Stochastic Mean Field Control and Games on Graph Limits: a Q-noise Formulation

Alex Dunyak

Department of Electrical Engineering
McGill University, Montreal

December 2024

A thesis submitted to McGill University in partial fulfillment of the requirements of the degree of Doctor of Philosophy

Abstract

The modelling of linear quadratic Gaussian optimal control problems on large complex networks is intractable computationally. Graphon theory provides an approach to overcome these issues by defining limit objects for infinite sequences of graphs. This permits one to approximate arbitrarily large networks by infinite dimensional operators. This is extended to stochastic systems by the use of Q-noise, a generalization of Wiener processes in finite dimensional spaces to processes in function spaces. This thesis concerns the synthesis of two types of stochastic system on large graphs: linear quadratic Gaussian problems with estimation and linear quadratic field tracking games.

The optimal control and estimation of linear quadratic problems on graphon systems with Q-noise disturbances are defined here and shown to be the limit of the corresponding finite graph optimal control problem. The theory is extended to low rank systems, and a fully worked special case is presented. In addition, the worst-case long-range average and infinite horizon discounted optimal control performance with respect to Q-noise distribution are computed for a set of standard graphon limits. The convergence of finite network linear system state estimates to their graphon limit counterparts is established. Computational examples of this convergence behaviour are illustrated with a set of standard graphon examples.

In this thesis, linear quadratic games on very large dense networks are modelled with discrete time linear quadratic graphon field games with Q-noise. In such a game, the agents are interconnected via an undirected network with one agent per node. Gaussian disturbances that are correlated over nodes affect each agent. The limit of the finite-sized linear quadratic network tracking game in discrete time is formulated, and it is shown that under the proper assumptions, the game has a graphon limit system with Q-noise. Then, the optimal control of the discrete-time system is found in closed form and the Nash equilibrium behavior of the game is demonstrated numerically. The infinite time horizon discounted case is also analyzed, and a closed-form feedback solution is presented in the special case where the underlying graphon is finite rank.

Résumé

La modélisation des problèmes de contrôle optimal linéaire, quadratique et gaussien sur de grands réseaux complexes est intraitable d'un point de vue informatique. La théorie des graphes fournit une approche pour surmonter ces problèmes en définissant des objets limites pour des séquences infinies de graphes. Cela permet d'approximer des réseaux de taille arbitraire par des opérateurs de dimension infinie. Cette approche est étendue aux systèmes stochastiques par l'utilisation du bruit Q, une généralisation des processus de Wiener dans les espaces de dimension finie aux processus dans les espaces de fonction. Cette thèse concerne la synthèse de deux types de systèmes stochastiques sur les grands graphes : les problèmes gaussiens quadratiques linéaires avec estimation et les jeux de suivi de champs quadratiques linéaires.

Le contrôle optimal et l'estimation des problèmes quadratiques linéaires sur les systèmes de graphes avec des perturbations de bruit Q sont définis ici et il est démontré qu'ils sont la limite du problème de contrôle optimal correspondant sur les graphes finis. La théorie est étendue aux systèmes de rang inférieur, et un cas spécial entièrement travaillé est présenté. En outre, les performances de contrôle optimal actualisé à long terme et à horizon infini les plus défavorables en ce qui concerne la distribution du bruit Q sont calculées pour un ensemble de limites de graphes standard. La convergence des estimations d'état des systèmes linéaires à réseau fini vers leurs équivalents en limite de graphon est établie. Des exemples de calcul de ce comportement de convergence sont illustrés avec un ensemble d'exemples de graphon standard.

Dans cette thèse, les jeux linéaires quadratiques sur de très grands réseaux denses sont modélisés à l'aide de modèles discrets.

For my parents.

Acknowledgements

I would like to thank my advisor, Peter E. Caines, for all of his support during my time at McGill.

I would also like to thank my advising committee members, Aditya Mahajan and Xiaozhe Wang. I'd like to thank Shuang Gao for all his help as I was adjusting to life as a PhD student.

Finally, I'd like to thank my friends and fellow PhD students Borna Sayedana and Tao Zhang.

Table of Contents

List of Figures

Figure

List of Tables

Table

Preface

This thesis consists of elements of five conference papers cowritten with my advisor, Peter E. Caines,

- *Large scale systems and SIR models: a featured graphon approach*, presented at the 2021 60th IEEE Conference on Decision and Control (CDC), 6928-6933,
- *Linear stochastic graphon systems with Q-space noise*, presented at the 2022 IEEE 61st Conference on Decision and Control (CDC), 3926-3932,
- *Graphon Field Tracking Games with Discrete Time Q-noise*, presented at the 2023 62nd IEEE Conference on Decision and Control (CDC), 8194-8199,
- *Stochastic Control on Large Networks: A Q-noise Formulation*, presented at the 2024 American Control Conference (ACC), 5219-5225, and
- Linear Stochastic Processes on Networks and Low Rank Graph Limits, presented at the International Conference on Complex Networks and Their Applications, 395-407.

In addition, the thesis contains work revised from three articles in review,

- *Stochastic graphon field tracking games with finite and infinite horizons*, under review for *Automatica*,
- *Quadratic Optimal Control of Graphon Q-noise Linear Systems*, under review for *Automatica*,
- *Optimal Filtering and Separation Principle for Graphon Q-noise Linear Systems*, to be submitted to *Communications in Information and Systems*.

In each article above, I, Alex Dunyak, am the first author, and my advisor, Peter E. Caines, is the second author. The work was split approximately 65 percent myself and 35 percent Professor Caines.

Chapter 1

Introduction

In modern society, the control and estimation of systems on large graphs is of vital importance. Large graphs naturally occur in many situations, from physical systems such as decentralized energy generation and distribution, to non-physical systems such as logistics networks, social media, and financial markets. From a practical perspective, modelling these systems directly is infeasible as they involve thousands or millions of agents acting in tandem. These large systems are often buffeted by stochastic shocks, which increases the difficulty of analysis from both a theoretical and a practical perspective. As such, the estimation and control of such systems in a computationally tractable manner is critical.

This thesis concerns optimization and control of continuous-time linear quadratic problems on very large, dense graphs with stochastic shocks. The systems considered can be broadly characterized as either optimal control problems of linear systems on large graphs with quadratic costs, or linear games with quadratic costs where each agent attempts to match its neighbors on the graph.

This document is structured in the following manner: Chapter 1 motivates the problems, defines relevant notation, and gives required background on graphons, a type of graph limit that allows functional analysis techniques to be applied to systems on graphs. Chapter 2 defines the variety of stochastic shock applied to the system, a generalization of multidimensional Wiener processes to Hilbert spaces, as well as defining the linear quadratic Gaussian

problem on large graphs, and demonstrates that the large graph state trajectory converges to the limit graphon system. Chapter 3 introduces Kalman filter-based state estimation for these systems, culminating in a Separation Principle for the control and estimation of systems on large graphs. In addition, Chapter 2 and Chapter 3 also show that when the graphon limit is finite rank, then the systems on large graphs can be modelled in a finite number of equations (typically orders of magnitude fewer equations than the full state of the graph system). Chapter 4 defines the graphon field-tracking game, where each agent in a discrete-time game with stochastic shocks attempts to match their neighbors in the graph. All chapters are supported with numerical examples.

1.1 Graphons

Large graphs are common objects in contemporary systems modelling and analysis, in particular for the purposes of optimization and control. Indeed, from the internet to electrical generation and distribution to social networks, complex networks have been a focus of research for decades. Many of these networks cannot be fully mapped; for example, it is not possible to determine all connections on the internet currently active, as connections are created and destroyed in real time. As such, global modelling and analysis problems are intractable with standard methods for all sufficiently large networks.

Graphons (short for graph functions, and described in detail by Lovasz [1]) are one method of providing qualitative properties to graph sequences of increasing size. Formally, a graphon is any bounded, symmetric function mapping the unit square to the unit interval. Individual graphs in a graph sequence can be mapped to the unit square by taking the adjacency matrix and mapping them to piecewise constant step functions on the unit square, where each partition denotes an entry in the adjacency matrix.

As explained by Lovasz, this sequence of piecewise constant step functions necessarily has a subsequence converging to the graphon under the cut distance, which essentially quantifies how closely two large graphs match if their nodes could be freely relabeled. To define the

cut distance, first it is necessary to define the *cut norm* as in [1],

$$||W||_{\square} = \sup_{S,T\subseteq[0,1]} \Big| \int_{S\times T} W(x,y)dxdy \Big|, \tag{1.1}$$

with the corresponding cut metric $d_{\square}(U,W) = ||U-W||_{\square}$. Further, let $S_{[0,1]}$ denote the set of all invertible measure preserving transformations of $[0,1]$ to $[0,1]$, and for a graphon W, let $W^{\phi}(x,y) := W(\phi(x),\phi(y))$. The *cut distance* is then found by taking the infimum over all such measure-preserving transformations of the second graphon onto the first,

$$\delta_{\square}(U,W) = \inf_{\phi\in S_{[0,1]}} d_{\square}(U,W^{\phi}). \tag{1.2}$$

Just as the adjacency matrix of a graph can have its rows and columns permuted without changing the underlying graph, an invertible measure-preserving transformation applied to the entries of a graphon does not change the underlying structure of the graphon. The cut distance captures this behavior.

The compactness of the set of graphons under the cut distance allows certain questions about large graphs to be answered by their graphon approximations. The difficulty with the cut distance, however, is the infimization over the set of invertible measure-preserving transformations. With this in mind, we restrict our consideration to graph sequences whose piecewise constant step function equivalents converge to a graphon in the standard $L^2[0,1]$ operator norm. Thus, the intention behind this work is to apply the convergence of systems on graphs to graphons in the $L^2[0,1]$ function space and relate it to the analysis of stochastic dynamic systems on large graphs. Medvedev [2] initiated the use of graphons as operators for linear systems, though the work continued with Gao and Caines applying linear control techniques to these graphon systems [3], [4].

The basic model is to map the adjacency matrix to a piecewise constant step function, and then to take the limit as the graph size tends to infinity. This procedure is demonstrated for a deterministic, continuous-time system on a graph in Figure 1.1.

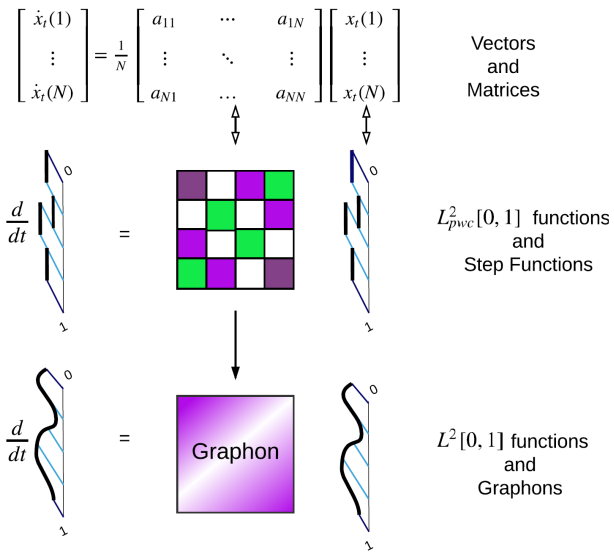

Figure 1.1: The finite-dimensional system (top) is mapped to the space of piecewise constant step functions on the unit interval. The graphon limit is found as the size of the graph tends to infinity. Picture credit: Shuang Gao.

Another important domain of this research is the approximation of large graph systems by finite rank systems. In particular, when the graphon limit is rank $M < \infty$, then a system on a sufficiently large graph can be approximated by an M-dimensional linear system. For deterministic systems, this finite rank convergence was first shown by Gao and Caines [3], [4].

This leads to the overall system model:

1. The system state on a finite graph is mapped to a piecewise constant step function on the unit interval.

2. The graph system state tends to the graphon limit as the cardinality of the graph tends to infinity.

3. Projecting onto M basis functions of the graphon limit yields a finite-dimensional approximation of the graphon limit system.

4. The M-dimensional system can be used to either model or control the finite graph system.

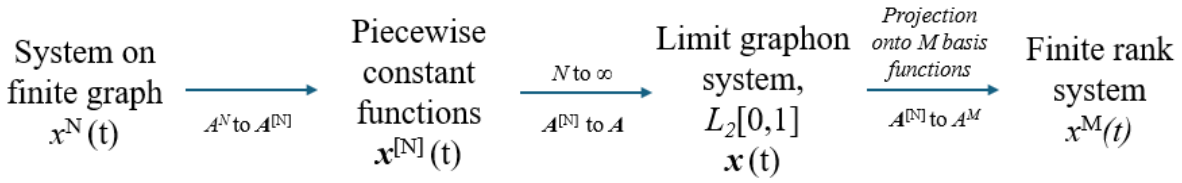

Figure 1.2: The system model that allows graphs with a large number of nodes to be approximated by a system with fewer dimensions.

This is summarized in Figure 1.2.

However, in classical control linear systems theory, it is common to assume that modelled systems have stochastic inputs. These inputs represent the fundamental limitations of the model as compared to reality. Due to analytical difficulties of random variables in function spaces, it is not straightforward to adapt the stochastic linear analysis in finite dimensions to stochastic analysis in infinite dimensions. Prior research in the area of networked system control via graphons is strictly deterministic ([3], [4]). Allowing the system to be influenced by random perturbations enriches the modelling capabilities of the graphon-systems approach and allows for important concepts such as state estimation under uncertainty to be well-defined.

1.2 Stochastic Processes in Hilbert spaces

The primary extension of this thesis is to demonstrate that stochastic systems on these large graphs also converge in a meaningful sense by using functional analytic techniques. The approach used is to refine the notion of Q-Wiener processes to specify Wiener processes on the unit interval. These processes, termed Q-noise, will be introduced formally in Chapter 2.

The extension of a random variable from having support in a finite-dimensional space to an infinite-dimensional space must be attempted carefully. Even standard properties of finite-dimensional analysis (such as the translation-invariance of the Lebesgue measure) may

fail to hold.

The space of square-integrable functions, $L^2[0,1]$, is an infinite-dimensional separable Hilbert space, so it is isomorphic to l_2, the space of square-summable sequences. This is a consequence of elements of a separable Hilbert space having an orthonormal basis—each basis element ϕ_k of $L^2[0,1]$ corresponds to the kth sequence element. Because of this fact, in the cases we consider it is often easier to study and construct these sequences than to analyze the corresponding square-integrable functions.

Pressingly, there is no random variable in a Hilbert space corresponding to an N-dimensional Gaussian random vector that is independent in its dimensions. In finite dimensions, a random Gaussian vector with independent dimensions has a well-defined covariance operator so long as the covariance between any dimensions is finite. A naive approach to constructing a "white noise" Gaussian random variable in the infinite-dimensional Hilbert space l_2 may have variance one for each index ($k, 1 \leq k < \infty$), and a covariance of zero for all ($j, j \neq k, 1 \leq j < \infty$). However, this yields a random variable that does not have a valid probability measure, a fact proven by Kolmogorov and Khinchin in 1925 ([5][6, Theorem 2.4]).

Instead, to construct an l_2 Gaussian random variable, $g^\infty = (g_1, g_2, ...)$, which is independent between indices i and j, $i \neq j$, it is necessary that the variances are summable. I.e., if $(w_1, w_2, ...)$ is a collection of independent Gaussian random variables, then g^∞ can be defined by

$$g^\infty = (\sqrt{\lambda_1}w_1, \sqrt{\lambda_2}w_2, ..., \sqrt{\lambda_k}w_k, ...) \in l_2, \tag{1.3}$$

$$\sum_{k=1}^{\infty} \lambda_k < \infty. \tag{1.4}$$

As in [6, Section 2.4], this constructs an l_2 valued Gaussian random variable. This approach can be extended to Gaussian processes in space and time, commonly called Q-Wiener processes (see e.g. [7], [8]). Rather than a collection of static independent Gaussian random

variables, consider a collection of Wiener processes $(W_1(t), W_2(t), ...)$; this defines the Q-Wiener process $g_{l_2}^{\infty}(t)$,

$$g^{\infty}(t) = \sum_{k=1}^{\infty} \sqrt{\lambda_k} W_k(t), \tag{1.5}$$

$$\sum_{k=1}^{\infty} \lambda_k < \infty. \tag{1.6}$$

This construction yields a time-varying l_2 random process. As l_2 is isomorphic to any separable Hilbert space by associating the indices of the sequence with the orthogonal dimensions of the alternate space, if $Q : L^2[0,1] \to L^2[0,1]$ is a self-adjoint operator with eigenvalues $(\lambda_k, 1 \leq k < \infty)$ and orthonormal eigenfunctions $(\phi_k, 1 \leq k < \infty)$, then $g_{l_2}^{\infty}(t)$ is equivalent to the $L^2[0,1]$-valued random process $g_{L^2}^{\infty}(t)$,

$$g^{\infty}(t) = \sum_{k=1}^{\infty} \sqrt{\lambda_k} \phi_k W_k(t) \tag{1.7}$$

$$\sum_{k=1}^{\infty} \lambda_k < \infty. \tag{1.8}$$

The space of square-integrable functions $L^2[0,1]$ is very well-studied, and many domain-specific geometric insights may be gained by considering the equivalent $L^2[0,1]$ process rather than the l_2 sequence process.

To demonstrate why the Q-noise framework is necessary for the modelling of very large linear systems, consider two linear stochastic systems of dimension $N = 300$. For each index $i \in \{1, ..., N\}$, the ith state of both systems satisfies the following stochastic differential equation with Brownian disturbance W_t^i,

$$\begin{aligned} dx_t^i =& \frac{1}{N} \sum_{j=1}^{N} \cos\left(\pi \left(\frac{i}{N} - \frac{j}{N}\right)\right) x_t^j dt + dW_t^i, \\ x_0^i =& 1. \end{aligned} \tag{1.9}$$

In the first system, assume that the covariance matrix Q of the Brownian motion disturbance between state i and state j is given entry-wise by $Q_{ij} = 1 - \max\left(\frac{i}{N}, \frac{j}{N}\right)$. This system converges to a Q-noise system in the $L^2[0,1]$ norm as the number of nodes increases. In the second system, assume that the Brownian motion disturbances W_t^i are independent. The result is a system where the noise of individual states overpowers the trajectory of the overall system. The sample trajectories of two such systems with terminal time $T = 1$ can be seen in Fig. 1.3. This simulation suggests a method of identifying when a Q-noise model is appropriate, as the system will have bounded variance.

In Dunyak and Caines ([9]), space-time Gaussian noise on the unit interval ([7] [8] [6]), termed Q-noise, was introduced as a limit object for sequences of systems on graphs with Brownian disturbances. Medvedev and Simpson [10] presented a numerical method of simulating such systems. Previous work on control via graphons has been primarily concerned with deterministic systems ([11][3]), though there have been prior efforts to introduce infinite-dimensional noise to graphon systems [12]. The intention behind defining Q-noise for graphon systems is to create a well-defined method of applying linear quadratic Gaussian control (the focus of Chapter 2) and estimation (Chapter 3) techniques to systems on large graph systems.

Linear quadratic Gaussian problems with Q-Wiener processes extend the standard linear quadratic Gaussian results to infinite-dimensional systems [13]. For two positive operators $\boldsymbol{M}$ and $\mathbf{R}$, the linear quadratic Gaussian problem infinimizes

$$\inf_{\boldsymbol{u}_t} \int_0^T \mathbb{E}[\langle \boldsymbol{x}_s, \boldsymbol{M}\boldsymbol{x}_s\rangle + \langle \boldsymbol{u}_t, \mathbf{R}\boldsymbol{u}_t\rangle ds] + \langle \boldsymbol{x}_T, \boldsymbol{M}\boldsymbol{x}_T\rangle. \tag{1.10}$$

This is commonly used to control infinite-dimensional distributed parameter systems, such as heat equations [14].

The Kalman filter is the optimal least-squares linear estimator of a state process (initially for discrete-time systems, but extended to continuous-time processes by Bucy [15]), i.e., for a

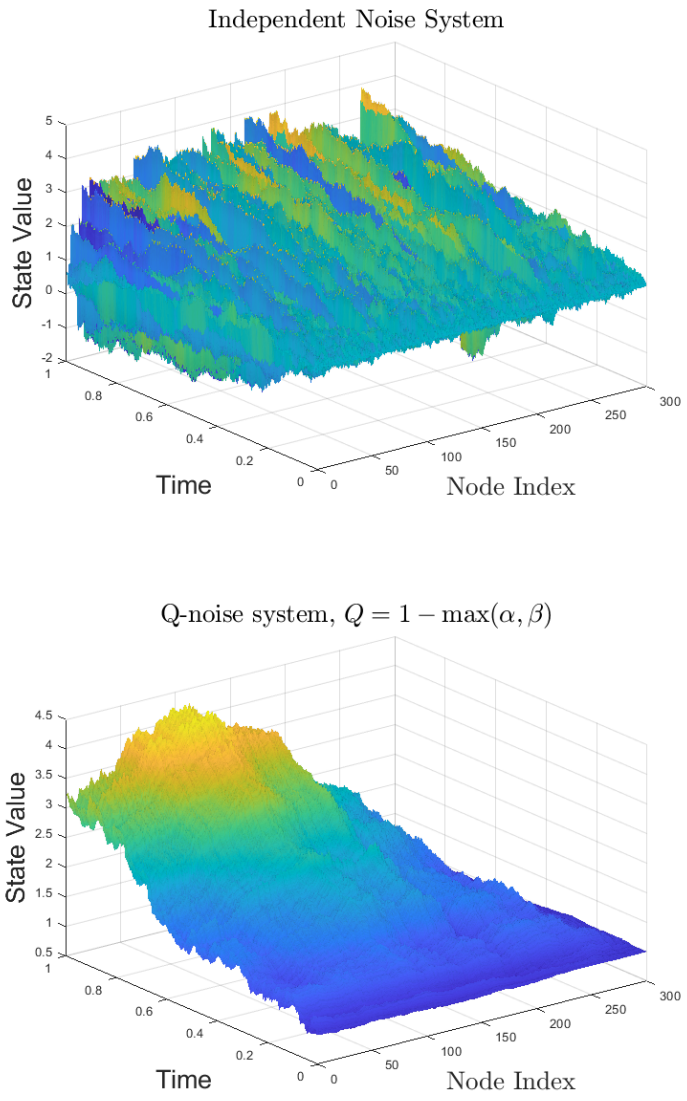

Figure 1.3: Top: Trajectory of system (1.9) with independent noise at each node. Because the magnitude of the independent noise is so high, there is no clear system structure in the state trajectory. Bottom: the state trajectory of system (1.9) with a Q-noise disturbance. While there is clearly noise present in the system, there is an overall structure suggesting that the limit will be continuous in both space and time.

stochastic linear state process x_t with an observation process y_t, the Kalman filter minimizes

$$\hat{x}_t = \min_{\xi_t} \mathbb{E}[x_t - \xi_t | y_t]. \tag{1.11}$$

We note that the Kalman filter for infinite-dimensional systems is well-known, initially characterized in 1975 by Falb [16], and later extended by Curtain [17]. Curtain and Ichikawa later classified a Separation Principle, showing that for infinite-dimensional systems the deterministic linear quadratic regulator problem and the least-squares state estimation problem can be solved independently [18]. Applying this Separation Principle to a convergent sequence of graph systems forms the culminating theorem in Chapter 3: the graphon state estimate of a large graph system can generate an approximately optimal control for the finite graph system. This allows the finite graph system to be controlled even when the exact data of the underlying adjacency matrices A^N and B^N are unknown, so long as they converge to the graphons $\boldsymbol{A}$ and $\boldsymbol{B}$.

In finite-dimensional graph systems, the Kalman filter has typically been used as a method of state estimation over sensor networks, as in [19]. Typically, it is modified to emphasize the distributed nature of sensor networks [20]. Much as how graphon theory assumes a particular graph property—density—these distributed Kalman filter methods exploit the structure of specific networks (for example, for bipartite graphs [21]) to overcome the difficulty of decentralized estimation and control.

1.3 Graphon Field Games

Adapting the definition of Q-noise from continuous time to discrete time, a linear quadratic game with correlated Gaussian disturbances on an infinitely large dense graph is investigated where each node represents a single agent is presented in Chapter 4. To distinguish this from the infinite-agent-per-node graphon mean-field game (GMFG) model, this approach was termed the graphon field game model. The fundamental difference between the GMFG

model investigated in [22], [23], [24], [25], [26] and the graphon field game model presented here is that each agent in the graphon field game is associated with a single node in the graph, rather than an infinite number of nodes. The GMFG model's strongest benefit is that agents only affect the game state as a mass—as there are an infinite number of agents at each node, the actions of a particular agent do not influence the average state of either the local node or the game as a whole. In both standard mean-field games and GMFGs, this is known as the mean-field game assumption. This assumption allows the trajectory of the limit game to be modelled as a Fokker-Planck-Kolmogorov equation [27] with an associated McKean-Vlasov equation. Continuous-time stochastic mean-field games on graphons with Q-Wiener processes were analyzed in [28]. GMFGs have been extended in particular to the case of large sparse graphs in [29], [30], and [31].

A difficulty with some interpretations of the GMFG approach is that idiosyncratic noise in space implicitly appears which would lead to singular random processes. One approach to averting this measurability issue by Aurell et al., for linear quadratic GMFGs is to use the Fubini extension [32], which was extended to bilinear epidemic games in [33]. The use of discrete-time Q-Wiener processes in Chapter 4 is another attempt to solve the measurability problem of applying idiosyncratic Wiener processes at each node.

The model presented in Chapter 4 is a stochastic, discrete-time version of a model first proposed by Gao et al., [34]. By introducing a definition for discrete-time Q-noise (which is much simpler than the continuous-time definition from an intuitive perspective, as it is a sequence of Hilbert space-valued random variables rather than a continuum), we find a closed-form solution to the game by using the mean-field game assumption and the graphon field definition.

1.4 Contributions

In Chapter 2, we:

- provide motivation for the approximation and control of stochastic processes on large graphs using Q-noise.
- Demonstrate that, under the proper conditions on the system parameters, a linear stochastic process on a finite graph converges to a graphon limit process.
- Show that the same convergence behavior holds true for linear quadratic Gaussian problems on large graphs.
- Define the infinite time horizon long-term averaging (LTA) problem for graphon systems, and we find a closed-form solution for a natural class of such LTA problems.

In Chapter 3, we:

- Extend the work of Chapter 2 by interpreting the infinite-dimensional Kalman filter (for infinite-dimensional linear systems driven by Q-Wiener processes) in the context of graphon systems.
- Show that the Separation Principle of estimation and control for infinite-dimensional systems holds, and that this allows a system on a large finite graph to be estimated and stabilized by its limit graphon system.

In Chapter 4, we:

- Modify the graphon field game definition of [34] to discrete-time stochastic linear quadratic games on graphons.
- Derive an optimal Nash equilibrium strategy for each agent in the game as an adapted backwards stochastic difference equation.
- Identify a possible solution to the infinite-horizon discounted game.

Chapter 2

Linear Quadratic Gaussian Control

2.1 Introduction

Large graphs are common objects in contemporary systems modelling and analysis, in particular for the purposes of optimization and control. Indeed, from the internet to electrical generation and distribution to social networks, complex networks have been a focus of research for decades. However, global modelling and analysis problems are intractable with standard methods for all sufficiently large networks.

One approach to handling large networks is to use the theory of graphons [1]. Informally, a graphon is a function on the unit square which represents a limit of the adjacency matrices of a sequence of graphs. Consequently, using graphons for modelling large systems allows for the approximation of very large networks within a functional analysis framework and hence enables their modelling, analysis, and design.

The use of graphons in system dynamics was initiated by Medvedev [2]. Previous work on control via graphons has been primarily concerned with deterministic systems ([11][3]), while stochastic mean-field games on graphons have been investigated in [22], [23], [24], [25], [26] and with Q-Wiener processes in [28]. Graphon Mean-Field Games have been extended in particular to the case of large sparse graphs in [29], [30], and [31]. The use of Q-Wiener processes solves the measurability problem of applying idiosyncratic Wiener processes at

each node, which was addressed by Aurell et al., for linear quadratic graphon mean-field games using the Fubini extension in [32] and for epidemic games in [33].

In Dunyak and Caines [9], space-time Gaussian noise on the unit interval ([7] [8] [6]), termed Q-noise, was introduced as a limit object for sequences of systems on graphs with Brownian disturbances. Medvedev and Simpson [10] presented a numerical method of simulating such systems. This chapter demonstrates that linear quadratic Gaussian (LQG) optimal control problems on large graphs can be approximately solved by the graphon limit of their system. The analysis relies on the Hilbert space methods in Ichikawa [13] which is extended here to long-range average and infinite discounted cost LQG problems, the former of which is derived with a limit argument and the latter of which is solved via the corresponding algebraic Riccati equation in the case of purely local controls.

In the following subsections, we provide the motivation for modelling linear quadratic Gaussian systems on large networks with their graphon and Q-noise limits. In Section 2.2.1, we define the notation used in this thesis, as well as summarize relevant prior results for Q-noise systems. In Section 2.2.4, we present the formal proof that the finite-dimensional linear quadratic Gaussian system converges to the infinite-dimensional linear quadratic Q-noise system, as well as presenting the long-range average and exponential discounting problems. Section 2.4 extends the analysis of low rank graphons presented in [4] to Q-noise systems. Section 2.5 demonstrates the utility of the Q-noise approach in that the solutions to LQG problems on large unweighted random graphs are shown to be well-approximated by lower-order systems derived from the graphon limit of the original system.

2.1.1 Motivation: Networked Systems and Graphons

Define two graphs $G_A^N = (V_N, E_A^N)$ and $G_B^N = (V_N, E_B^N)$ with $N < \infty$ vertices, with associated adjacency matrices A^N and B^N. Let $x^N : [0,T]^N \to \mathbb{R}$ be a vector of states, where the ith value is associated with the ith vertex of the graph, and let $u^N : [0,T]^N \to \mathbb{R}^N$ be the control input at each vertex. For clarity of notation, systems where each node has

a scalar state are considered below. The theory extends to systems with vector states at each node in a straightforward manner. Let the (i, j)th entry of the matrices A^N and B^N represent the impact of the state and control input at node i on node j, respectively. For each node, define a Brownian motion such that the N-component Brownian motion W^N has a strictly positive covariance matrix Q^N. Let a_N and b_N be constants describing the impact of the state of a node and its control on itself.

Finally, define a network-averaged control system [3] on a graph with the following equation for each node,

$$dx_t^i = (a_N x_t^i + \sum_{j=1}^{N} A_{ij}^N x_t^j + b_N u_t^i + \sum_{j=1}^{N} B_{ij}^N u_t^j)dt + dW_i^N(t), \tag{2.1}$$

or in vector form,

$$dx_t^N = ((A^N + a_N)x_t^N + (B^N + b_N)u_t^N)dt + dW^N(t). \tag{2.2}$$

Subject only to the assumption that the entries of A^N and B^N are uniformly bounded in N, the sequences of adjacency matrices $\{A^N\}$ and $\{B^N\}$, $1 \leq N < \infty$, defined on the unit square converge, as N tends to infinity, to their (not necessarily unique) associated graphon limits [1], which are bounded measurable functions mapping $[0, 1] \times [0, 1] \to [0, 1]$. These are denoted $\boldsymbol{A}$ and $\boldsymbol{B}$ (as in [3]). In order to disambiguate the convergence of the adjacency matrix A^N to the graphon $\boldsymbol{A}$, the scaling term $\frac{1}{N}$ is omitted when A^N is acting as an operator. This scaling is to ensure that the summation $A^N x^N$ is bounded and converges to the correct integral. When the underlying graph is undirected, its graphon is also symmetric. Denote the graphon limit system as

$$d\boldsymbol{x}_t = ((\boldsymbol{A} + a\mathbb{I})\boldsymbol{x}_t + (\boldsymbol{B} + b\mathbb{I})\boldsymbol{u}_t)dt + d\boldsymbol{w}_t, \tag{2.3}$$

where $\boldsymbol{x}_t$ and $\boldsymbol{u}_t$ are square-integrable functions on the unit interval, $\boldsymbol{A}$ and $\boldsymbol{B}$ are graphons,

a and b are real constants, $\mathbb{I}$ is the identity operator, and $\boldsymbol{w}_t$ is a Q-noise, a generalization of Gaussian noise from finite-dimensional vectors to random time-varying functions the unit interval as defined in Section 2.2.2, together with the conditions in Theorem 2.2.3 for the existence of the limit in mean-square.

2.1.2 Linear Quadratic Q-noise Control

Let x_t^N be the state of a networked control system on a graph G^N as given in equation (2.2). Suppose that M^N is an $N \times N$ positive matrix, and R^N is an $N \times N$ strictly positive matrix. Then the associated linear quadratic Gaussian optimal control problem for a control system with terminal time T is defined via the infimization of the performance function:

$$\inf_{u_0^T} J(x_0, u) = \inf_{u_0^T} \mathbb{E}\left[\int_0^T x_t^{N*} M^N x_t^N + u_t^{N*} R^N u_t^N dt\right]. \tag{2.4}$$

The solution of the limit problem takes the same form as the standard finite-dimensional LQG problem, but the equations have operator-valued coefficients and the solutions are operator-valued. This work analyzes the properties of the operator limits of such sequences of network-averaged optimal control problems and it is shown that the solutions of the limit problems are obtained via the operator limits of the associated Riccati equations.

2.1.3 The Special Case of Finite Rank Systems

The systems described in the prior section are defined in the space of square-integrable functions on the unit interval, $L^2[0,1]$. In general, it is not possible to find a closed-form solution for such a system. However, when a system's associated graphon parameters and Q-noise covariance function are finite-rank, then the state of the system evolves on a finite-dimensional space. This is explored in Section 2.4.

2.2 Preliminaries

2.2.1 Notation

- The set of vectors of real numbers of dimension m is denoted $\mathcal{R}^m$.
- Graphons (i.e. bounded symmetric $[0,1]^2$ functions used as the kernels of linear integral operators) are denoted in italicized bold capital letters, such as $\boldsymbol{A}$, $\boldsymbol{B}$, and $\boldsymbol{M}$.
- $L^2[0,1]$ denotes the Hilbert space of real square-integrable functions on the unit interval. In addition, $L^2[0,1]$ is equipped with the standard inner product, denoted $\langle \boldsymbol{u}, \boldsymbol{v} \rangle$. For any function $\boldsymbol{v}$, $\boldsymbol{v}^*$ denotes the adjoint of $\boldsymbol{v}$. As such, $\langle \boldsymbol{u}, \boldsymbol{v} \rangle$ is sometimes written as $\boldsymbol{v}^* \boldsymbol{u}$.
- The identity operator in both $L^2[0,1]$ and finite-dimensional spaces is denoted $\mathbb{I}$.
- Operators of the form $\mathbb{A}$ and $\mathbb{B}$ have the structure $\mathbb{A} = \boldsymbol{A} + a\mathbb{I}$, where $\boldsymbol{A}$ is a graphon and a is a real scalar. Let $\mathcal{M}$ denote the set of these operators.
- A linear integral operator with the kernel $\mathbf{Q} : [0,1]^2 \to \mathcal{R}$ acting on a function $\boldsymbol{f} \in L^2[0,1]$ is defined by

$$(\mathbf{Q}\boldsymbol{f})(x) = \int_0^1 \mathbf{Q}(x,y)\boldsymbol{f}(y)dy, \quad \forall\ x \in [0,1]. \tag{2.5}$$

- The operators $\mathbf{Q}$ are equipped with the standard operator norm $||\mathbf{Q}||_{\text{op}}$. When unambiguous, the argument is dropped.
- A symmetric function $\mathbf{Q} : [0,1]^2 \to \mathcal{R}$ is non-negative if the following inequality is satisfied for every function $\boldsymbol{f} \in L^2[0,1]$,

$$\begin{aligned} 0 &\leq \int_0^1 \int_0^1 \mathbf{Q}(x,y)\boldsymbol{f}^*(x)\boldsymbol{f}(y)dxdy \\ &:= \langle \mathbf{Q}\boldsymbol{f}, \boldsymbol{f} \rangle < \infty. \end{aligned} \tag{2.6}$$

Additionally, denote $\mathcal{Q}$ to be the set of bounded symmetric non-negative functions. The set $\mathcal{Q}$ serves as the set of valid covariance functions for the class of stochastic processes called Q-noise processes.

- For a given linear system $\boldsymbol{x}_t$ satisfying $\dot{\boldsymbol{x}}_t = \boldsymbol{A}_t\boldsymbol{x}_t$, $\Phi(t,s)$ denotes the semigroup solution operator solving $\boldsymbol{x}_t = \Phi(t,s)\boldsymbol{x}_s$ for any given initial condition $\boldsymbol{x}_s$.

- Q-noise processes (stochastic processes over the time interval $[0,T]$) will be denoted as $\boldsymbol{w}_t$. For each $t \in [0,T]$, $\boldsymbol{w}_t$ is an $L^2[0,1]$ function. The precise definition of a Q-noise process is given in Section 2.2.2.

- A partition of the unit interval of N increments is denoted $P^N = \{P_1, \cdots, P_N\}$, where $P_1 = [0, \frac{1}{N}]$ and $P_i = (\frac{i-1}{N}, \frac{i}{N}]$. An $L^2[0,1]$ function which is piece-wise constant on the unit interval is denoted $\boldsymbol{v}^{[N]}$, and a self-adjoint $L^2[0,1]$ operator $\boldsymbol{M}$ which is piece-wise constant on the Cartesian product $P^N \times P^N$ is denoted $\boldsymbol{M}^{[N]}$ (or $\mathbb{M}^{[N]}$, if it is of the form $\mathbb{M}^{[N]} = \boldsymbol{M}^{[N]} + m\mathbb{I}$). This formulation is necessary for mapping $N \times N$ adjacency matrices of networks to functions on the unit square, as in Section 2.2.5.

2.2.2 Q-noise Axioms

Q-noise processes, first applied to graphon systems in [9], are $L^2[0,1]$ valued random processes that satisfy the following axioms.

1. Let $\mathbf{Q} \in \mathcal{Q}$, and let $([0,1] \times [0,T] \times \Omega, \mathcal{B}([0,1] \times [0,T] \times \Omega), \mathbb{P})$ be a probability space with the measurable random variable $\boldsymbol{w}(\alpha, t, \omega) : [0,1] \times [0,T] \times \Omega \to \mathcal{R}$ for all $t \in [0,T], \alpha \in [0,1]$, $\omega \in \Omega$. For notation, ω is suppressed when the meaning is clear.

2. For all $\alpha \in [0,1]$, $\boldsymbol{w}(\alpha,t) - \boldsymbol{w}(\alpha,s)$ is a Wiener process increment in time for all $t, s \in [0,T]$, with $\boldsymbol{w}(\alpha,t) - \boldsymbol{w}(\alpha,s) \sim \mathcal{N}(0, |t-s|\mathbf{Q}(\alpha,\alpha))$ where $\boldsymbol{w}(\alpha,0) = 0$ for all $\alpha \in [0,1]$.

3. Let $\boldsymbol{w}_{t-t'}(\alpha) = \boldsymbol{w}(\alpha, t) - \boldsymbol{w}(\alpha, t')$. Then,

$$\mathbb{E}[\boldsymbol{w}_{t-t'}(\alpha)\boldsymbol{w}_{s-s'}(\beta)] = |[t, t'] \cap [s, s']| \cdot \mathbf{Q}(\alpha, \beta).$$

4. For almost all $s, t \in [0, T]$, $\alpha, \beta \in [0, 1]$, and $\omega \in \Omega$, $\boldsymbol{w}(\alpha, t, \omega) - \boldsymbol{w}(\beta, s, \omega)$ is Bochner-integrable as a function taking values in the Banach space of a.s. piece-wise continuous functions of $[s, t] \in [0, T]$. The Bochner integral of a random variable $X : (\Omega, \mathcal{B}, \mu) \to E$ where E is a Banach space is defined as the limit of the sum of simple functions taking a finite set of values $X_n(\omega)$, analogous to Lebesgue integration [8, Sec. 1.1.3].

An orthonormal basis example: Let $\{W_1, W_2, \cdots\}$ be a sequence of independent Brownian motions. Let $\mathbf{Q} \in \mathcal{Q}$ have a diagonalizing orthonormal basis $\{\phi_k\}_{k=1}^{\infty}$ with eigenvalues $\{\lambda_k\}_{k=1}^{\infty}$. Then

$$g(\alpha, t, \omega) = \sum_{k=1}^{\infty} \sqrt{\lambda_k}\phi_k(\alpha)W_k(t, \omega) \tag{2.7}$$

is a Q-noise process. The common name for this formulation in the literature is Q-Wiener process ([7] [8]).

2.2.3 Operators on Q-noise

The following theorems on the action of operators on Q-noise were originally presented by Dunyak and Caines in [35].

Definition 2.2.1 *$\mathcal{M}$ shall denote the set of operators of the form $\mathbb{M} = \boldsymbol{W} + c\mathbb{I}$, where $\boldsymbol{W}$ is a bounded self-adjoint Hilbert-Schmidt integral operator (hence possessing square-summable eigenvalues) mapping $L^2[0, 1]$ to $L^2[0, 1]$, $c > 0$ is a positive constant, and $\mathbb{I}$ is the identity operator on $L^2[0, 1]$.*

Definition 2.2.2 (Operators on Q-Space Noise) *Let $\mathbf{Q} \in \mathcal{Q}$ and $\boldsymbol{w}_t$ be a Q-space noise. Let $\mathbb{M} \in \mathcal{M}$, and let $s < t \in [0, T]$. Then the action of $\mathbb{M}$ on $\boldsymbol{w}_{t-s}(\cdot) := \boldsymbol{w}(\cdot, t) - \boldsymbol{w}(\cdot, s)$ is*

defined by the following Lebesgue integral for $s,t \in [0,T],\ \alpha \in [0,1]$,

$$(\mathbb{M}\boldsymbol{w}_{t-s}(\cdot))(\alpha) = \int_0^1 \mathbb{M}(\alpha,z)\boldsymbol{w}_{t-s}(z)dz. \tag{2.8}$$

Lemma 2.2.1 *Let* $\mathbb{M} = \boldsymbol{W} + c\mathbb{I} \in \mathcal{M}$. *Then* $(\mathbb{M}\boldsymbol{w}_{t-s})(\alpha)$ *is a centered random variable for all* $\alpha \in [0,1]$ *and* $s,t \in [0,T]$.

Proof: As $\boldsymbol{W}$ is a bounded operator, $\mathbb{E}[\boldsymbol{w}_{t-s}] = 0$ by Axiom 2, and since $\boldsymbol{w}_{t-s}$ is assumed to be Bochner-integrable by Axiom 4, the expected value is

$$\begin{aligned}\mathbb{E}[\mathbb{M}\boldsymbol{w}_{t-s}](\alpha) &= \mathbb{E}[\boldsymbol{W}\boldsymbol{w}_{t-s}](\alpha) + c\mathbb{E}[\boldsymbol{w}_{t-s}](\alpha)\\ &= (\boldsymbol{W} + c\mathbb{I})\mathbb{E}[\boldsymbol{w}_{t-s}](\alpha) = 0. \quad \square\end{aligned} \tag{2.9}$$

By associativity, an operator $\mathbb{W}$ acting on an operator $\mathbb{M}$ acting on a function $\boldsymbol{x}$ is denoted $(\mathbb{W}(\mathbb{M}\boldsymbol{x}))(\alpha) = (\mathbb{W}\mathbb{M}\boldsymbol{x})(\alpha)$ when the following iterated integral exists,

$$((\mathbb{W}\mathbb{M})\boldsymbol{x})(\alpha) = \int_0^1 \mathbb{W}(\alpha,z)\int_0^1 \mathbb{M}(z,y)\boldsymbol{x}(y)dydz. \tag{2.10}$$

Theorem 2.2.2 *Let* $\boldsymbol{w}_{t-t'}(\cdot) = \boldsymbol{w}(\cdot,t) - \boldsymbol{w}(\cdot,t')$ *and* $\boldsymbol{w}_{s-s'}(\cdot) = \boldsymbol{w}(\cdot,s) - \boldsymbol{w}(\cdot,s')$ *be two time increments of a Q-space process,* $\mathbf{Q} \in \mathcal{Q}$, *and* $\mathbb{M} \in \mathcal{M}$ *with* $\mathbb{M}\mathbf{Q}\mathbb{M}^* \in \mathcal{Q}$. *Then,*

$$cov((\mathbb{M}\boldsymbol{w}_{t-t'})(\alpha),(\mathbb{M}\boldsymbol{w}_{s-s'})(\beta)) = |[t,t'] \cap [s,s']|(\mathbb{M}\mathbf{Q}\mathbb{M}^*)(\alpha,\beta) \tag{2.11}$$

Proof: Recalling Lemma 2.2.1 the covariance is given by

$$\operatorname{cov}((\mathbb{M}\boldsymbol{w}_{t-t'})(\alpha),(\mathbb{M}\boldsymbol{w}_{s-s'})(\beta)) = \mathbb{E}[(\mathbb{M}\boldsymbol{w}_{t-t'})(\alpha)((\boldsymbol{w}_{s-s'})^*\mathbb{M}^*)(\beta)] \tag{2.12}$$

As $\boldsymbol{w}_{t-s}$ is Bochner-integrable by Axiom 4 and $\mathbb{M}$ is a bounded self-adjoint operator, the

operator $\mathbb{M}$ can be exchanged with the expectation,

$$\begin{aligned}
&\operatorname{cov}((\mathbb{M}\boldsymbol{w}_{t-t'})(\alpha), (\mathbb{M}\boldsymbol{w}_{s-s'})(\beta)) \\
&\quad = (\mathbb{M}\mathbb{E}[\boldsymbol{w}_{t-t'}\boldsymbol{w}^*_{s-s'}]\mathbb{M}^*)(\alpha,\beta) \\
&\quad = |[t,t'] \cap [s,s']| \int_0^1 \int_0^1 \mathbb{M}(\alpha,y)\mathbf{Q}(y,z)\mathbb{M}^*(z,\beta)dydz. \quad \square
\end{aligned} \tag{2.13}$$

2.2.4 Linear Dynamical Control Systems

Definition 2.2.3 (Q-noise Dynamical Systems) *Let $\boldsymbol{x} : [0,1]\times[0,T] \to \mathcal{R}$ be an $L^2[0,1]\times[0,T]$ function with a given initial condition $\boldsymbol{x}(\cdot,0) = \boldsymbol{x}_0$. Let $\mathbb{A}_t, \mathbb{B}_t \in \mathcal{M}$ be bounded linear operators from $L^2[0,1]$ to $L^2[0,1]$ such that $\mathbb{A}_t\mathbf{Q}\mathbb{A}_t^* \in \mathcal{Q}$. This defines a Q-noise denoted $\boldsymbol{w}_t$. Let a control input $\boldsymbol{u}_t : [0,T] \to L^2[0,1]$ be a function adapted to the filtration $\mathcal{F}_t$, consisting of all measurable functions of the state of the system $\boldsymbol{x}_s, 0 \le s \le t$.*

Then, a linear dynamical system with Q-noise is an infinite-dimensional differential system satisfying the following equation,

$$d\boldsymbol{x}_t(\alpha) = ((\mathbb{A}_t\boldsymbol{x}_t)(\alpha) + (\mathbb{B}_t\boldsymbol{u}_t)(\alpha))dt + d\boldsymbol{w}(\alpha,t), \tag{2.14}$$

where for a partition of $[0,t]$, $[0,t_2,\cdots,t_{N-2},t]$,

$$\int_0^t d\boldsymbol{w}(\alpha,s) = \lim_{N\to\infty}\sum_{k=1}^{N}(\boldsymbol{w}(\alpha,t_{k+1}) - \boldsymbol{w}(\alpha,t_k)) \tag{2.15}$$

in the mean-squared convergence sense.

Definition 2.2.4 (Mild solution) *A mild solution (see [7, Sec. 3.1]) to a system $\boldsymbol{x}_t : [0,T]\times\Omega \to L^2[0,1]$ satisfying*

$$d\boldsymbol{x}_t = (\mathbb{A}_t\boldsymbol{x}_t + \mathbb{B}_t\boldsymbol{u}_t)dt + d\boldsymbol{w}_t,\ \boldsymbol{x}_0 \in L^2[0,1] \tag{2.16}$$

on $[0,T]$ *is given by*

$$\boldsymbol{x}_t = \Phi(t,0)\boldsymbol{x}_0 + \int_0^t \Phi(t,s)\mathbb{B}_t\boldsymbol{u}_t ds + \int_0^t \Phi(t,s)d\boldsymbol{w}_s. \tag{2.17}$$

In the development of this theory, $\mathbb{A}$ and $\mathbb{B}$ will be taken to be bounded, time-invariant operators. When $\mathbb{A}_t$ is constant, then $\Phi(t,s) = e^{\mathbb{A}(t-s)}$.

2.2.5 Networks

Consider a network-averaged control system of the form (2.2),

$$dx_t = ((A^N x_t + B^N u_t) + \alpha_N x_t + \beta_N u_t)dt + dW^N(t). \tag{2.18}$$

The finite-dimensional system is mapped to piecewise constant functions on the unit square (see [3]). Define the uniform partition on the unit interval as $P^N = \{P_1, \cdots, P_N\}$, where $P_1 = [0, \frac{1}{N}]$ and $P_i = (\frac{i-1}{N}, \frac{i}{N}]$. Then, the following step function graphon for N nodes corresponding to A^N is defined for all $\alpha, \beta \in [0,1]$:

$$\boldsymbol{A}^{[N]}(\alpha,\beta) = \sum_{i=1}^N \sum_{j=1}^N A_{ij}^N \mathbb{1}_{P_i}(\alpha)\mathbb{1}_{P_j}(\beta). \tag{2.19}$$

A similar function can be defined for $\boldsymbol{B}^{[N]}(\cdot,\cdot)$. One can define the step function control $\boldsymbol{u}_t^{[N]} : [0,1] \times [0,T] \to \mathcal{R}$ for such a graphon system using the control u_t,

$$\boldsymbol{u}_t^{[N]}(\alpha) = \sum_{i=1}^N \mathbb{1}_{P_i}(\alpha)u_t(i) \quad \alpha \in [0,1]. \tag{2.20}$$

Finally, define the covariance of the disturbance as a piecewise constant function analogously to the finite-dimensional adjacency matrix. Let $\boldsymbol{w}^{[N]} : [0,1] \times [0,1] \to \mathcal{R}$ be a Q-noise with covariance defined by the following equation,

$$\mathbf{Q}^{[N]}(\alpha,\beta)=\sum_{i=1}^{N}\sum_{j=1}^{N}Q_{ij}^{N}\mathbb{1}_{P_i}(\alpha)\mathbb{1}_{P_j}(\beta). \tag{2.21}$$

A piecewise constant partition section of the unit interval $\{\mathbb{S}_k^N\}_{k=1}^N$ mapping $[0,1]\to\mathcal{R}$ is defined via

$$\mathbb{S}_k^N(\alpha):=\mathbb{1}_{P_k}(\alpha),\ \alpha\in[0,1]. \tag{2.22}$$

This defines an orthogonal set corresponding to the standard $\mathcal{R}^N$ basis $\{e_1,e_2,...,e_N\}$.

Then the corresponding systems in $L^2[0,1]$ can be expressed as

$$d\boldsymbol{x}_t^{[N]}=((\boldsymbol{A}^{[N]}+\alpha_N\mathbb{I})\boldsymbol{x}_t^N+(\boldsymbol{B}^{[N]}+\beta_N\mathbb{I})\boldsymbol{u}_t^{[N]})dt+d\boldsymbol{w}_t^{[N]}, \tag{2.23}$$

where

$$\boldsymbol{w}_t^N(\alpha):=\sum_{k=1}^{N}\mathbb{S}_k^N(\alpha)\sum_{r=1}^{\infty}c_{k,r}^N W_r(t), \tag{2.24}$$

in which $\{W_r\}_{r=1}^\infty$ is a sequence of independent Brownian motions, and denote the $L^2[0,1]$ limit by

$$\boldsymbol{w}_t^\infty(\alpha):=\lim_{N\to\infty}\boldsymbol{w}_t^{[N]}(\alpha)=\sum_{r=1}^{\infty}\sqrt{\lambda_r}\phi_r(\alpha)W_r(t). \tag{2.25}$$

By Mercer's Theorem (see, e.g. [36]), $\mathbf{Q}$ has the eigenvalue and basis representation:

$$\mathbf{Q}(\alpha,\beta)t=\sum_{r=1}^{\infty}\sqrt{\lambda_r}\phi_r(\alpha)\phi_r(\beta)=\mathbb{E}[\boldsymbol{w}_t^\infty(\alpha)\boldsymbol{w}_t^\infty(\beta)]. \tag{2.26}$$

To ensure the existence of this limit, we explicitly require the processes constructed in (2.24) to be Cauchy in the $L^2[0,1]$ norm, i.e., for all $\epsilon>0$, there exists $M>N>N_0(\epsilon)$ such that

$$\begin{aligned}&\mathbb{E}[||\boldsymbol{w}_t^{[N]}-\boldsymbol{w}^{[M]}||_2^2] \\ &\leq\sum_{r=1}^{\infty}\int_0^1\left(\sum_{j=1}^{M}\mathbb{S}_j^M(\alpha)c_{j,r}^M-\sum_{k=1}^{N}\mathbb{S}_k^N(\alpha)c_{k,r}^N\right)^2 d\alpha<\epsilon.\end{aligned} \tag{2.27}$$

Finally, we observe that as a result of the specifications above, the state process $\boldsymbol{x}_t^{[N]}$ on partition P_i has a one-to-one correspondence with the state of the ith node of x_t^N given by

$$[x_t^N]_i := \boldsymbol{x}_t^{[N]}(\alpha) \text{ for } \alpha \in P_i,\ 1 \leq i \leq N. \tag{2.28}$$

2.2.5.1 Common Graphons

There are a few common graphons that will be further investigated in Sec. 2.5. In this subsection, a small set of common graphons and their associated dynamical systems properties are further investigated. In this thesis, these are primarily used to generate random graphs using the W-random graph method [1]. Jackson [37] also provides a good overview of random graph generation in the context of social and economic networks.

Erdős-Renyi graphs are one of the most common methods of generating random graphs. In an ER graph for every two vertices i and j in a graph of size N, an (undirected) edge $e_{i,j}$ exists with probability p. That is,

$$\mathbb{P}(A_{i,j}^N = 1) = p, \quad 1 \leq i, j \leq N. \tag{2.29}$$

From this, it is clear that the graphon limit of an ER graph is simply the constant function $\boldsymbol{W}(\alpha, \beta) = p,\ \alpha, \beta \in [0, 1]$.

Uniform Attachment Graphs [1] are a more sophisticated increasing random graph model which possesses a smooth graphon limit. It is constructed inductively. Start with a single-node graph G^1 (with associated adjacency matrix $A^1 = 0$). Then, given a UAG G^{N-1}, add a node and connect each pair of non-adjacent nodes with probability $\frac{1}{N}$ to create G^N. This has the graphon limit:

$$\boldsymbol{W}(\alpha, \beta) = 1 - \max(\alpha, \beta), \quad \alpha, \beta \in [0, 1]. \tag{2.30}$$

Small World Graphs [38] model networks with a high level of local clustering, a low level of

global clustering, and a low graph diameter, which demonstrates degree behavior sometimes observed in graphs such as the Internet. Medvedev [2] presents one potential model of such graphs called a W-small world graphon. Here, we propose a limit model of small world graphs where the node connection probability is given by the sum of two truncated Gaussian functions of variance σ^2 on each horizontal in the unit square (2.31), these are shifted by an offset γ so that the resulting surface (2.32) is symmetrically distributed with respect to the diagonal; it is normalized to have a maximum value of one on the diagonal,

$$\boldsymbol{G}_{SW}(\alpha,\beta) = \exp\left(-\frac{1}{2}\left(\frac{\alpha-\beta}{\sigma}\right)^2\right), \quad \alpha,\beta \in [0,1], \tag{2.31}$$

$$\boldsymbol{W}_{\mathrm{SW}}(\alpha,\beta) = 0.5\boldsymbol{G}_{SW}(\alpha-\gamma,\beta) + 0.5\boldsymbol{G}_{SW}(\alpha,\beta-\gamma). \tag{2.32}$$

Identifying 0 with the 0-degree position on a circle, 1 with the π location and invoking symmetry shows this graphon shares some of the required SW network properties listed above.

Low rank graphons are a special class of graphons which possess a finite number of eigenfunctions. These are explored further in Sec. 2.4.

The convergence of the finite-order network system to the infinite limit graphon system can now be analyzed.

Theorem 2.2.3 *Let $\boldsymbol{x}_t^{[N]}$ solve the following graphon stochastic differential equation,*

$$d\boldsymbol{x}_t^{[N]} = \mathbb{A}^{[N]}\boldsymbol{x}_t^{[N]}dt + d\boldsymbol{w}_t^{[N]}, \quad \boldsymbol{x}_0^{[N]} \in L^2[0,1], \tag{2.33}$$

where $\mathbf{Q}^{[N]}$ is the covariance operator of $\boldsymbol{w}^{[N]}$. Let $\Phi^{[N]}(t,s)$ and $\Phi^{[M]}(t,s)$ refer to the semigroup solutions to the state systems $\boldsymbol{x}_t^{[N]}$ and $\boldsymbol{x}_t^{[M]}$ respectively. Assume for each triple $\epsilon_0,\epsilon_1,\epsilon_2 > 0$ there exists N_0 such that for all $N > M > N_0$,

$$||\boldsymbol{x}_0^{[N]} - \boldsymbol{x}_0^{[M]}||_2^2 < \epsilon_0, \qquad \textit{(A0)} \tag{2.34}$$

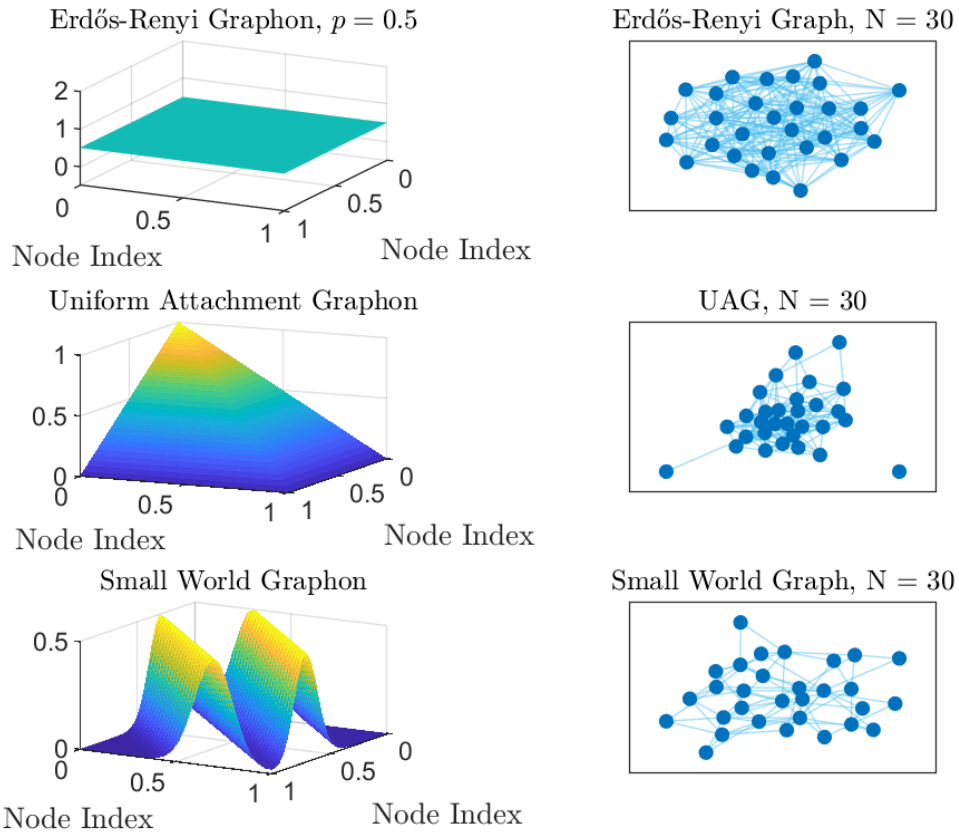

Figure 2.1: Top row: An Erdős-Renyi graphon and sample graph. Middle row: A uniform attachment graphon and graph. Bottom row: A small world graphon.

$$||\Phi^{[N]}(t,s) - \Phi^{[M]}(t,s)||_{op}^2 < \epsilon_1, \qquad \textit{(A1)} \tag{2.35}$$

$$\mathbb{E}[||\boldsymbol{w}_t^{[N]} - \boldsymbol{w}_t^{[M]}||_2^2] < \epsilon_2, \qquad \textit{(A2)} \tag{2.36}$$

and there exist $\alpha, C < \infty$, *such that, for all* N,

$$\sum_{k=1}^{N}\sum_{r=1}^{N} |c_{k,r}^N|^2 \leq C, \qquad \textit{(B0)} \tag{2.37}$$

$$\int_0^s ||\Phi^{[N]}(t,s)||_{op}^2 ds \leq \alpha, \quad t \in [0,T]. \qquad \textit{(B1)} \tag{2.38}$$

Then, for each $\epsilon > 0$, *there exists* N_0' *such that for all* $N, M > N_0'$

$$\mathbb{E}[||\boldsymbol{x}_t^{[N]} - \boldsymbol{x}_t^{[M]}||_2] < \epsilon. \tag{2.39}$$

Hence, there exists an $L^2[0,1]$ *limit process* $\boldsymbol{x}_t^\infty$ *constituting the unique mild solution of (2.14) satisfying* $\mathbb{E}[||\boldsymbol{x}_t^{[N]} - \boldsymbol{x}_t^\infty||_2] \to 0$ *as* N *goes to infinity, that is,*

$$d\boldsymbol{x}_t = \mathbb{A}\boldsymbol{x}_t + d\boldsymbol{w}_t, \ \boldsymbol{x}_0 \in L^2[0,1]. \tag{2.40}$$

□

The proof relies on the convergence of the operator norms of $\Phi^{[N]}(t,s)$ to $\Phi^{[N]}(t,s)$ implying L^2 convergence of $\Phi^{[N]}(t,s)\boldsymbol{v}$ for any $\boldsymbol{v} \in L^2[0,1]$ and is given in Section 2.6.1.

Remark: This result was provided Dunyak and Caines in [9] in the time-invariant operator case. When $\mathbb{A}_t^{[N]} = \mathbb{A}^{[N]}$ and $\mathbb{A}_t^{[M]} = \mathbb{A}^{[M]}$ for all $t \in [0,T]$, assumption (A1) can be relaxed to

$$||\mathbb{A}^{[N]} - \mathbb{A}^{[M]}||_{\text{op}}^2 < \epsilon_1, \tag{2.41}$$

i.e., the piecewise constant graphons corresponding to the finite graphs A^N and A^M converge in the L^2 operator norm.

2.3 Linear Quadratic Control

2.3.1 Finite Time Horizon

Given a linear stochastic dynamical system of type (2.47), a linear quadratic Gaussian optimal control problem with Q-noise is given by the following performance function:

$$\begin{aligned} J(\boldsymbol{u}, \boldsymbol{x}_0) =& \mathbb{E}[\int_0^T (\boldsymbol{x}_t^* \mathbb{M} \boldsymbol{x}_t + \boldsymbol{u}_t^* \mathbb{R} \boldsymbol{u}_t) dt + \boldsymbol{x}_T^* \mathbb{M}_T \boldsymbol{x}_t], \\ & \boldsymbol{x}_t, \boldsymbol{u}_t \in L^2[0,1], \end{aligned} \tag{2.42}$$

where $\mathbb{M} = \boldsymbol{M} + m\mathbb{I}$ and $\mathbb{R} = \mathbf{R} + r\mathbb{I}$ are bounded functionals composed of a non-negative compact operator $\boldsymbol{M} \geq 0$ and $\mathbf{R} > 0$, with $m \geq 0$ and $r > 0$ respectively. A control input $\boldsymbol{u}_t$ is admissible when it is adapted to the sigma algebra generated by $\boldsymbol{w}_t$ and where $\int_0^T |\boldsymbol{u}_t|^2 dt < \infty$. Problems of this variety will henceforth be referred to as Q-LQG problems, and denoted by their system parameters $\{\mathbb{A}, \mathbb{B}, \mathbf{Q}, \mathbb{M}, \mathbb{M}_T, \mathbb{R}\}$.

Theorem 2.3.1 ([13]) *Suppose that $\mathbb{M}, \mathbb{R}, \mathbb{M}_T$ are bounded positive self-adjoint $L^2[0,1]$ operators, and that $\mathbb{R} : L^2[0,1] \to L^2[0,1]$ is invertible. Then, the performance function (2.42) is minimized with $\boldsymbol{u}_t = -\mathbb{R}^{-1}\mathbb{B}^* S_t \boldsymbol{x}_t$, where $S : [0,1] \times [0,1] \times [0,T] \to \mathcal{R}$ is an $L^2[0,1]$ linear operator for all t whose kernel satisfies the following Riccati equation,*

$$\begin{aligned} -\frac{d}{dt}\langle S_t \boldsymbol{v}, \boldsymbol{v} \rangle =& 2\langle \mathbb{A}\boldsymbol{v}, S_t \boldsymbol{v} \rangle - \langle S_t \mathbb{B}\mathbb{R}^{-1}\mathbb{B}^* S_t \boldsymbol{v}, \boldsymbol{v} \rangle, + \langle \mathbb{M}\boldsymbol{v}, \boldsymbol{v} \rangle, \qquad \forall \boldsymbol{v} \in L^2[0,1] \\ S_T =& \mathbb{M}_T. \end{aligned} \tag{2.43}$$

Proof: See [13, Sec. 4] with $F = \mathbb{I},\ D = 0,\ C = 0$ (hence $\Gamma(\cdot) = 0$ and $\Delta(S_t) = 0$). □

Corollary 2.3.1.1 ([13]) *Given a Q-LQG problem with parameters $\{\mathbb{A}, \mathbb{B}, \mathbf{Q}, \mathbb{M}, \mathbb{M}_T, \mathbb{R}\}$ where S_t is the self-adjoint $L^2[0,1]$ operator solving (2.43), S_t is unique in the space of $L^2[0,1]$ non-negative operators.*

In addition, the value function is given by

$$V(\boldsymbol{x}_t, t) = \boldsymbol{x}_t^* S_t \boldsymbol{x}_t + \int_t^T trace(S_r \mathbf{Q}) dr. \tag{2.44}$$

□

As expected, the intensity of the Q-noise does not change the optimal control $\boldsymbol{u}_t$, but does impact the value function of the Q-LQG problem. In order to show that the finite-dimensional linear quadratic Gaussian problem on a network converges to an infinite-dimensional Q-LQG problem in the sense of converging value functions, state, and control functions, it must first be shown that the solution $S_t^{[N]}$ of the piece-wise constant Q-LQG problem is bounded in operator norm uniformly in $N \in \mathcal{Z}$.

Lemma 2.3.2 (Dunyak and Caines, [35]) *Let A^N and B^N be bounded self-adjoint $L^2[0,1]$ operators, M^N and M_T^N be bounded positive $L^2[0,1]$ operators, and R^N be a bounded strictly positive $L^2[0,1]$ operator converging to A, B, M, M_T, and R respectively in the operator norm sense for $\{A^N, B^N, M^N, M_T^N, R^N\}$. Let S_t^N be a positive, self-adjoint L^2 operator satisfying*

$$\begin{aligned} -\dot{S}_t^N &= A^N S_t^N + S_t^N A^N - S_t^N B^N R^{-1} B^N S_t^N + M^N \\ S_T^N &= M_T^N. \end{aligned} \tag{2.45}$$

Then, there exists $0 < c_N < \infty$ such that

$$||S_t^N||_{op} \leq 2||M_T||_{op} + (T-t)c_N. \tag{2.46}$$

Proof: See Section 2.6.2.

From Theorem 3.1, the minimizing controls to the limit Q-LQG problem and the piece-

wise constant Q-LQG problem are respectively

$$\boldsymbol{u}_t = -\mathbb{R}^{-1}\mathbb{B}^* S_t \boldsymbol{x}_t$$

and

$$\boldsymbol{u}_t^{[N]} = -(\mathbb{R}^{[N]})^{-1}\mathbb{B}^{[N]*} S_t^{[N]} \boldsymbol{x}_t^{[N]}$$

.

Theorem 2.3.3 (Q-LQG Convergence, Dunyak and Caines [35]) *Let $\boldsymbol{x}_t$ be a system of the form*

$$d\boldsymbol{x}_t = (\mathbb{A}\boldsymbol{x}_t + \mathbb{B}\boldsymbol{u}_t)dt + d\boldsymbol{w}_t, \tag{2.47}$$

and let $\boldsymbol{x}_t^{[N]}$ be a system of the form

$$d\boldsymbol{x}_t^{[N]} = (\mathbb{A}^{[N]}\boldsymbol{x}_t^{[N]} + \mathbb{B}^{[N]}\boldsymbol{u}_t^{[N]})dt + d\boldsymbol{w}_t^{[N]}, \tag{2.48}$$

where $\mathbb{A}^{[N]} \to \mathbb{A}$, $\mathbb{B}^{[N]} \to \mathbb{B}$, and $\mathbf{Q}^{[N]} \to \mathbf{Q}$ in the L^2 operator norm sense, and let assumptions (A0)-(A2), (B0), and (B1) of Theorem 2.2.3 be satisfied. In addition, let $\mathbb{R}^{[N]}$, $\mathbb{M}^{[N]}$, and $\mathbb{M}_T^{[N]}$ be bounded, positive, self-adjoint operators converging to $\mathbb{R}$, $\mathbb{M}$, and $\mathbb{M}_T$ in the operator norm sense.

Let S_t and S_t^N be the positive, bounded self-adjoint operators solving the functional Riccati equation (2.43) for $(\mathbb{A}, \mathbb{B}, \mathbb{R}, \mathbb{M}, \mathbb{M}_T)$ and $(\mathbb{A}^{[N]}, \mathbb{B}^{[N]}, \mathbb{R}^{[N]}, \mathbb{M}^{[N]}, \mathbb{M}_T^{[N]})$ respectively. Then, for every $\epsilon > 0$, there exists an $N(\epsilon)$ such that for all $N > N(\epsilon)$,

$$\mathbb{E}[||\boldsymbol{x}_t^{[N]} - \boldsymbol{x}_t||_2] < \epsilon. \tag{2.49}$$

Proof: See Section 2.6.3.

As the control input and state trajectory converge in the L^2 sense for all time, the

optimally controlled finite-dimensional network performance function value

$$\inf_{u_t^N} \mathbb{E}\left[\int_0^T (x_t^N)^* M^N x_t^N + (u_t^N)^* R^N u_t^N dt\right] \tag{2.50}$$

converges to the value of the infinite-dimensional graphon system value

$$\begin{aligned} &\inf_{\boldsymbol{u}} \mathbb{E}[\int_0^T (\boldsymbol{x}_t^* \mathbb{M} \boldsymbol{x}_t + \boldsymbol{u}_t^* \mathbb{R} \boldsymbol{u}_t) dt + \boldsymbol{x}_T^* \mathbb{M}_T \boldsymbol{x}_t], \\ &\boldsymbol{x}_0, \boldsymbol{u}_t \in L^2[0,1]. \end{aligned} \tag{2.51}$$

2.3.2 Long-Range Average

In contrast to deterministic systems, the infinite time horizon optimal control problem does not have a finite value. Hence, we consider the long-range average Q-LQG problem given by:

$$\begin{aligned} V_\infty(\boldsymbol{x}_0) :=& \inf_{\boldsymbol{u}} \lim_{T\to\infty} J_T(\boldsymbol{u}, \boldsymbol{x}_0) \\ =& \inf_{\boldsymbol{u}} \lim_{T\to\infty} \frac{1}{T} \mathbb{E}[\int_0^T (\boldsymbol{x}_t^* \mathbb{M} \boldsymbol{x}_t + \boldsymbol{u}_t^* \mathbb{R} \boldsymbol{u}_t) dt], \\ =& \lim_{T\to\infty} \frac{1}{T} (\boldsymbol{x}_0^* S_0 \boldsymbol{x}_0 + \int_0^T \operatorname{trace}(S_r \mathbf{Q}) dr). \end{aligned} \tag{2.52}$$

The solution to the long-range average Q-LQG problem is given via the unique positive solution S_∞ to the algebraic Riccati equation [8]:

$$\begin{aligned} 0 =& 2\langle \mathbb{A}\boldsymbol{v}, S_\infty \boldsymbol{v}\rangle - \langle S_\infty \mathbb{B}\mathbb{R}^{-1}\mathbb{B}^* S_\infty \boldsymbol{v}, \boldsymbol{v}\rangle \\ &+ \langle \mathbb{M}\boldsymbol{v}, \boldsymbol{v}\rangle, \quad \forall \boldsymbol{v} \in L^2[0,1]. \end{aligned} \tag{2.53}$$

The solution S_t to equation (2.43) converges to S_∞ exponentially, yielding

$$V_\infty(\boldsymbol{x}_0) = V_\infty := \operatorname{trace}(S_\infty \mathbf{Q}) \ \ \forall \boldsymbol{x}_0 \in L^2[0,1]. \tag{2.54}$$

In particular, below we show that when $\mathbb{B} = \mathbb{R} = \mathbb{I}$, and $\mathbb{A}$ is symmetric, this can be solved with

$$S_\infty = \mathbb{A} + (\mathbb{A}^2 + \mathbb{M})^{\frac{1}{2}}, \tag{2.55}$$

where, for a positive operator M, $(M)^{\frac{1}{2}}$ is the positive operator solving $(M)^{\frac{1}{2}*}(M)^{\frac{1}{2}} = M$.

Note that the rate of loss is given by $\text{trace}(S_\infty \mathbf{Q})$ which is the Hilbert-Schmidt inner product. Given an orthornormal basis of $L^2[0,1]$, $\{\phi_k\}_k^\infty$:

$$\text{trace}(S_\infty \mathbf{Q}) = \sum_k \langle S_\infty \phi_k, \mathbf{Q}\phi_k \rangle. \tag{2.56}$$

Restricting ourselves to the case where $\mathbb{M} = \mathbb{I}$, $||\mathbf{Q}||_{\text{HS}} = 1$ and $||\boldsymbol{A}||_{\text{HS}} = 1$, this is maximized for the eigenfunction corresponding to the largest eigenvalue of $\boldsymbol{A}$.

Lemma 2.3.4 (Maximum Trace Lemma) *Let $\mathbb{M} = \mathbb{I}$, and let $\{\phi_k\}_{k=0}^\infty$ be the set of orthonormal eigenvectors of $\boldsymbol{A}$ with eigenvalues $\{\lambda_k\}_{k=0}^\infty$. Let $\overline{\lambda} = \sup_k \lambda_k$ and $\underline{\lambda} = \inf_k \lambda_k$ with associated eigenfunctions $\overline{\phi}$ and $\underline{\phi}$ respectively if $\overline{\lambda}$ and $\underline{\lambda}$ are obtained for a finite k. Then, for systems driven by of the form $\mathbb{A} = \boldsymbol{A} + a\mathbb{I}$,*

$$\sup_{||\mathbf{Q}||_{HS}=1} \text{trace}(S_\infty \mathbf{Q}) = \sup_{||\mathbf{Q}||_{HS}=1} \sum_k \langle S_\infty \phi_k, \mathbf{Q}\phi_k \rangle \tag{2.57}$$

$$= (\overline{\lambda} + a) + \sqrt{(\overline{\lambda} + a)^2 + 1}. \tag{2.58}$$

and attains the supremum for $\mathbf{Q} = \langle \cdot, \overline{\phi} \rangle$ when $\overline{\lambda}$ is obtained for a finite k, and respectively obtains the infimum for $\mathbf{Q} = \langle \cdot, \underline{\phi} \rangle$ when $\underline{\phi}$ is attained for finite k.

Proof: Note that the operator $(\mathbb{A}^2 + \mathbb{I})$ can be expressed as

$$\mathbb{A}^2 + \mathbb{I} = \boldsymbol{A}^2 + 2a\boldsymbol{A} + (a^2 + 1)\mathbb{I} \tag{2.59}$$

$$= \sum_{k=1}^\infty \lambda_k^2 \langle \cdot, \phi_k \rangle \phi_k + 2a\lambda_k \langle \cdot, \phi_k \rangle \phi_k + (a^2 + 1)\langle \cdot, \phi_k \rangle \phi_k$$

$$= \sum_{k=1}^{\infty} (\lambda_k^2 + 2a\lambda_k + a^2 + 1)\langle \cdot, \phi_k \rangle \phi_k$$
$$= \sum_{k=1}^{\infty} ((\lambda_k + a)^2 + 1)\langle \cdot, \phi_k \rangle \phi_k.$$

Taking the positive root of the (necessarily positive) eigenvalues gives us the operator root,

$$(\mathbb{A}^2 + \mathbb{I})^{\frac{1}{2}} = \sum_{k=0}^{\infty} \sqrt{(\lambda_k + a)^2 + 1} \langle \cdot, \phi_k \rangle, \tag{2.60}$$

which then yields

$$S_\infty = \sum_{k=0}^{\infty} \left((\lambda_k + a) + \sqrt{(\lambda_k + a)^2 + 1} \right) \langle \cdot, \phi_k \rangle \phi_k. \tag{2.61}$$

First, suppose that $\overline{\phi}$ is attained for a finite k. Then, setting $\mathbf{Q} = \langle \cdot, \overline{\phi} \rangle$ yields

$$\text{trace}(S_\infty \mathbf{Q}) = (\overline{\lambda} + a) + \sqrt{(\overline{\lambda} + a)^2 + 1}. \tag{2.62}$$

As $\mathbf{Q}$ is constrained by $||\mathbf{Q}||_{\text{HS}} = 1$ and the eigenbasis is orthonormal, assigning any positive value to a different eigenfunction cannot increase this value.

Likewise, if the infimum $\underline{\lambda}$ is attained for finite k, the minimum value is attained for $\mathbf{Q} = \langle \cdot, \underline{\phi} \rangle$ and

$$\text{trace}(S_\infty \mathbf{Q}) = (\underline{\lambda} + a) + \sqrt{(\underline{\lambda} + a)^2 + 1}. \tag{2.63}$$

If the supremum (or infimum, respectively) is not attained for finite k, then the limit $\lambda_{k \to \infty} = 0$ implies that the supremum (respectively infimum) value is

$$\text{trace}(S_\infty \mathbf{Q}) = a + \sqrt{a^2 + 1} \tag{2.64}$$

which can be made arbitrarily close by setting $\mathbf{Q} = \langle \cdot, \phi_k \rangle$ for arbitrarily large k. □

2.3.3 Exponential Discounting

The infinite time horizon problem with exponential discounting is presented below. Unlike the long-term averaging problem, the value function is found by explicitly solving a Hamilton-Jacobi-Bellman equation.

Lemma 2.3.5 (Infinite Horizon Discounting) *Let $\rho > 0$. Then the infinite horizon discounted cost performance functional is given by*

$$J_\rho(\boldsymbol{x}_0, \boldsymbol{u}) = \mathbb{E}[\int_0^\infty e^{-\rho t}(\boldsymbol{x}_t^* \mathbb{M} \boldsymbol{x}_t + \boldsymbol{u}_t^* \mathbb{R} \boldsymbol{u}_t) dt]. \tag{2.65}$$

This is minimized by $\boldsymbol{u}_t = -\mathbb{R}^{-1}\mathbb{B}^* S_\infty$, where S_∞ solves the discounted Algebraic Riccati equation

$$\rho S_\infty = S_\infty \mathbb{A}^* + \mathbb{A} S_\infty - S_\infty \mathbb{B}\mathbb{R}^{-1}\mathbb{B}^* S_\infty + \mathbb{M}. \tag{2.66}$$

When $\mathbb{B} = \mathbb{R} = \mathbb{I}$ and $\mathbb{A}$ is symmetric, the unique positive symmetric solution is given by

$$S_\infty^\rho = (\mathbb{A} - \frac{\rho}{2}\mathbb{I}) + ((\mathbb{A} - \frac{\rho}{2}\mathbb{I})^2 + \mathbb{M})^{\frac{1}{2}}. \tag{2.67}$$

Proof: For the existence and uniqueness of the solution, refer to [8, Section 2.6.1.3]. For a function $V : L^2[0,1] \to \mathcal{R}^1$, let DV be the Frechet derivative of V. Define the value function $V_\rho : L^2[0,1] \to \mathcal{R}^1$

$$V_\rho(\boldsymbol{x}) = \langle \boldsymbol{x}, S_\infty^\rho \boldsymbol{x} \rangle + \frac{1}{\rho}\text{trace}(\mathbf{Q} S_\infty^\rho), \quad \boldsymbol{x} \in L^2[0,1] \tag{2.68}$$

be a classical solution of the Hamilton-Jacobi-Bellman equation of an infinite horizon discounted cost performance problem, satisfying

$$\rho V_\rho - \frac{1}{2}\text{trace}(\mathbf{Q} D^2 V_\rho) - \langle \mathbb{A}\boldsymbol{x}, DV_\rho \rangle \tag{2.69}$$

$$-\inf_{\boldsymbol{u}}\{\langle \mathbb{B}\boldsymbol{u}, DV_\rho\rangle + \langle \boldsymbol{x}, \mathbb{M}\boldsymbol{x}\rangle + \langle \boldsymbol{u}, \mathbb{R}\boldsymbol{u}\rangle\} = 0.$$

After evaluating the Frechet derivatives $DV_\rho = 2S_\infty^\rho \boldsymbol{x}$ and $D^2V_\rho = 2S_\infty^\rho$, this is equivalent to

$$\begin{aligned}\rho(\langle \boldsymbol{x}, S_\infty^\rho \boldsymbol{x}\rangle + \frac{1}{\rho}\text{trace}(\mathbf{Q}S_\infty^\rho)) \\ - \text{trace}(\mathbf{Q}S_\infty^\rho) - 2\langle \mathbb{A}\boldsymbol{x}, S_\infty^\rho \boldsymbol{x}\rangle \\ - \inf_{\boldsymbol{u}}\{2\langle \mathbb{B}\boldsymbol{u}, S_\infty^\rho \boldsymbol{x}\rangle + \langle \boldsymbol{x}, \mathbb{M}\boldsymbol{x}\rangle + \langle \boldsymbol{u}, \mathbb{R}\boldsymbol{u}\rangle\} = 0.\end{aligned} \tag{2.70}$$

Noting that the infimization holds for $\boldsymbol{u} = -\mathbb{R}\mathbb{B}^* S_\infty^\rho \boldsymbol{x}$, this is equivalent to

$$\begin{aligned}\langle \boldsymbol{x}, \rho S_\infty^\rho \boldsymbol{x}\rangle =& 2\langle \mathbb{A}\boldsymbol{x}, S_\infty^\rho \boldsymbol{x}\rangle - \langle \mathbb{B}\mathbb{R}^{-1}\mathbb{B}S_\infty^\rho \boldsymbol{x}, S_\infty^\rho \boldsymbol{x}\rangle, \\ &+ \langle \boldsymbol{x}, \mathbb{M}\boldsymbol{x}\rangle, \quad \forall \boldsymbol{x} \in L^2[0,1]\end{aligned} \tag{2.71}$$

and the result follows. □

Remark: In the special case of $\mathbb{B} = \mathbb{R} = \mathbb{M} = \mathbb{I}$, the optimal discounted performance control decreases the control input along all the directions of all eigenfunctions. This results in a weaker control input for all actuators compared to the long-range averaging solution.

To illustrate Lemma 2.3.4 and Lemma 2.3.5, a selection of worst-case scenarios are presented in Table 1, comparing the S_∞ value to the S_t value at $T = 1$ (with the local forcing term $a = 0$). In each example, the underlying graphon $\boldsymbol{A}$ has only non-negative eigenvalues, and the best case scenario has the same cost (namely, $\text{trace}(S_\infty \mathbf{Q}) = 1$). Notably, the Erdos-Renyi Graphon $\boldsymbol{A}(\alpha, \beta) = 0.5$ and $\boldsymbol{A}(\alpha, \beta) = \cos(2\pi(\alpha - \beta))$ have the same worst case value, due to the fact that they have the same maximum eigenvalue.

When the relevant operators are infinite-dimensional, the system cannot be fully simulated. However, when the operators are finite-dimensional, the system can be fully analyzed as an N-dimensional system.

Graphon	Max eigenvalue of $\boldsymbol{A}$	$\|\|S_\infty \mathbf{Q}\|\|^2_{\text{H.S.}}$	$\|\|S^\rho_\infty \mathbf{Q}\|\|^2_{\text{H.S.}}$, $\rho = 1$
$\boldsymbol{A}(x,y) = (x^2-1)(y^2-1)$	0.533	1.666	1.034
$\boldsymbol{A}(x,y) = 0.5$ (Erdos-Renyi)	0.5	1.618	1.000
$\boldsymbol{A}(x,y) = \cos(2\pi(x-y))$	0.5	1.618	1.000
$\boldsymbol{A}(x,y) = 1 - \max(x,y)$ (UAG)	0.405	1.484	0.910
S.W. ($\sigma = 0.1, \gamma = 0.3$)	0.183	1.200	0.783

Table 2.1: A comparison of the worst case performance of various graphons with Hilbert-Schmidt norm bounded noise covariance $\mathbf{Q}$. Calculating the H.S. norm $(\text{trace}(S_\infty \mathbf{Q}))^2$ agrees with the maximum value calculated by Eq. (2.58). As expected, the discounting problem with discount factor $\gamma = 1$ has a lower expected cost than the long-time averaging problem.

2.4 Low Rank Graphons

Here, the theory described in [4] is extended to Q-noise systems. The initial extension for uncontrolled systems was shown by Dunyak and Caines in [39]. Define an invariant subspace of a linear operator $\mathbb{T}$ by $\mathcal{S} \subset L^2[0,1]$ to be a subspace of $L^2[0,1]$ such that, for all $\boldsymbol{x} \in \mathcal{S}$,

$$\boldsymbol{x} \in \mathcal{S} \implies \mathbb{T}\boldsymbol{x} \in \mathcal{S}. \tag{2.72}$$

Denote the orthogonal complement of $\mathcal{S}$ to be the subspace $\mathcal{S}^\perp$, such that for all $\boldsymbol{v} \in \mathcal{S}$ and all $\breve{\boldsymbol{v}} \in \mathcal{S}^\perp$, $\langle \boldsymbol{v}, \breve{\boldsymbol{v}} \rangle = 0$. This partitions $L^2[0,1]$ into the two orthogonal spaces, $\mathcal{S}$ and $\mathcal{S}^\perp$, and hence $L^2[0,1] = \mathcal{S} \oplus \mathcal{S}^\perp$. An operator $\mathbb{T}$ is said to be low rank (with respect to an invariant subspace $\mathcal{S}$) when, for all $\breve{\boldsymbol{v}} \in \mathcal{S}^\perp$, $\mathbb{T}\breve{\boldsymbol{v}} = 0$.

For a given linear Q-noise graphon process as generated by (2.14), with $\mathbb{A} = \boldsymbol{A} + a\mathbb{I}$, $\mathbb{B} = \boldsymbol{B} + b\mathbb{I}$, and a Q-noise $\boldsymbol{w}_t$ with covariance operator $\mathbf{Q}$, make the following Low Rank Graphon (LRG) assumptions:

- (**LRG1**) $\mathcal{S}$ is spanned by a finite number of orthonormal $L^2[0,1]$ functions denoted $\boldsymbol{f} = (\boldsymbol{f}_1, \ldots \boldsymbol{f}_N)$.
- (**LRG2**) The operators $\boldsymbol{A}$ and $\boldsymbol{B}$ are finite rank self-adjoint graphon operators which share the non-trivial invariant subspace $\mathcal{S}$. That is, for all $\breve{\boldsymbol{v}} \in \mathcal{S}^\perp$, $\boldsymbol{A}\breve{\boldsymbol{v}} = 0$ and

$\boldsymbol{B}\breve{\boldsymbol{v}} = 0$.

- **(LRG3)** $\boldsymbol{w}_t$ is finite-dimensional, and has a representation of the form

$$\boldsymbol{w}_t = \sum_{k=1}^{N} \sqrt{\lambda_k} \boldsymbol{f}_k W_t^k. \tag{2.73}$$

  Equivalently, the covariance operator $\mathbf{Q}$ is low rank with respect to $\mathcal{S}$.

By (LRG1), the state process of a linear Q-noise graphon process as generated by (2.14) can be decomposed into two orthogonal components

$$\boldsymbol{x}_t =: \boldsymbol{x}_t^{\boldsymbol{f}} + \breve{\boldsymbol{x}}_t, \quad \boldsymbol{x}^{\boldsymbol{f}} \in \mathcal{S}, \quad \breve{\boldsymbol{x}} \in \mathcal{S}^{\perp} \tag{2.74}$$

where $\boldsymbol{x}_t^{\boldsymbol{f}} = (\boldsymbol{x}_t|\mathcal{S})$ is the orthogonal projection of $\boldsymbol{x}_t$ into $\mathcal{S}$ and $\breve{\boldsymbol{x}}_t = (\boldsymbol{x}_t|\mathcal{S}^{\perp})$ is the orthogonal projection into $\mathcal{S}^{\perp}$. Hence, $\boldsymbol{x}_t^{\boldsymbol{f}}$ consists of a linear combination of elements of $\mathcal{S}$ and $\breve{\boldsymbol{x}}$ consists of a linear combination of elements of $\mathcal{S}^{\perp}$. Similarly, decompose $\boldsymbol{u}_t$ into

$$\boldsymbol{u}_t =: \boldsymbol{u}_t^{\boldsymbol{f}} + \breve{\boldsymbol{u}}_t. \tag{2.75}$$

By the Q-noise axioms, $\boldsymbol{w}_t$ is defined as a sum of weighted Wiener processes, each associated with an eigenbasis of $\mathbf{Q}$. Consequently, $\boldsymbol{w}_t$ can also be decomposed into its orthogonal components with respect to $\mathcal{S}$ and $\mathcal{S}^{\perp}$. This has the general form

$$\boldsymbol{w}_t = \boldsymbol{w}_t^{\boldsymbol{f}} + \breve{\boldsymbol{w}}_t, \tag{2.76}$$

where

$$\begin{aligned} \boldsymbol{w}_t^{\boldsymbol{f}} :=& (\boldsymbol{w}_t|\mathcal{S}) \\ =& \sum_{r=1}^{N} \langle \sum_{k=1}^{\infty} \sqrt{\lambda_k} \phi_k W_t^k, \boldsymbol{f}_r \rangle \boldsymbol{f}_r \end{aligned} \tag{2.77}$$

$$= \sum_{r=1}^{N} \left(\sum_{k=1}^{\infty} \sqrt{\lambda_k} \langle \phi_k, \boldsymbol{f}_r \rangle W_t^k \right) \boldsymbol{f}_r,$$

$$\breve{\boldsymbol{w}}_t := (\boldsymbol{w}_t | \mathcal{S}^{\perp}) = \boldsymbol{w}_t - \boldsymbol{w}_t^{\boldsymbol{f}}. \tag{2.78}$$

By (LRG3), $\boldsymbol{w}_t$ is low rank with respect to the common invariant subspace $\mathcal{S}$ of $\boldsymbol{A}$ and $\boldsymbol{B}$, hence $\boldsymbol{w}_t^{\boldsymbol{f}} = \boldsymbol{w}$, $\breve{\boldsymbol{w}}_t = 0$, and $\breve{\boldsymbol{x}}_t$ is deterministic. Consequently, these processes evolve according to

$$d\boldsymbol{x}_t^{\boldsymbol{f}} = ((\boldsymbol{A} + a\mathbb{I})\boldsymbol{x}_t^{\boldsymbol{f}} + (\boldsymbol{B} + b\mathbb{I})\boldsymbol{u}_t^{\boldsymbol{f}})dt + d\boldsymbol{w}_t, \tag{2.79}$$

$$d\breve{\boldsymbol{x}}_t = (a\breve{\boldsymbol{x}}_t + b\breve{\boldsymbol{u}}_t)dt, \tag{2.80}$$

$$\boldsymbol{x}_0^{\boldsymbol{f}} \in \mathcal{R}^N, \quad \breve{\boldsymbol{x}}_0 \in L^2[0,1]. \tag{2.81}$$

Notably, by the low rank assumptions on $\boldsymbol{A}$ and $\boldsymbol{B}$, the orthogonal process $\breve{\boldsymbol{x}}_t$ is diagonal—each point on the unit interval evolves as a single-dimensional linear differential equation. Because of this decomposition, the system can be modelled as a finite-dimensional system.

2.4.1 Projections onto the Invariant Subspace $\mathcal{S}$

To project the low rank linear Q-noise graphon system to the finite-dimensional invariant subspace $\mathcal{S}$, define the $\mathcal{R}^N$-valued state processes $x_t^{\boldsymbol{f}}$, $u_t^{\boldsymbol{f}}$:

$$x_t^{\boldsymbol{f}} := [\langle \boldsymbol{x}_t^{\boldsymbol{f}}, \boldsymbol{f}_1 \rangle, \langle \boldsymbol{x}_t^{\boldsymbol{f}}, \boldsymbol{f}_2 \rangle, ..., \langle \boldsymbol{f}_N, \boldsymbol{x}_t^{\boldsymbol{f}} \rangle], \tag{2.82}$$

$$u_t^{\boldsymbol{f}} := [\langle \boldsymbol{u}_t^{\boldsymbol{f}}, \boldsymbol{f}_1 \rangle, \langle \boldsymbol{u}_t^{\boldsymbol{f}}, \boldsymbol{f}_2 \rangle, ..., \langle \boldsymbol{f}_N, \boldsymbol{u}_t^{\boldsymbol{f}} \rangle], \tag{2.83}$$

i.e., $x_t^{\boldsymbol{f}}$ and $u_t^{\boldsymbol{f}}$ are projections onto the coordinate space defined by $\boldsymbol{f}$.

Similarly, define the following $N \times N$ matrices

$$A_{ij} := \langle \boldsymbol{A}\boldsymbol{f}_i, \boldsymbol{f}_j \rangle, \quad B_{ij} := \langle \boldsymbol{B}\boldsymbol{f}_i, \boldsymbol{f}_j \rangle, \tag{2.84}$$

$$Q = \mathrm{diag}(\{\lambda_k\}_{k=1}^N), \tag{2.85}$$

and let $W_t^{\boldsymbol{f}}$ be an N dimensional Wiener process with covariance matrix Q. Then the state process $x_t^{\boldsymbol{f}}$ equivalently evolves according to the finite-dimensional differential equation

$$dx_t^{\boldsymbol{f}} = ((A + aI)x_t^{\boldsymbol{f}} + (B + bI)u_t^{\boldsymbol{f}})dt + dW_t^{\boldsymbol{f}}, \tag{2.86}$$

$$x_0^{\boldsymbol{f}} = [\langle \boldsymbol{x}_0^{\boldsymbol{f}}, \boldsymbol{f}_1 \rangle, \langle \boldsymbol{x}_0^{\boldsymbol{f}}, \boldsymbol{f}_2 \rangle, ..., \langle \boldsymbol{f}_N, \boldsymbol{x}_0^{\boldsymbol{f}} \rangle]. \tag{2.87}$$

This construction allows for a low-dimensional analysis of $\boldsymbol{x}_t^{\boldsymbol{f}}$ and $\boldsymbol{u}_t^{\boldsymbol{f}}$, which can then be mapped back into the $L^2[0,1]$ space by associating each element $[u_t^{\boldsymbol{f}}]_k$ with its respective basis function $\boldsymbol{f}_k$,

$$\boldsymbol{u}_t^{\boldsymbol{f}} = \sum_{k=1} [u_t^{\boldsymbol{f}}]_k \boldsymbol{f}_k =: u_t^{\boldsymbol{f}} \circ \boldsymbol{f}. \tag{2.88}$$

This approach is particularly useful for linear-quadratic problems on low-rank graphon systems.

2.4.2 Low Rank Linear Quadratic Control

Consider a graphon Q-LQG optimal control problem with the operators $\mathbb{A} = \boldsymbol{A} + a\mathbb{I}$ and $\mathbb{B} = \boldsymbol{B} + b\mathbb{I}$, and cost operators $\mathbb{M}$, $\mathbb{M}_T$, and $\mathbf{R}$.

As with the standard Q-LQG problem, the objective function is

$$J(\boldsymbol{u}, \boldsymbol{x}_0) = \mathbb{E}[\int_0^T (\boldsymbol{x}_t^* \mathbb{M} \boldsymbol{x}_t + \boldsymbol{u}_t^* \mathbf{R} \boldsymbol{u}_t)dt + \boldsymbol{x}_T^* \mathbb{M}_T \boldsymbol{x}_T]. \tag{2.89}$$

By taking the orthogonal decomposition of $\boldsymbol{x}_t$ and $\boldsymbol{u}_t$,

$$\begin{aligned} \boldsymbol{x}_t^* \mathbb{M} \boldsymbol{x}_t =& (\boldsymbol{x}_t^{\boldsymbol{f}} + \breve{\boldsymbol{x}}_t)^* \mathbb{M} (\boldsymbol{x}_t^{\boldsymbol{f}} + \breve{\boldsymbol{x}}_t) \\ =& (\boldsymbol{x}_t^{\boldsymbol{f}})^* \mathbb{M} \boldsymbol{x}_t^{\boldsymbol{f}} + (\breve{\boldsymbol{x}}_t)^* \mathbb{M} \breve{\boldsymbol{x}}_t \end{aligned} \tag{2.90}$$

and

$$\boldsymbol{u}_t^* \mathbf{R} \boldsymbol{u}_t = (\boldsymbol{u}_t^{\boldsymbol{f}})^* \mathbf{R} (\boldsymbol{u}_t^{\boldsymbol{f}}) + (\breve{\boldsymbol{u}}_t)^* \mathbf{R} (\breve{\boldsymbol{u}}_t). \tag{2.91}$$

As with the $\boldsymbol{A}$ and $\boldsymbol{B}$ operators, the $N \times N$ real matrices M and R can be defined as

$$M_{ij} := \langle \mathbb{M} \boldsymbol{f}_i, \boldsymbol{f}_j \rangle, \quad R_{ij} := \langle \mathbf{R} \boldsymbol{f}_i, \boldsymbol{f}_j \rangle, \tag{2.92}$$

$$M_{Tij} = \langle \mathbb{M}_T \boldsymbol{f}_i, \boldsymbol{f}_j \rangle. \tag{2.93}$$

Then, the optimal control problem can be decomposed into the following $-N$-dimensional LQG optimal control problem (which can be solved using standard Riccati equation methods) and an $L^2[0,1]$ deterministic orthogonal process,

$$J(\boldsymbol{u}, \boldsymbol{x}_0) = J^{\boldsymbol{f}}(u^{\boldsymbol{f}}, x_0^{\boldsymbol{f}}) + \breve{J}(\breve{\boldsymbol{u}}, \breve{\boldsymbol{x}}_0), \tag{2.94}$$

$$\begin{aligned} J^{\boldsymbol{f}}(u^{\boldsymbol{f}}, x_0^{\boldsymbol{f}}) :=& \mathbb{E}[\int_0^T ((x_t^{\boldsymbol{f}})^* M x_t^{\boldsymbol{f}} + (u_t^{\boldsymbol{f}})^* R u_t^{\boldsymbol{f}}) dt \\ &+ (x_T^{\boldsymbol{f}})^* M_T x_T^{\boldsymbol{f}}], \end{aligned} \tag{2.95}$$

$$dx_t^{\boldsymbol{f}} = ((A + aI) x_t^{\boldsymbol{f}} + (B + bI) u_t^{\boldsymbol{f}}) dt + dC_t^{\boldsymbol{f}}, \tag{2.96}$$

$$x_0^{\boldsymbol{f}} = [\langle \boldsymbol{x}_0^{\boldsymbol{f}}, \boldsymbol{f}_1 \rangle, ..., \langle \boldsymbol{x}_0^{\boldsymbol{f}}, \boldsymbol{f}_N \rangle], \quad x_0^{\boldsymbol{f}} \in \mathcal{R}^N, \tag{2.97}$$

$$\breve{J}(\breve{\boldsymbol{u}}, \breve{\boldsymbol{x}}_0) = \int_0^T (\breve{\boldsymbol{x}}_t^* \mathbb{M} \breve{\boldsymbol{x}}_t + \breve{\boldsymbol{u}}_t^* \mathbf{R} \breve{\boldsymbol{u}}_t) dt + \breve{\boldsymbol{x}}_T^* \mathbb{M}_T \breve{\boldsymbol{x}}_T, \tag{2.98}$$

$$d\breve{\boldsymbol{x}}_t = (a \breve{\boldsymbol{x}}_t + b \breve{\boldsymbol{u}}_t) dt. \tag{2.99}$$

$$\breve{\boldsymbol{x}}_0 \in L^2[0,1] \tag{2.100}$$

Further, when $\mathbb{M}$, $\mathbb{M}_T$, and $\mathbf{R}$ are low rank with respect to $\boldsymbol{f}$ except for a diagonal constant, then the minimizing solution to $\breve{J}(\breve{\boldsymbol{u}}, \breve{\boldsymbol{x}}_0)$ is effectively one-dimensional, as the feedback control is diagonal with identical coefficients for each $\alpha \in [0,1]$.

Theorem 2.4.1 *Define a Q-LQG problem with coefficients* $\{\boldsymbol{A}+a\mathbb{I}, \boldsymbol{B}+b\mathbb{I}, \mathbf{Q}, \boldsymbol{M}+m\mathbb{I}, \boldsymbol{M}_T+$

$m_t\mathbb{I}, \mathbf{R} + r\mathbb{I}\}$ *where all operators are rank* N *with respect to an orthogonal subspace* $\mathcal{S}$*, whose projections onto* $\mathcal{S}$ *are denoted* $\{A, B, Q, M, M_T, R\}$ *respectively. Then, the optimizing control* $\boldsymbol{u}_t^0$ *is given by*

$$\boldsymbol{u}_t^0 := \boldsymbol{u}_t^{\boldsymbol{f}} + \breve{\boldsymbol{u}}_t, \quad \boldsymbol{u}_t^0 \in L^2[0,1], \quad t \in [0,T] \tag{2.101}$$

$$\boldsymbol{u}_t^{\boldsymbol{f}} := \sum_{k=1} [-(R + rI)^{-1}(B + bI)^* P_t x_t^{\boldsymbol{f}}]_k \boldsymbol{f}_k, \tag{2.102}$$

$$\breve{\boldsymbol{u}}_t := -\frac{b^2}{r} p_t \breve{\boldsymbol{x}}_t, \tag{2.103}$$

where P_t *and* p_t *are time-varying operators solving the following* N*-dimensional and one-dimensional Riccati equations respectively,*

$$\begin{aligned} -\dot{P}_t =& (A + aI)^* P_t + P_t(A + aI) \\ & - P_t(B + bI)^*(R + rI)^{-1}(B + bI)P_t \\ & + (M + mI), \end{aligned} \tag{2.104}$$

$$P_T = (M_T + m_T I), \quad P_t \in \mathcal{R}^{N \times N} \tag{2.105}$$

$$\dot{p}_t = 2ap_t - \frac{b^2}{r} p_t^2 + m, \tag{2.106}$$

$$p_T = m_T. \tag{2.107}$$

Proof: This result is analogous to the deterministic finite-dimensional graphon LQR solution shown in [4]. The Riccati equations (2.104-2.105) give the standard N-dimensional and one-dimensional operator solution P_t and p_t respectively. Using the solution P_t, the optimizing controls for the finite-rank subspace LQG problem (with respect to the N-dimensional state vector $x_t^{\boldsymbol{f}}$ is given by

$$u_t^{\boldsymbol{f}} = -(R + rI)^{-1}(B + bI)^* P_t x_t^{\boldsymbol{f}}. \tag{2.108}$$

By associating the kth entry of the control vector with the corresponding basis function $\boldsymbol{f}_k$,

the finite-dimensional controls can be mapped back to the original space.

Similarly, while the orthogonal state complement $\breve{\boldsymbol{x}}_t$ is infinite-dimensional, the feedback gain is one-dimensional due to the diagonal nature of the state process, and the optimal control can be found with by solving the scalar Riccati equations (2.106-2.107).

This gives the optimal controls for $\boldsymbol{u}_t^{\boldsymbol{f}}$ and $\breve{\boldsymbol{u}}_t$, and hence for $\boldsymbol{u}_t^0$. □

2.5 Numerical Examples

For the following numerical examples, the unit interval $[0, 1]$ is partitioned into N segments, and the kth partition segment I_k is denoted as

$$I_1 := [0, \frac{1}{N}], \quad I_k := (\frac{k-1}{N}, \frac{k}{N}]. \tag{2.109}$$

In each example, $N = 50$, and the state of the simulated systems follows the form

$$d\boldsymbol{x}_t^{[N]} = (\mathbb{A}^{[N]}\boldsymbol{x}_t^{[N]} + \mathbb{B}^{[N]}\boldsymbol{u}_t^{[N]})dt + d\boldsymbol{w}_t^{[N]}, \tag{2.110}$$

as in equation (2.23). This discretized system is used as an approximate solution to the infinite-dimensional system.

In the following sections, $\mathbb{A} = \boldsymbol{A} + 0.1\mathbb{I}$ and $\mathbb{B} = 0.1\mathbb{I}$, where $\boldsymbol{A}$ is a symmetric graphon and $\mathbb{I}$ is the identity operator. To simulate the Q-LQG problems, we set a terminal time of $T = 1$ and implemented Euler's method with a time increment of $\Delta t = 0.001$.

There are three key results to be presented: first, the convergence of a linear quadratic Gaussian finite graph system to a graphon system. Next, that a graph system with a low rank graphon limit can be efficiently represented by a low rank decomposition. Finally, we demonstrate that the finite time horizon feedback solution converges to the infinite time horizon solution. In order to compare trajectories, we introduce the root squared distance

of two system trajectories $\boldsymbol{x}_t$ and $\boldsymbol{y}_t$ at time t,

$$rmd(\boldsymbol{x}_t, \boldsymbol{y}_t) = \sqrt{\langle \boldsymbol{x}_t - \boldsymbol{y}_t, \boldsymbol{x}_t - \boldsymbol{y}_t \rangle}. \tag{2.111}$$

2.5.1 Low Rank Finite Graph Convergence

Consider a finite graph generated using the following W-random graph [1] kernel:

$$\boldsymbol{A}(\alpha, \beta) = (\alpha^2 - 1)(\beta^2 - 1), \quad \alpha, \beta \in [0, 1]. \tag{2.112}$$

Clearly, $\boldsymbol{A}$ is a rank one graphon, with a basis function given by

$$\boldsymbol{f}(\alpha) = \frac{(\alpha^2 - 1)}{\sqrt{\int_0^1 (\beta^2 - 1)^2 d\beta}}, \quad \alpha \in [0, 1]. \tag{2.113}$$

For each pair of gridpoints of the partition I, independently sample a Bernoulli random variable to generate an edge between that pair, with edge probability given by

$$\mathcal{P}(e_{ij} = 1) = \boldsymbol{A}(\alpha_i, \alpha_j), \ \alpha_i, \alpha_j \in [0, 1], \ i, j \in \{1, ..., N\}. \tag{2.114}$$

This creates a graph of 50 nodes, shown in Fig. 2.2 along with its adjacency matrix. Despite having a rank-one limit, the finite adjacency matrix $A^{[N]}$ is full rank.

As with Section 2.3.2, to simulate the worst case scenario, the Q-noise disturbance is placed on the basis function $\boldsymbol{f}$,

$$\boldsymbol{w}_t(\alpha) = \boldsymbol{f}(\alpha) W_t, \quad \alpha \in [0, 1]. \tag{2.115}$$

Then, the finite graph LQG problem can be solved with standard methods, and the limit system can be solved with Theorem 2.3.3. The finite graph system trajectory is shown in Fig. 2.3-I, and the low rank system created by projecting $\boldsymbol{A}^{[N]}$ onto the normal basis function $\boldsymbol{f}$

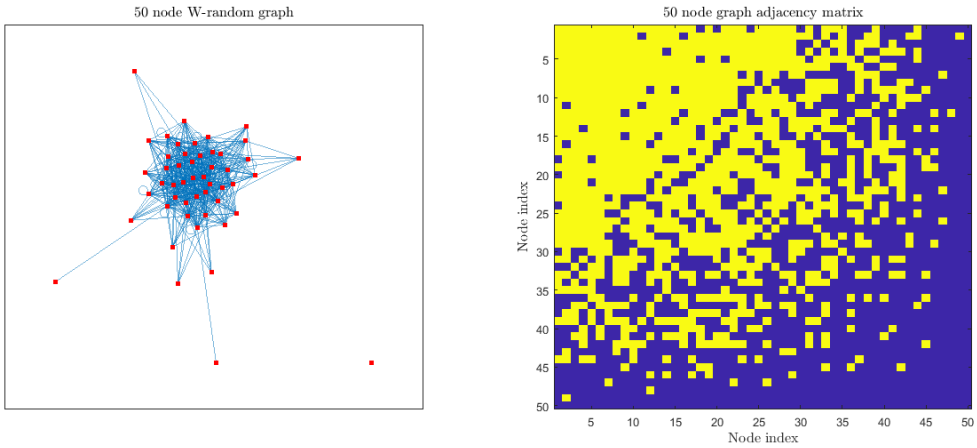

Figure 2.2: Left: a fifty-node W-random graph. Right: the associated adjacency matrix to be used for the numerical examples. Yellow squares represent an edge, blue squares represent a lack of an edge. The adjacency matrix is rank 49, despite the limit system being rank one.

is given by Fig. 2.3-II. This is accomplished by simulating the system

$$dx_t^{\boldsymbol{f}} = \left((\langle \boldsymbol{A}^{[N]}\boldsymbol{f}, \boldsymbol{f}\rangle + 0.1)x_t^{\boldsymbol{f}} + 0.1u_t^{\boldsymbol{f}}\right)dt + dW_t^{\boldsymbol{f}}, \tag{2.116}$$

$$d\breve{\boldsymbol{x}}_t = (0.1\breve{\boldsymbol{x}}_t + 0.1\breve{\boldsymbol{u}}_t)dt, \quad t \in [0,1], \tag{2.117}$$

$$x_0^{\boldsymbol{f}} \in \mathcal{R}^1, \ \breve{\boldsymbol{x}}_0 \in L^2[0,1], \tag{2.118}$$

where $\langle \boldsymbol{A}^{[N]}\boldsymbol{f}, \boldsymbol{f}\rangle + 0.1$ is simply equal to the constant 1.7251. Even though the finite graph's adjacency matrix is full rank, the (piecewise constant) system projected onto the eigenspace spanned by $\boldsymbol{f}$ captures the behavior of the finite graph trajectory.

The limit system generated with $\boldsymbol{A}$ in place of $\boldsymbol{A}^{[N]}$ is shown in Fig. 2.4-I, and the root squared difference over time of the trajectory of the finite graph system and the limit system are shown in Fig. 2.4-II.

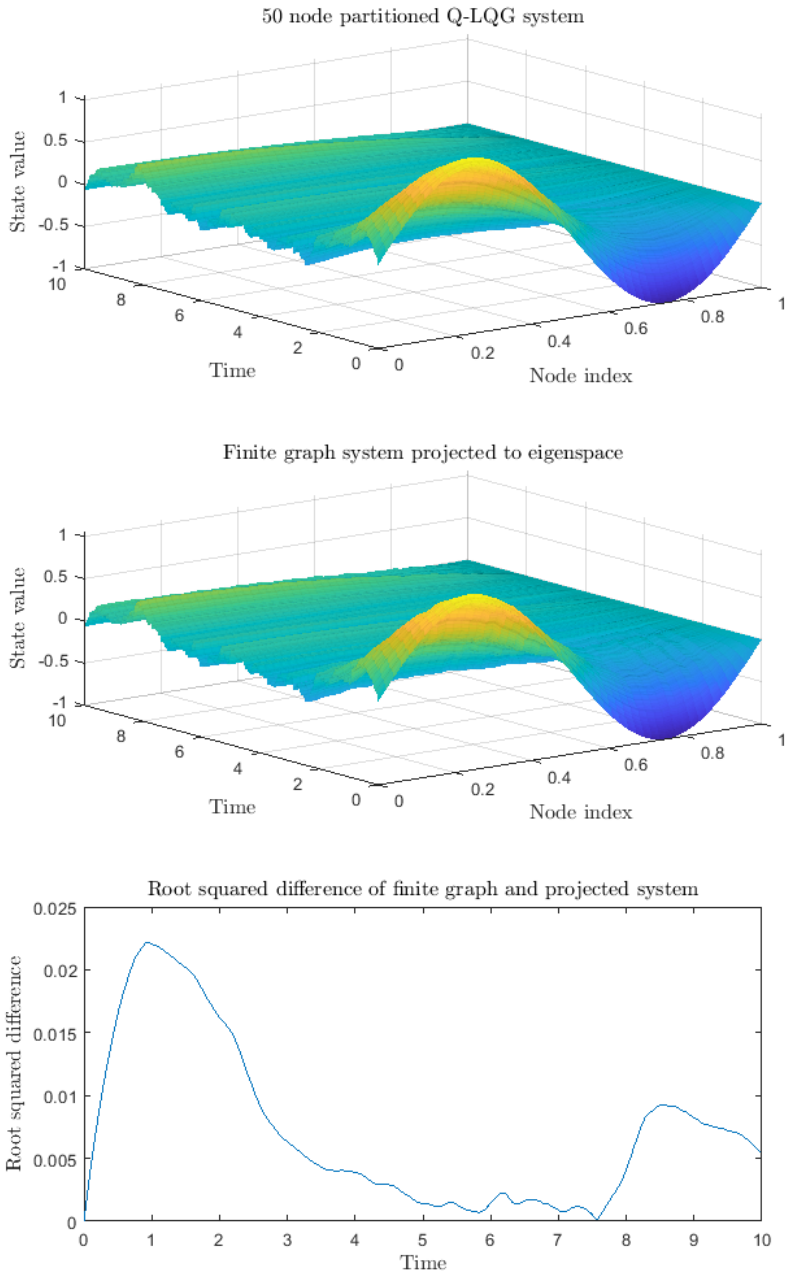

Figure 2.3: I–Top: the system generated with the finite graph using the piecewise constant graphon $\boldsymbol{A}^{[N]}$. II–Middle: The system trajectory generated when $\boldsymbol{A}^{[N]}$ is projected onto the eigenspace spanned by $\boldsymbol{f}$. III–Bottom: the root squared distance of the finite graph system trajectory and the projected graph system trajectory. The root squared distance has a maximum deviation of 0.023, showing that the two trajectory surfaces are very similar. The transient is a result of the spectral difference between the finite graph and the graphon.

2.5.2 Long-Range Average Comparison

This can be found using the analysis of Section 2.3.2. We apply the infinite horizon control found using the algebraic Riccati equation solution (2.55), and the resulting trajectory is shown for a terminal time of $T = 10$ in Fig. 2.5-I. A comparison of the Hilbert-Schmidt norms of both S_t, the time-varying solution to the differential Riccati equation associated with the system and the infinite horizon solution of the algebraic Riccati equation is shown in Fig. 2.5-II. The time varying Riccati solution converges exponentially to the algebraic Riccati solution in the interval $t = [0, 8]$ as t tends to 0, and it diverges from the infinite horizon solution as t approaches the terminal time.

2.6 Proofs

2.6.1 Proof of Theorem 2.2.3

Recall

$$\boldsymbol{x}_t^{[N]} = \Phi^{[N]}(t,0)\boldsymbol{x}_0 + \int_0^t \Phi^{N]}(t,s)d\boldsymbol{w}_s^{[N]}. \tag{2.119}$$

Then,

$$\begin{aligned} &\mathbb{E}[||\boldsymbol{x}_t^{[N]} - \boldsymbol{x}_t^{[M]}||_2] \\ &\leq \mathbb{E}[||\Phi^{[N]}(t,0)\boldsymbol{x}_0^{[N]} - \Phi^{[M]}(t,0)\boldsymbol{x}_0^{[M]}||_2] \\ &\quad + \mathbb{E}[||\int_0^t \Phi^{[N]}(t,s)d\boldsymbol{w}_s^{[N]} - \int_0^t \Phi^{[M]}(t,s)d\boldsymbol{w}_s^{[M]}||_2]. \end{aligned} \tag{2.120}$$

The Cauchy condition is established in two steps. To address the first expectation, $e^{\mathbb{A}^{[N]}t}\boldsymbol{x}^{[M]}$ is added and subtracted inside the norm, which allows assumptions (A0, A1) in conjunction with (B1) to be invoked to bound the term by any $\epsilon_0' > 0$ for sufficiently large N and M.

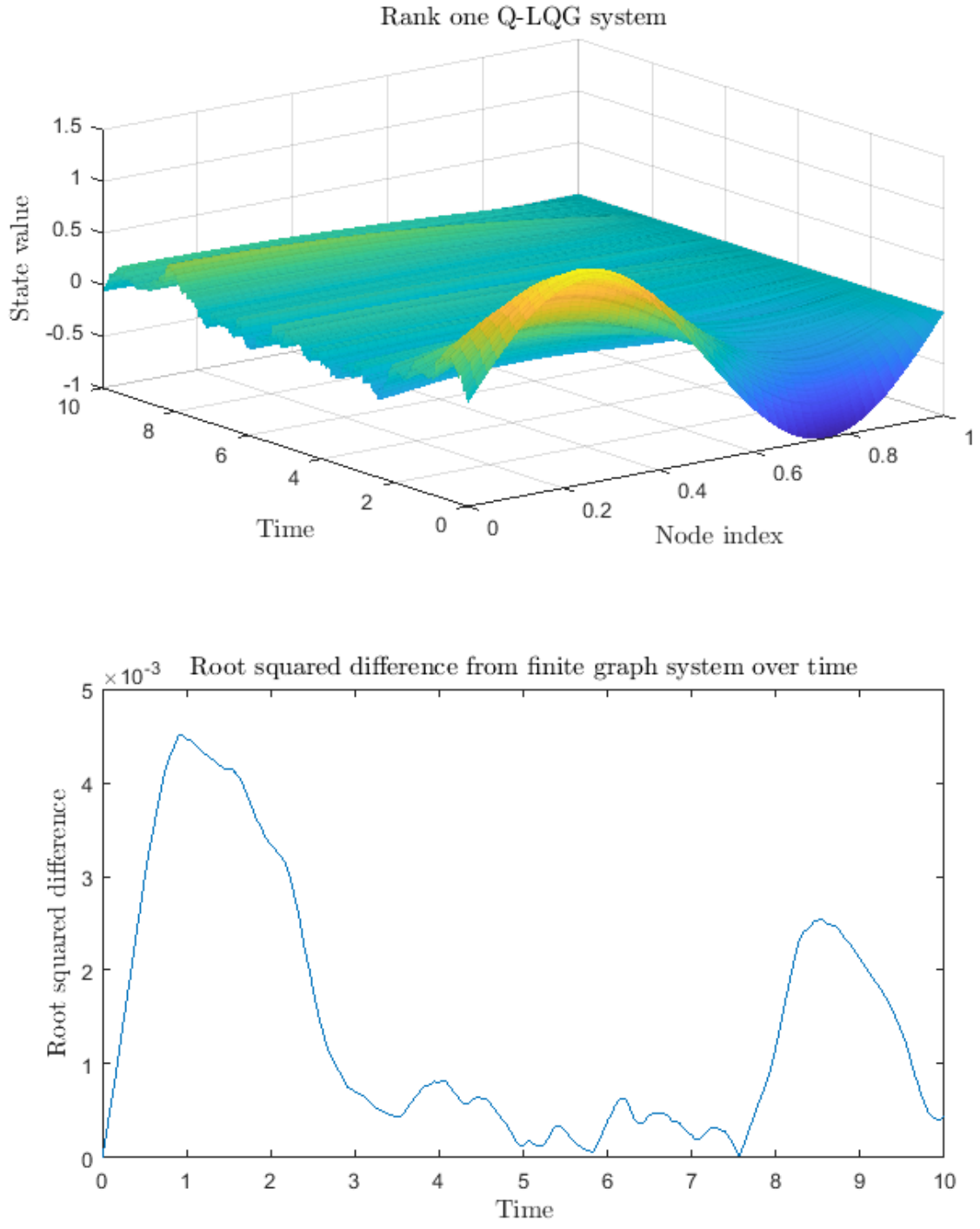

Figure 2.4: Top: the trajectory of the system under the rank one limit control. Bottom: the positive root of the squared distance between the finite graph system and the limit system over time.

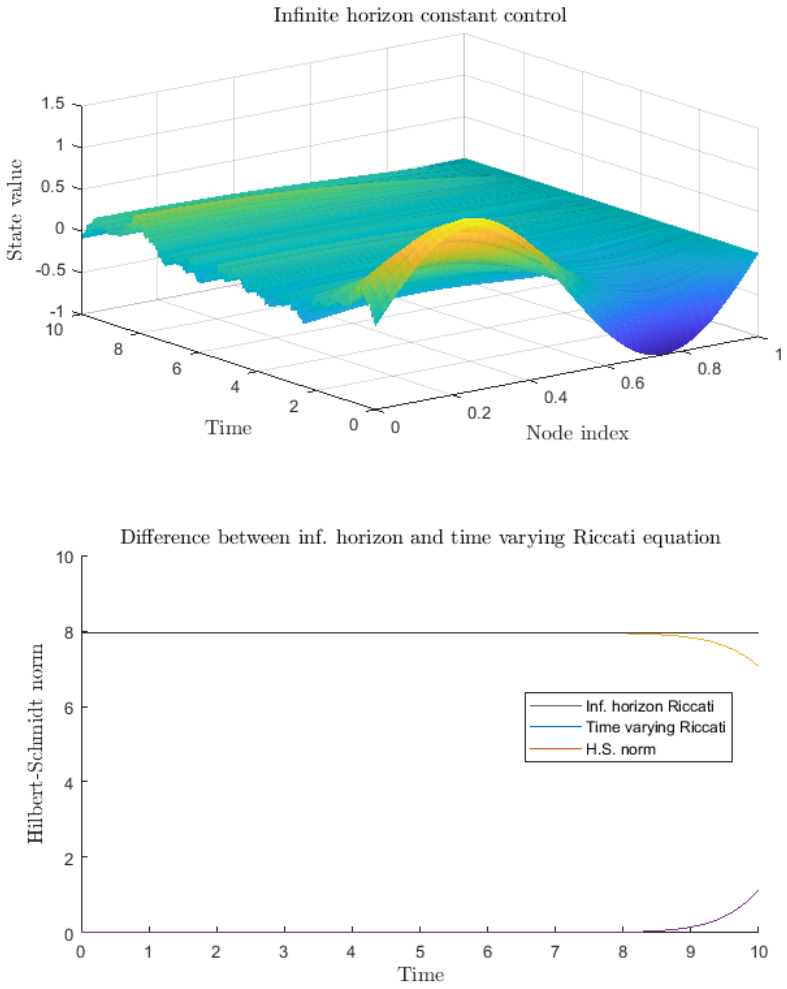

Figure 2.5: I: the trajectory of a system under infinite horizon control. II: The Hilbert-Schmidt norms of the infinite horizon Riccati equation solution and the time-varying Riccati equation solution.

Next, define $\tilde{\boldsymbol{x}}_t^{[N]}$ by:

$$\tilde{\boldsymbol{x}}_t^{[N]} = \int_0^t \Phi^{[N]}(t,s) d\boldsymbol{w}_s^{[N]}. \tag{2.121}$$

Then, the second expectation can be evaluated by using the Ito isometry for one-dimensional adapted processes,

$$\mathbb{E}[|| \int_0^T X_t dw_t ||_2^2] = \mathbb{E}[\int_0^T ||X_t||_2^2 dt]. \tag{2.122}$$

Then, via the same approach of adding and subtracting $\sum_{k=1}^N e^{\mathbb{A}^{[N]}} \mathbb{S}_k^M c_{k,r}^M$, the definition of the operator norm gives

$$\begin{aligned} &\mathbb{E}[|| \int_0^t \Phi^{[N]}(t,s) d\boldsymbol{w}_s^{[N]} - \int_0^t \Phi^{[M]}(t,s) d\boldsymbol{w}_s^{[M]} ||_2^2] \\ &\leq \int_0^t \left(||\Phi^{[N]}(t,s)||_{\text{op}}^2 \cdot \sum_{r=1}^M ||(\sum_{i=1}^N \mathbb{S}_i^N c_{i,r}^N - \sum_{j=1}^M \mathbb{S}_j^M c_{j,r}^M)||_2^2 \right) ds \\ &\quad + \int_0^t \left(||\Phi^{[N]}(t,s) - \Phi^{[M]}(t,s)||_{\text{op}}^2 \cdot \sum_{j=1}^M \sum_{r=1}^M ||\mathbb{S}_j^M c_{j,r}^M||_2^2 \right) ds \\ &\quad + \int_0^t ||\Phi^{[N]}(t,s)||_{\text{op}}^2 ds \sum_{r=M+1}^N \sum_{i=1}^N ||\mathbb{S}_i^N||_2^2 |c_{i,r}^N|^2. \end{aligned} \tag{2.123}$$

Hence, by the Cauchy property assumptions (A1, A2), the boundedness assumption (B0), and noting that for all i, $||\mathbb{S}_i^N||^2 = \frac{1}{N^2}$, and by choosing a smaller ϵ_2 if necessary, we see that for any $\epsilon_1' > 0$, and all sufficiently large N and M,

$$\begin{aligned} &\mathbb{E}[||\tilde{\boldsymbol{x}}_t^{[N]} - \tilde{\boldsymbol{x}}_t^{[M]}||_2^2] \\ &< \left(\int_0^t ||\Phi^{[N]}(t,s)||_{\text{op}}^2 ds \ \epsilon_2 + \epsilon_1 \ \frac{C}{N^2} \right. \\ &\qquad \left. + \int_0^t ||\Phi^{[N]}(t,s)||_{\text{op}}^2 ds \ \frac{C}{N^2} \right) < \epsilon_1'. \end{aligned} \tag{2.124}$$

By the Cauchy-Schwartz inequality applied to the inner product $\langle X, Y \rangle = \mathbb{E}[XY]$,

$$\mathbb{E}[||\tilde{\boldsymbol{x}}^{[N]} - \tilde{\boldsymbol{x}}^{[M]}||_2] = \sqrt{\mathbb{E}[1 \cdot ||\tilde{\boldsymbol{x}}^{[N]} - \tilde{\boldsymbol{x}}^{[M]}||_2]} \tag{2.125}$$

$$\leq \sqrt{\mathbb{E}[1^2]}\sqrt{\mathbb{E}[||\tilde{\boldsymbol{x}}^{[N]} - \tilde{\boldsymbol{x}}^{[M]}||_2^2]}$$
$$< \sqrt{\epsilon_1'}$$

Hence for any $\epsilon > 0$, there exists N and M sufficiently large such that $\sqrt{\epsilon_1'} < \frac{\epsilon}{2}$ and $\epsilon_0 < \frac{\epsilon}{2}$ giving $\mathbb{E}[||\boldsymbol{x}_t^{[N]} - \boldsymbol{x}_t^{[M]}||_2] < \epsilon$. Then, by completeness of $L^2[0,1]$, there exists $\boldsymbol{x}_t^{\infty}$ such that $\mathbb{E}[||\boldsymbol{x}_t^{[N]} - \boldsymbol{x}_t^{\infty}||_2] \to 0$ as N goes to infinity, yielding the desired result. □

2.6.2 Proof of Lemma 2.3.2

Apply the operator norm to both sides of equation (2.45). As $\mathbb{R}$ (and hence $\mathbb{R}^{-1}$) is strictly positive, $-S_t^N \mathbb{B}^N \mathbb{R}^{-1} \mathbb{B}^N S_t^N$ is negative, and by assumption $\{A^N, B^N, Q^N, M^N, M_T^N, R^N\}$ converges to $\{A, B, Q, M, M_T, R\}$ in the operator norm sense,

$$||S_t^N||_{\text{op}} \leq ||\mathbb{M}_T^N||_{\text{op}} + \int_t^T (||\mathbb{A}^N S_t^N + S_t^N \mathbb{A}^N$$
$$- S_t^N B^N R^{-1} B^N S_t^N + M^N||_{\text{op}})dt \tag{2.126}$$
$$\leq ||\mathbb{M}_T^N||_{\text{op}} + \int_t^T (4||\mathbb{A}||_{\text{op}}||S_t^N||_{\text{op}} + 2||\mathbb{M}||_{\text{op}})dt. \tag{2.127}$$

Then, by Gronwall's inequality, $||S_t^N||_{\text{op}}$ satisfies

$$||S_t^N||_{\text{op}} \leq (2||\mathbb{M}_T||_{\text{op}} + 2(T-t)||\mathbb{M}||_{\text{op}})$$
$$\cdot \exp(4(T-t)||\mathbb{A}||_{\text{op}}). \tag{2.128}$$

By assumption, $\mathbb{A}, \mathbb{M}, \mathbb{M}_T, \mathbb{R}$ are bounded, and hence there exists $0 < c_N < \infty$ such that

$$||S_t^N||_{\text{op}} \leq 2||\mathbb{M}_T||_{\text{op}} + (T-t)c_N, \ \forall t \in [0,T], \ N > N_0. \tag{2.129}$$

□

2.6.3 Proof of Theorem 2.3.3

Recall that the linear quadratic Q-noise problem is solved by

$$\boldsymbol{u}_t = -\mathbb{R}^{-1}\mathbb{B}^* S_t \boldsymbol{x}_t, \quad t \in [0,T], \tag{2.130}$$

$$\boldsymbol{u}_t^{[N]} = -(\mathbb{R}^{[N]})^{-1}\mathbb{B}^{[N]*} S_t^{[N]} \boldsymbol{x}_t^{[N]}, \quad t \in [0,T], \tag{2.131}$$

which places the system in linear feedback form. Then, by Theorem 2.2.3, $\boldsymbol{x}_t^{[N]}$ converges to $\boldsymbol{x}_t$ if

$$\lim_{N\to\infty} S_t^{[N]} = S_t, \quad 0 \le t \le T \tag{2.132}$$

in the operator norm sense. Let

$$\Delta_t^N := S_t - S_t^{[N]}, \quad 0 \le t \le T. \tag{2.133}$$

Define the evolution of Δ_t^N in terms of the evolution of S_t and $S_t^{[N]}$,

$$\begin{aligned}
\dot{\Delta}_t^N =& \dot{S}_t - \dot{S}_t^{[N]} \qquad (2.134)\\
=& (\mathbb{A}^{[N]} S_t^{[N]} - \mathbb{A} S_t) + (S_t^{[N]}\mathbb{A}^{[N]*} - S_t\mathbb{A}^*)\\
&- (S_t^{[N]}\mathbb{B}^{[N]}\mathbb{R}^{[N]^{-1}}\mathbb{B}^{[N]*} S_t^{[N]} - S_t\mathbb{B}\mathbb{R}^{-1}\mathbb{B}^* S_t)\\
&+ (\mathbb{M}^{[N]} - \mathbb{M}),\\
\Delta_T^N =& \mathbb{M}_T - \mathbb{M}_T^{[N]}, \qquad (2.135)
\end{aligned}$$

and hence

$$\begin{aligned}
\Delta_t^N =& \mathbb{M}_T - \mathbb{M}_T^{[N]} \qquad (2.136)\\
&+ \int_t^T (\mathbb{A}^{[N]} S_t^{[N]} - \mathbb{A} S_t) + (S_t^{[N]}\mathbb{A}^{[N]*} - S_t\mathbb{A}^*)\\
&- (S_t^{[N]}\mathbb{B}^{[N]}\mathbb{R}^{[N]^{-1}}\mathbb{B}^{[N]*} S_t^{[N]} - S_t\mathbb{B}\mathbb{R}^{-1}\mathbb{B}^* S_t)
\end{aligned}$$

$$+ (\mathbb{M}^{[N]} - \mathbb{M})dt.$$

Focusing on the first term $\mathbb{A}^{[N]}S_t^{[N]} - \mathbb{A}S_t$:

$$\begin{aligned}\mathbb{A}^{[N]}S_t^{[N]} - \mathbb{A}S_t &= \mathbb{A}^{[N]}S_t^{[N]} - \mathbb{A}S_t + \mathbb{A}^{[N]}S_t - \mathbb{A}^{[N]}S_t \\ &= (\mathbb{A}^{[N]} - \mathbb{A})S_t - \mathbb{A}^{[N]}\Delta_t^N. \end{aligned} \tag{2.137}$$

Similarly,

$$S_t^{[N]}\mathbb{A}^{[N]*} - S_t\mathbb{A}^* = S_t(\mathbb{A}^{[N]*} - \mathbb{A}^*) - \Delta_t^N\mathbb{A}^{[N]*} \tag{2.138}$$

For the quadratic term, let

$$\begin{gathered} H = \mathbb{B}\mathbb{R}^{-\frac{1}{2}}, \quad H^{[N]} = \mathbb{B}^{[N]}\mathbb{R}^{[N]^{-\frac{1}{2}}}, \\ \text{where } \mathbb{R}^{-1} = \mathbb{R}^{-\frac{1}{2}}\mathbb{R}^{-\frac{1}{2}*}. \end{gathered} \tag{2.139}$$

Then,

$$S_tHH^*S_t = S_t\mathbb{B}\mathbb{R}^{-1}\mathbb{B}^*S_t, \tag{2.140}$$

$$S_t^{[N]}H^{[N]}H^{[N]*}S_t^{[N]} = S_t^{[N]}\mathbb{B}^{[N]}\mathbb{R}^{[N]^{-1}}\mathbb{B}^{[N]*}S_t^{[N]}, \tag{2.141}$$

$$\begin{aligned} &S_t^{[N]}H^{[N]}H^{[N]*}S_t^{[N]} - S_tHH^*S_t \\ &\quad = S_t^{[N]}H^{[N]}H^{[N]*}S_t^{[N]} - S_tHH^*S_t \\ &\qquad + S_tHH^{[N]*}S_t^{[N]} - S_tHH^{[N]*}S_t^{[N]} \\ &\qquad + S_tH(H^{[N]*}S_t^{[N]} - H^*S_t) \end{aligned} \tag{2.142}$$

Employing the identities of the form used in (2.137) and (2.138) with $\mathbb{A} = H$ and $\mathbb{A}^{[N]} = H^{[N]}$, this is equal to

$$\begin{aligned} & S_t^{[N]} H^{[N]} H^{[N]*} S_t^{[N]} - S_t H H^* S_t \\ & \quad = \left(S_t (H^{[N]} - H) - \Delta_t^N H^{[N]} \right) H^{[N]*} S_t^{[N]} \\ & \qquad + S_t H \left((H^* - H^{[N]*}) S_t - H^{[N]*} \Delta_t^N \right). \end{aligned} \tag{2.143}$$

Using equations (2.137), (2.138), (2.143), define the operator valued functions P^N, Y^N,

$$\begin{aligned} P^N(t) :=& (\mathbb{M}^{[N]} - \mathbb{M}) + (\mathbb{A}^{[N]} - \mathbb{A}) S_t \\ & + S_t (\mathbb{A}^{[N]*} - \mathbb{A}^*) \\ & + S_t (H^{[N]} - H) H^{[N]*} S_t^{[N]} \\ & + S_t H (H^* - H^{[N]*}) S_t, \end{aligned} \tag{2.144}$$

$$\begin{aligned} Y^N(t, \Delta_t^N) :=& - (\mathbb{A}^{[N]} \Delta_t^N + \Delta_t^N \mathbb{A}^{[N]*} \\ & + \Delta_t^N H^{[N]} H^{[N]*} S_t^{[N]} + S_t H H^{[N]*} \Delta_t^N), \end{aligned} \tag{2.145}$$

in terms of which (94) yields

$$\Delta_t^N = (\mathbb{M}_T - \mathbb{M}_T^{[N]}) + \int_t^T P^N(t) + Y^N(t, \Delta_t^N) dt. \tag{2.146}$$

Then,

$$\begin{aligned} ||\Delta_t^N||_{\text{op}} \leq & \int_t^T ||P^N(s) + Y^N(s, \Delta_s^N)||_{\text{op}} ds \\ & + ||\mathbb{M}_T - \mathbb{M}_T^{[N]}||_{\text{op}} \\ \leq & \int_t^T ||P^N(s)||_{\text{op}} ds + \int_t^T ||Y^N(s, \Delta_s^N)||_{\text{op}} ds \end{aligned} \tag{2.147}$$

$$+ ||\mathbb{M}_T - \mathbb{M}_T^{[N]}||_{\text{op}}. \tag{2.148}$$

Further, define the time process $Z^N(t) : [0, T] \to \mathbb{R}$,

$$\begin{aligned} ||Y^N(t, \Delta_t^N)||_{\text{op}} \leq & (2||\mathbb{A}^{[N]}||_{\text{op}} + ||H^{[N]} H^{[N]*} S_t^{[N]}||_{\text{op}} \\ & + ||S_t H H^{[N]*}||_{\text{op}})||\Delta_t^N||_{\text{op}} \\ =: & Z^N(t)||\Delta_t^N||_{\text{op}}. \end{aligned} \tag{2.149}$$

Then, by applying Gronwall's inequality to $||\Delta_t^N||_{\text{op}}$ in (2.149),

$$\begin{aligned} ||\Delta_t^N||_{\text{op}} \leq & (||\mathbb{M}_T - \mathbb{M}_T^{[N]}||_{\text{op}} \\ & + \int_t^T ||P^N(s)||_{\text{op}} ds) \exp(\int_t^T ||Z^N(s)||_{\text{op}} ds). \end{aligned} \tag{2.150}$$

By assumption $\mathbb{A}^{[N]} \to \mathbb{A}$, $H^{[N]} \to H$, $\mathbb{M}^{[N]} \to \mathbb{M}$, $\mathbb{M}_T^{[N]} \to \mathbb{M}_T$ in operator norm, and as $S_t, S_t^{[N]}$ are uniformly bounded operators for all N, t,

$$\begin{aligned} & ||P^N(t)||_{\text{op}} \\ & = ||(\mathbb{M}^{[N]} - \mathbb{M}) + (\mathbb{A}^{[N]} - \mathbb{A}) S_t \\ & + S_t(\mathbb{A}^{[N]*} - \mathbb{A}^*) \\ & + S_t(H^{[N]} - H) H^{[N]*} S_t^{[N]} \\ & + S_t H(H^* - H^{[N]*}) S_t||_{\text{op}} \end{aligned} \tag{2.151}$$

$$\begin{aligned} \leq & ||(\mathbb{M}^{[N]} - \mathbb{M})||_{\text{op}} + ||(\mathbb{A}^{[N]} - \mathbb{A})||_{\text{op}} ||S_t||_{\text{op}} \\ & + ||S_t||_{\text{op}} ||(\mathbb{A}^{[N]*} - \mathbb{A}^*)||_{\text{op}} \\ & + ||S_t||_{\text{op}} ||(H^{[N]} - H)||_{\text{op}} ||H^{[N]*}||_{\text{op}} ||S_t^{[N]}||_{\text{op}} \\ & + ||S_t||_{\text{op}} ||H||_{\text{op}} ||(H^* - H^{[N]*})||_{\text{op}} ||S_t||_{\text{op}}. \end{aligned} \tag{2.152}$$

Hence, by the convergence of $\mathbb{M}_T^{[N]} \to \mathbb{M}_T$ and equation (2.152), as $N \to \infty$,

$$(||\mathbb{M}_T - \mathbb{M}_T^{[N]}||_{\text{op}} + \int_t^T ||P^N(s)||_{\text{op}} ds) \to 0 \tag{2.153}$$

$$\text{and } ||Z(t)||_{\text{op}} < \infty \implies \exp(\int_t^T ||Z(s)||_{\text{op}} ds) < \infty. \tag{2.154}$$

Hence, by (2.150)

$$||\Delta_t^N||_{\text{op}} \to 0. \tag{2.155}$$

As $||\Delta_t^N||_{\text{op}}$ converges to zero, $S_t^{[N]}$ converges to S_t in the operator norm sense as N increases to infinity. Then the finite-dimensional network operator $(\mathbb{A}^{[N]} - \mathbb{B}^{[N]}\mathbb{K}_t^{[N]})$ converges to the operator on the graphon system $(\mathbb{A} - \mathbb{B}\mathbb{K}_t)$ and Theorem 2.2.3 can be applied, yielding

$$\mathbb{E}[||\boldsymbol{x}_t^{[N]} - \boldsymbol{x}_t||_2] < \epsilon, \tag{2.156}$$

as required. □

Chapter 3

State Estimation

3.1 Introduction

Previous work on graphon systems has been primarily concerned with deterministic analysis and control ([11][3][2]), while stochastic mean-field games on graphons have been investigated in ([22] [23] [24] [25]). As the systems were deterministic (with potentially a non-deterministic initial condition), there was no great need for estimation.

Dunyak and Caines [9] showed that Gaussian noise on the unit interval ([7] [8] [6]), termed Q-noise, is an appropriate limit object for sequences of systems on graphs with Wiener process disturbances. This model, as well as its extensions to control, were demonstrated in Chapter 2. Medvedev and Simpson [10] provide a numerical scheme for simulating such systems.

This work builds on the results of infinite-dimensional filtering ([17], [16]) and applies them to systems on large graphs; it is established that for systems on large graphs the Kalman filter state estimation processes converge to the filter processes generated by the limit filter systems on the limit graphon networks. The Separation Principle for control and estimation of these limit graph systems is then defined as a natural consequence of the linear filtering and control. The chapter concludes with some computational examples in which these convergence properties are illustrated with a set of standard graphons.

3.1.1 Motivation: partially observed network systems

As in Chapter 2, define two graphs $G_A^N = (V_N, E_A^N)$ and $G_B^N = (V_N, E_B^N)$ with $N < \infty$ vertices, with associated adjacency matrices A^N and B^N. Let $x^N : [0,T]^N \to \mathcal{R}$ be a vector of states where the ith value is associated with the ith vertex of the graph, and let $u^N : [0,T]^N \to \mathcal{R}^N$ be the control input at each vertex. For clarity of notation, we consider systems where each node has a single state. The theory extends to systems with vectors of states at each node in a straightforward manner. Let the (i,j)th entry of the matrices A^N and B^N represent the impact of the state and control input at node i on node j, respectively. For each node, define a Wiener process W^N disturbance with instantaneous positive covariance matrix Q^N. Let a_N and b_N be constants describing the impact of the state of a node and its control on itself.

Finally, define a network-averaged control system [3] on a graph with the following equation for each node,

$$dx_t = ((A^N + a_N\mathbb{I})x_t + (B^N + b_N\mathbb{I})u_t)dt + dW_t^N, \tag{3.1}$$

with the l-dimensional instantaneous system observations given by the operator $C^N : \mathcal{R}^N \to \mathcal{R}^l$ with a Wiener process disturbance v^N with instantaneous covariance matrix R^N,

$$dy_t^N = C^N x_t^N dt + dv_t^N. \tag{3.2}$$

The processes W^N and v^N are orthogonal to each other and to the initial condition x_0^N.

Given these system parameters, the Kalman filter [15] generates the least squares estimate of the system state $\hat{x}_t^N$, with estimation error covariance matrix P_t^N satisfying

$$\begin{aligned} d\hat{x}_t^N =& [(A^N + a_N)\hat{x}_t^N + (B^N + b_N)u_t^N]dt \quad 0 \le t \le T \\ &+ P_t^N (C^N)^{\mathrm{T}} (R^N)^{\mathrm{T}} (dy_t^N - C^N x_t^N dt), \end{aligned} \tag{3.3}$$

$$\frac{d}{dt}P_t^N = (A^N + a_N\mathbb{I})P_t^N + P_t^N(A^N + a_N\mathbb{I})^{\mathrm{T}} \quad 0 \le t \le T,$$
$$+ Q^N - P_t^N(C^N)^{\mathrm{T}}(R^N)^{-1}C^N P_t^N, \tag{3.4}$$
$$P_0^N = \mathrm{Cov}(\hat{x}_0^N - x_0^N, \hat{x}_0^N - x_0^N). \tag{3.5}$$

As the graph becomes larger, the networked system adjacency matrices A^N and B^N converge in the cut-norm sense to their associated graphons [1], which are bounded measurable functions mapping $[0,1] \times [0,1] \to [0,1]$, denoted $\boldsymbol{A}$ and $\boldsymbol{B}$ (as in [3]). When the underlying graph is undirected, its graphon is also symmetric. As the cut norm is difficult to manipulate we henceforth consider only graphs which converge in the stronger $L^2[0,1]$ operator norm sense to limits which are assumed to be unique. Denote the graphon limit system as

$$d\boldsymbol{x}_t = ((\boldsymbol{A} + a\mathbb{I})\boldsymbol{x}_t + (\boldsymbol{B} + b\mathbb{I})\boldsymbol{u}_t)dt + d\boldsymbol{w}_t, \quad \boldsymbol{x}_0 \in L^2[0,1] \tag{3.6}$$

where $\boldsymbol{x}_t$ and $\boldsymbol{u}_t$ are square-integrable functions on the unit interval, $\boldsymbol{A}$ and $\boldsymbol{B}$ are graphons, a and b are real constants, $\mathbb{I}$ is the identity operator, and $\boldsymbol{w}_t$ is a Q-noise, a generalization of Gaussian noise from finite-dimensional vectors to the unit interval [9]. The observations are necessarily finite-dimensional from a practical standpoint and from the requirement that the observation noise have an invertible covariance operator [14]. The corresponding l-dimensional limit observation process $\boldsymbol{y}_t$ satisfies

$$d[\boldsymbol{y}_t]_k := [\boldsymbol{C}\boldsymbol{x}_t]_k dt + d[v_t]_k \tag{3.7}$$
$$= \langle c_k, \boldsymbol{x}_t\rangle dt + d[v_t]_k, \quad k = \{1, ..., l\},$$

where the process v_t is an l-dimensional real centered Wiener process with covariance operator $\mathbf{R}$. This section also shows that the finite rank nature of the filter necessarily cannot model the system trajectory when the graphon limit system and its associated Q-noise is higher (or infinite) dimensional.

Section 3.4 summarizes some results of linear quadratic control on these stochastic graphon systems, and shows a Separation Principle for the control and estimation of linear stochastic graphon systems with quadratic costs.

Relying on classical results of Kalman filters in Hilbert spaces ([17], [16]), we show that the Kalman filter of the finite graph $\hat{x}_t^N$ is well-approximated by the graphon Kalman filter process $\hat{\boldsymbol{x}}_t$.

3.2 Preliminaries

We adopt the same notation as Chapter 2, Section 2.2.1. With the addition of the observation process, we slightly modify the definition of a linear Q-noise system.

Definition 3.2.1 (Partially Observed Q-noise Dynamical Systems) *As in Chapter 2, define the state trajectory $\boldsymbol{x} : [0,1] \times [0,T] \to \mathcal{R}$ be an $L^2[0,1] \times [0,T]$ function with a given initial condition $\boldsymbol{x}(\cdot, 0) = \boldsymbol{x}_0$. Let $\mathbb{A}, \mathbb{B} \in \mathcal{M}$ be bounded linear operators from $L^2[0,1]$ to $L^2[0,1]$ such that $\mathbb{A}\mathbf{Q}\mathbb{A}^* \in \mathcal{Q}$. This defines a Q-noise noise denoted $\boldsymbol{w}_t$. Let a control input $\boldsymbol{u}_t : [0,T] \to L^2[0,1]$ be a function adapted to the filtration $\mathcal{F}_t$, consisting of all measurable functions of the state of the system $\boldsymbol{x}_s, 0 \leq s \leq t$. In addition, let $\boldsymbol{y}_t$ be a finite-dimensional observation process, $\boldsymbol{C} : L^2[0,1] \to \mathcal{R}^l$ be a finite-dimensional operator, and $\boldsymbol{v}_t$ be an l-dimensional Wiener process observation noise with instantaneous covariance operator $\mathbf{R} \in \mathcal{R}^{l \times l}$.*

A partially observed linear dynamical system with Q-noise is an infinite-dimensional differential system satisfying the following equation,

$$d\boldsymbol{x}_t(\alpha) = ((\mathbb{A}\boldsymbol{x}_t)(\alpha) + \mathbb{B}\boldsymbol{u}_t(\alpha))dt + d\boldsymbol{w}(\alpha, t), \tag{3.8}$$

$$d\boldsymbol{y}_t = \boldsymbol{C}\boldsymbol{x}_t dt + d\boldsymbol{v}_t \tag{3.9}$$

where for a partition of $[0,t]$, $(0,t_2,\cdots,t_{N-2},t)$,

$$\int_0^t d\boldsymbol{w}(\alpha,s) = \lim_{N\to\infty}\sum_{k=1}^{N}(\boldsymbol{w}(\alpha,t_{k+1}) - \boldsymbol{w}(\alpha,t_k)) \tag{3.10}$$

in the mean-squared convergence sense.

Definition 3.2.2 (Mild solution) *A mild solution (see [7, Sec. 3.1]) to a state and observation process of type (3.8) is the function* $\boldsymbol{x}_t : [0,T]\times\Omega \to L^2[0,1]$ *given by*

$$\boldsymbol{x}_t = e^{\mathbb{A}t}\boldsymbol{x}_0 + \int_0^t e^{\mathbb{A}(t-s)}\mathbb{B}\boldsymbol{u}_s ds + \int_0^t e^{\mathbb{A}(t-s)}d\boldsymbol{w}_s, \tag{3.11}$$

$$\boldsymbol{y}_t = \boldsymbol{C}\big[\Phi(t,0)\boldsymbol{x}_0 + \int_0^t \Phi(t,s)\mathbb{B}\boldsymbol{u}_s ds + \int_0^t \Phi(t,s)d\boldsymbol{w}_s\big] + \boldsymbol{v}_t \tag{3.12}$$

3.3 Network Models and Limit Processes

For convenience, we reiterate the definition of a graph system (Equation 2.2) here, which is a networked control system of the form (3.1),

$$\begin{aligned} dx_t^N &= ((A^N + a_N\mathbb{I})x_t^N + (B^N + b_N\mathbb{I})u_t^N)dt + dW^N(t),\\ x_t^N &\in \mathcal{R}^N, \end{aligned} \tag{3.13}$$

with the standard map to piecewise constant step functions on the unit interval to piecewise constant functions on the unit interval ([3]).

3.3.1 Kalman Filtering in Finite and Infinite Dimensions

Theorem 3.3.1 ([17]) *Consider a linear Q-noise state system satisfying*

$$\begin{aligned} d\boldsymbol{x}_t &= ((\boldsymbol{A} + a\mathbb{I})\boldsymbol{x}_t + (\boldsymbol{B} + b\mathbb{I})\boldsymbol{u}_t)dt + d\boldsymbol{w}_t,\\ \boldsymbol{x}_0 &\in L^2[0,1], \end{aligned} \tag{3.14}$$

with the observation process

$$d\boldsymbol{y}_t = \boldsymbol{C}\boldsymbol{x}_t dt + d\boldsymbol{v}_t, \quad \boldsymbol{y}_t \in \mathcal{R}^l \tag{3.15}$$

where the observation noise $\boldsymbol{v}_t$ *is a Wiener process with instantaneous covariance matrix* $\mathbf{R}$. *Let* P_t *be the* $L^2[0,1]$ *linear operator satisfying the following Riccati equation for any* $\boldsymbol{f}, \boldsymbol{g} \in L^2[0,1]$

$$\left\langle \left[\frac{d\boldsymbol{P}_t}{dt} - \mathbb{A}\boldsymbol{P}_t - \boldsymbol{P}_t\mathbb{A}^* - \mathbf{Q} + \boldsymbol{P}_t\boldsymbol{C}^*\mathbf{R}^{-1}\boldsymbol{C}\boldsymbol{P}_t \right] \boldsymbol{f}, \boldsymbol{g} \right\rangle = 0 \tag{3.16}$$

$$\boldsymbol{P}_0 = Cov(\hat{\boldsymbol{x}}_0 - \boldsymbol{x}_0, \hat{\boldsymbol{x}}_0 - \boldsymbol{x}_0), \tag{3.17}$$

and let the filter gain $\boldsymbol{K}_t$ *be defined by*

$$\boldsymbol{K}_t = \boldsymbol{P}_t\boldsymbol{C}^*\mathbf{R}^{-1}. \tag{3.18}$$

Then, the $L^2[0,1]$ *estimation process of system 3.14 is generated by the stochastic differential equation*

$$d\hat{\boldsymbol{x}}_t = (\mathbb{A}\hat{\boldsymbol{x}}_t + \mathbb{B}\boldsymbol{u}_t)dt + \boldsymbol{K}_t(d\boldsymbol{y}_t - \boldsymbol{C}\hat{\boldsymbol{x}}_t dt), \tag{3.19}$$

$$\hat{\boldsymbol{x}}_0 = \mathbb{E}[\boldsymbol{x}_0]. \tag{3.20}$$

□

Note that by substitution of $d\boldsymbol{y}_t := \boldsymbol{C}\boldsymbol{x}_t dt + d\boldsymbol{v}_t$

$$\begin{aligned} d\hat{\boldsymbol{x}}_t &= (\mathbb{A}\hat{\boldsymbol{x}}_t + \mathbb{B}\boldsymbol{u}_t)dt + K_t(d\boldsymbol{y}_t - \boldsymbol{C}\hat{\boldsymbol{x}}_t dt) \\ &= [(\mathbb{A} - \boldsymbol{K}_t\boldsymbol{C})\hat{\boldsymbol{x}}_t + \mathbb{B}\boldsymbol{u}_t]dt + \boldsymbol{K}_t\boldsymbol{C}\boldsymbol{x}_t dt + \boldsymbol{K}_t d\boldsymbol{v}_t. \end{aligned} \tag{3.21}$$

As in the finite-dimensional case, the solution $\boldsymbol{P}_t$ to equation (3.16) can be interpreted as

the covariance of the error process [14],

$$\boldsymbol{P}_t = \mathbb{E}[(\boldsymbol{x}_t - \hat{\boldsymbol{x}}_t)(\boldsymbol{x}_t - \hat{\boldsymbol{x}}_t)^*]. \tag{3.22}$$

Recalling from Equations (3.3)–(3.5), the Kalman filter generates the least-squares state estimate given the observations y_t of equation (3.13). For clarity, we restate the equations here.

$$\begin{aligned} d\hat{x}_t^N =& (A^N + a_N\mathbb{I})\hat{x}_t^N + (B^N + b_N\mathbb{I})u_t^N \\ &+ P_t(C^N)^{\mathrm{T}}(R^N)^{\mathrm{T}}(dy_t^N - C^N x_t^N dt), \end{aligned} \tag{3.23}$$

$$\begin{aligned} \frac{d}{dt}P_t^N =& (A^N + a_N\mathbb{I})P_t^N + P_t^N(A^N + a_N\mathbb{I})^{\mathrm{T}} \\ &+ Q^N - P_t^N(C^N)^{\mathrm{T}}(R^N)^{-1}C^N P_t^N, \end{aligned} \tag{3.24}$$

$$P_0^N = \mathrm{cov}(\hat{x}_0^N - x_0^N, \hat{x}_0^N - x_0^N). \tag{3.25}$$

The following theorem establishes that the state estimation process generated by the filter for a system defined on a graph with N nodes converges to the state estimation process generated by the limit Kalman filter on the limit graph. For simplicity, we assume that the control $\boldsymbol{u}_t$ is equivalent to $\boldsymbol{u}_t^{[N]}$.

Theorem 3.3.2 *Let the piecewise constant process $\boldsymbol{x}_t^{[N]}$ converge to the graphon process $\boldsymbol{x}_t$ under the assumptions of Theorem 2.2.3, and let $\hat{\boldsymbol{x}}_t^{[N]}$ be the N-dimensional Kalman filter process estimating the state process $\boldsymbol{x}_t^{[N]}$. Then, in addition to assumptions A0-A2, B0, and B1 of Theorem 2.2.3 (restated below for clarity), assume there exists an N_0 such that for any tuple $\{\epsilon_k\}_{k=0}^5$ where, for $N > N_0$,*

$$||\boldsymbol{x}_0^{[N]} - \boldsymbol{x}_0^{[M]}||_2^2 < \epsilon_0, \qquad \textit{(A0)} \tag{3.26}$$

$$||\Phi^{[N]}(t,s) - \Phi^{[M]}(t,s)||_{op}^2 < \epsilon_1, \qquad \textit{(A1)} \tag{3.27}$$

$$\mathbb{E}[||\boldsymbol{w}_t^{[N]} - \boldsymbol{w}_t^{[M]}||_2^2] < \epsilon_2, \qquad \textit{(A2)} \tag{3.28}$$

$$\sum_{k=1}^{N}\sum_{r=1}^{N}|c_{k,r}^{N}|^2 \leq C, \qquad \textit{(B0)} \tag{3.29}$$

$$\int_0^s ||\Phi^{[N]}(t,s)||_{op}^2 ds \leq \alpha, \quad t \in [0,T]. \qquad \textit{(B1)} \tag{3.30}$$

$$||R^N - R||_{op} < \epsilon_3, \qquad \textit{(C1)} \tag{3.31}$$

$$||\boldsymbol{C}^{[N]} - \boldsymbol{C}||_{op} < \epsilon_4, \qquad \textit{(C2)} \tag{3.32}$$

$$||\hat{\boldsymbol{x}}_0^{[N]} - \hat{\boldsymbol{x}}_0||_2 < \epsilon_5, \qquad \textit{(C3)} \tag{3.33}$$

and that the l-dimensional observation processes y_t^N and $\boldsymbol{y}_t$ share the observation noise process $\boldsymbol{v}_t$. Then

$$\mathbb{E}[||\hat{\boldsymbol{x}}_t^{[N]} - \hat{\boldsymbol{x}}_t||_2] < \epsilon. \tag{3.34}$$

Proof: First, we note that by Theorem 2.2.3, first demonstrated in [40], when $(\mathbb{A}^{[N]}, \boldsymbol{C}^{[N]}, \mathbf{Q}^{[N]}, R^N)$ converges to the tuple $(\mathbb{A}, \boldsymbol{C}, \mathbf{Q}, R)$, then the associated Riccati equation converges. This shows that the filter gain $\boldsymbol{K}_t^{[N]}$ corresponding to the finite graph converges to the graphon filter gain $\boldsymbol{K}_t$.

In a similar manner, define

$$\eta_t^N = \hat{\boldsymbol{x}}_t - \hat{\boldsymbol{x}}_t^{[N]}. \tag{3.35}$$

Unlike in [40], η_t^N is stochastic, hence a Gronwall's inequality argument cannot be applied directly. However, using equation (3.21),

$$\begin{aligned} d\eta_t^N =& d\hat{\boldsymbol{x}}_t - d\hat{\boldsymbol{x}}_t^{[N]} \\ =& [(\mathbb{A} - \boldsymbol{K}_t\boldsymbol{C})\hat{\boldsymbol{x}}_t + \mathbb{B}\boldsymbol{u}_t]dt + \boldsymbol{K}_t\boldsymbol{C}\boldsymbol{x}_t dt + \boldsymbol{K}_t d\boldsymbol{v}_t \\ & - [(\mathbb{A}^{[N]} - \boldsymbol{K}_t^{[N]}\boldsymbol{C}^{[N]})\hat{\boldsymbol{x}}_t^{[N]} + \mathbb{B}^{[N]}\boldsymbol{u}_t^{[N]}]dt \\ & - \boldsymbol{K}_t^{[N]}\boldsymbol{C}^{[N]}\boldsymbol{x}_t^{[N]}dt - \boldsymbol{K}_t^{[N]}d\boldsymbol{v}_t. \end{aligned} \tag{3.36}$$

To shorten this equation, introduce the notation

$$\boldsymbol{H}_t := \mathbb{A} - \boldsymbol{K}_t\boldsymbol{C}, \quad \boldsymbol{H}_t^N := \mathbb{A}^{[N]} - \boldsymbol{K}_t^{[N]}\boldsymbol{C}^{[N]}. \tag{3.37}$$

Then, by assumption, $\boldsymbol{u}_t = \boldsymbol{u}_t^{[N]}$, and $d\eta_t^N$ has the form

$$\begin{aligned} d\eta_t^N =&[\boldsymbol{H}_t\hat{\boldsymbol{x}}_t]dt + \boldsymbol{K}_t\boldsymbol{C}\boldsymbol{x}_t dt + \boldsymbol{K}_t d\boldsymbol{v}_t \\ &- [\boldsymbol{H}_t^N\hat{\boldsymbol{x}}_t^{[N]}]dt - \boldsymbol{K}_t^{[N]}\boldsymbol{C}^{[N]}\boldsymbol{x}_t^{[N]}dt - \boldsymbol{K}_t^{[N]}d\boldsymbol{v}_t. \end{aligned} \tag{3.38}$$

By adding and subtracting $(\boldsymbol{H}_t\hat{\boldsymbol{x}}^{[N]} + \boldsymbol{K}_t\boldsymbol{C}\boldsymbol{x}_t^{[N]})dt$, equation (3.38) can be rewritten as

$$\begin{aligned} d\eta_t^N =&[\boldsymbol{H}_t(\hat{\boldsymbol{x}}_t - \hat{\boldsymbol{x}}_t^{[N]}) + (\boldsymbol{H}_t - \boldsymbol{H}^N)\hat{\boldsymbol{x}}_t^{[N]} \\ &+ K_t\boldsymbol{C}(\boldsymbol{x}_t - \boldsymbol{x}_t^{[N]}) + (\boldsymbol{K}_t\boldsymbol{C} - \boldsymbol{K}_t^{[N]}\boldsymbol{C}^{[N]})\boldsymbol{x}_t^{[N]}]dt \\ &+ \boldsymbol{K}_t d\boldsymbol{v}_t - \boldsymbol{K}_t^{[N]}d\boldsymbol{v}^{[N]} \\ =&[\boldsymbol{H}_t\eta_t^N + (\boldsymbol{H}_t - \boldsymbol{H}_t^N)\hat{\boldsymbol{x}}_t^{[N]} + \boldsymbol{K}_t\boldsymbol{C}(\boldsymbol{x}_t - \boldsymbol{x}_t^{[N]}) \\ &+ (\boldsymbol{K}_t\boldsymbol{C} - \boldsymbol{K}_t^{[N]}\boldsymbol{C}^{[N]})\boldsymbol{x}_t^{[N]}]dt \\ &+ (\boldsymbol{K}_t - \boldsymbol{K}_t^{[N]})d\boldsymbol{v}_t. \end{aligned} \tag{3.39}$$

Note that only the first term depends on the trajectory of η_t. Letting $\Phi(t,s)$ be the evolution operator generated by $\boldsymbol{H}_t$, applying the Ito integral from 0 to t yields

$$\begin{aligned} \eta_t^N =&\Phi(t,0)\eta_0^N + \int_0^t (\boldsymbol{H}_s - \boldsymbol{H}_s^N)\hat{\boldsymbol{x}}_s^{[N]}ds \\ &+ \int_0^t \Phi(t,s)\boldsymbol{K}_s\boldsymbol{C}(\boldsymbol{x}_s - \boldsymbol{x}_s^{[N]})ds \\ &+ \int_0^t \Phi(t,s)(\boldsymbol{K}_s\boldsymbol{C} - \boldsymbol{K}_s^{[N]}\boldsymbol{C}^{[N]})\boldsymbol{x}_s^{[N]}ds \\ &+ \int_0^t \Phi(t,s)(\boldsymbol{K}_s - \boldsymbol{K}_s^{[N]})d\boldsymbol{v}_s. \end{aligned} \tag{3.40}$$

Applying $\mathbb{E}[||\cdot||_2]$ to η_t^N, the definition of the operator norm, the triangle inequality, and

Jensen's inequality yields

$$\begin{aligned}\mathbb{E}[||\eta_t^N||_2] \leq & \mathbb{E}[||\Phi(t,0)||_{\text{op}}||\eta_0^N||_2] \\ & + \mathbb{E}[\int_0^t ||(\boldsymbol{H}_s - \boldsymbol{H}_s^N)||_{\text{op}}||\hat{\boldsymbol{x}}_s^{[N]}||_2 ds] \\ & + \mathbb{E}[\int_0^t ||\Phi(t,s)||_{\text{op}}||\boldsymbol{K}_s\boldsymbol{C}||_{\text{op}}||\boldsymbol{x}_s - \boldsymbol{x}_s^{[N]}||_2 ds] \\ & + \mathbb{E}[\int_0^t ||\Phi(t,s)||_{\text{op}}\ ||(\boldsymbol{K}_s\boldsymbol{C} - \boldsymbol{K}_s^{[N]}\boldsymbol{C}^{[N]})||_{\text{op}}||\boldsymbol{x}_s^{[N]}||_2 ds] \\ & + \mathbb{E}[||\int_0^t \Phi(t,s)(\boldsymbol{K}_s - \boldsymbol{K}_s^{[N]})d\boldsymbol{v}_s||_2].\end{aligned} \tag{3.41}$$

The first term of (3.41) converges by assumption (C3), and the second, third, and fourth terms converge via the convergence of the operator norms of $(\mathbb{A}, \boldsymbol{C}, \mathbf{Q}, R)$.

The fifth term can be shown to converge, as follows from the Cauchy-Schwarz inequality applied to the inner product $\langle X, Y\rangle = \mathbb{E}[XY]$ and the Ito Isometry [7, Theorem 2.3]. By the boundedness of $\Phi(t,s)$ and the convergence of $\boldsymbol{K}_t^{[N]}$ to $\boldsymbol{K}_t$ in operator norm, for every $\epsilon > 0$, there exists an N such that

$$\begin{aligned}&\mathbb{E}||\int_0^t \Phi(t,s)(\boldsymbol{K}_s - \boldsymbol{K}_s^{[N]})d\boldsymbol{v}_s||_2 \\ &\leq \sqrt{\mathbb{E}[1^2]}\sqrt{\mathbb{E}||\int_0^t \Phi(t,s)(\boldsymbol{K}_s - \boldsymbol{K}_s^{[N]})d\boldsymbol{v}_s||_2^2} \\ &= \left(\int_0^t ||\Phi(t,s)(\boldsymbol{K}_s - \boldsymbol{K}_s^{[N]})||_{\text{op}}^2 ds\right)^{1/2} \quad \text{(by the Ito Isometry)} \\ &\leq \left(\int_0^T ||\Phi(t,s)||_{\text{op}}^2||\boldsymbol{K}_s - \boldsymbol{K}_s^{[N]}||_{\text{op}}^2 ds\right)^{1/2} \\ &< \epsilon.\end{aligned} \tag{3.42}$$

This yields the desired boundedness in expected norm. □

Note: The requirement that the finite graph system and the limit system have identical observation disturbances $\boldsymbol{v}_t$ is intuitive. As N increases, the graph becomes more complex,

but the same number of observations is taken.

3.3.2 Observability and Finite Rank Decomposition

As in [3] and [35], when the underlying graphon limits of the system are finite rank (that is, $\mathbb{A}$ and $\mathbf{Q}$ have finite rank), then the Kalman filter may be expressed as the solution of a finite number of equations. Thus, even when the large, finite graph has a nearly full rank adjacency matrix A^N, the Kalman filter can be calculated efficiently due to the finite rank nature of the limit. First, recall the notion of (approximate) observability ([41, Sec. 6.2]).

3.3.2.1 Observability

For deterministic systems, this is the property that the initial condition can be uniquely determined as a function of the output and input processes.

Definition 3.3.1 (Observability, [41], Corr. 6.2.15) *For a linear Q-noise system with a state operator of the form $\mathbb{A} = \boldsymbol{A} + a\mathbb{I}$ generating the evolution operator $\Phi(t,s)$ and the observation operator $\boldsymbol{C}$, $(\boldsymbol{C}, \mathbb{A})$ is observable if*

$$\boldsymbol{C}\Phi(s,0)\boldsymbol{v} = 0 \ \forall \ s \in [0,T] \implies \boldsymbol{v} = 0. \tag{3.43}$$

□

Recall that for $\mathbb{A} = \boldsymbol{A} + a\mathbb{I}$, where $\boldsymbol{A}$ is a graphon with distinct eigenvalues $\{\lambda_k, \lambda_1 > \lambda_2 > \cdots\}_{k=1}^{\infty}$ with multiplicity r_k corresponding to the orthonormal basis $\{\phi_{n_j}, j = 1, 2, \cdots r_k\}$ of $L^2[0,1]$, $\mathbb{A}$ acting on a function $\boldsymbol{f} \in L^2[0,1]$ can be expressed as the operator

$$\mathbb{A}\boldsymbol{f} = \sum_{n=1}^{\infty}(\lambda_n + a)\sum_{j=1}^{r_n}\langle\phi_{r_j}, \boldsymbol{f}\rangle\phi_{r_j}. \tag{3.44}$$

The following observability test for $(\boldsymbol{C}, \mathbb{A})$ is given in [41, Theorem 6.3.4].

Theorem 3.3.3 ([41]) *Given a system evolution operator $\mathbb{A}$ of the form 3.44 and a finite-dimensional observation operator $\boldsymbol{C}$ of the form*

$$\begin{aligned} &\boldsymbol{C}\boldsymbol{f} = [\langle c_1, \boldsymbol{f}\rangle \ \langle c_2, \boldsymbol{f}\rangle \ \cdots \ \langle c_l, \boldsymbol{f}\rangle]^T, \\ &c_k \in L^2[0,1] \ \forall \ k = (1, ..., l), \end{aligned} \tag{3.45}$$

$(\mathbb{A}, \boldsymbol{C})$ is observable if and only if for all n

$$rank \begin{bmatrix} \langle c_1, \phi_{n_1}\rangle & \cdots & \langle c_l, \phi_{n_1}\rangle \\ \vdots & & \vdots \\ \langle c_1, \phi_{n_{r_n}}\rangle & \cdots & \langle c_l, \phi_{n_{r_n}\rangle} \end{bmatrix} = r_n. \tag{3.46}$$

□

This implies that if $\boldsymbol{A}$ is finite rank (i.e., has a finite-dimensional range), the system is necessarily unobservable in an infinite number of subspaces.

In the context of Q-noise systems, it is natural to couple the notions of observable and unobservable spaces with the notions of noise-controllable and noise-uncontrollable subspaces. By duality of observability and controllability, if the tuple $(\boldsymbol{C}, \boldsymbol{A})$ is observable, then $(\boldsymbol{C}^*, \boldsymbol{A}^*)$ is controllable [41, Lemma 6.2.14]. The noise-controllable and observable subspaces can then be decomposed as in standard finite-dimensional analysis.

Definition 3.3.2 *For a Q-noise system with the parameters $(\boldsymbol{C}, \mathbb{A}, \mathbf{Q})$, for all $t \in (0, T]$, the following hold:*

The unobservable subspace $UNOB$ is the span of the set of functions $\boldsymbol{v} \in L^2[0,1]$ such that

$$\boldsymbol{C}\Phi(s, 0)\boldsymbol{v} = 0 \ \forall \ s \in [0, t]. \tag{3.47}$$

The observable subspace OB is the orthogonal complement of $UNOB$.

The noise-uncontrollable subspace $UNCON_{\mathbf{Q}}$ *is the set of functions* $\boldsymbol{v} \in L^2[0,1]$ *such that*

$$\mathbf{Q}\Phi^*(s,0)\boldsymbol{v} = 0 \ \forall \ s \in [0,t]. \tag{3.48}$$

The noise-controllable subspace is the orthogonal complement of $CON_{\mathbf{Q}}$.

The noise controllable and observable subspace is the intersection of OB *and* $CON_{\mathbf{Q}}$ *is denoted* $CON_{\mathbf{Q}}OB$.

Remark: As the unobservable subspace $UNOB$ is the largest subspace invariant with respect to $\Phi(\cdot,0)$ contained in $\ker \boldsymbol{C}$, and $CON_{\mathbf{Q}}$ is the smallest subspace invariant with respect to $\Phi(\cdot,0)$ containing the range of $\mathbf{Q}$, then the noise-controllable and unobservable subspace is equivalent to

$$CON_{\mathbf{Q}}UNOB = (\ker(\boldsymbol{C}\Phi(\cdot,0))) \cap (\mathrm{ran}(\Phi(\cdot,0)\mathbf{Q})). \tag{3.49}$$

Even if $(\boldsymbol{C}, \mathbb{A})$ contains unobservable modes, when the initial condition of the system $\boldsymbol{x}_0$ is an element of OB, $\boldsymbol{w}_t$ is $\boldsymbol{A}$-invariant, the space of initial condtions $\boldsymbol{X}_0$ is $\boldsymbol{A}$-invariant, and the noise-controllable and unobservable subspace $CON_{\mathbf{Q}}UNOB$ is empty, the system trajectory is fully contained in the observable subspace. This distinction is important, as when $\mathbb{A}$ and $\boldsymbol{C}$ have finite rank, the system necessarily has unobservable modes. With this in mind, we introduce the observable $\boldsymbol{A}$-invariant subspace and the notion of Q-observability.

Definition 3.3.3 *For any graphon* $\boldsymbol{A}$*, the subspace* $\mathcal{S}^{\boldsymbol{A}}$ *graphon* $\boldsymbol{A}$ *is the largest* $\boldsymbol{A}$*-invariant subspace of* OB*, i.e.,*

$$\mathcal{S}^{\boldsymbol{A}} = \{\boldsymbol{f} \in OB s.t. \boldsymbol{A}\boldsymbol{f} \in OB\}. \tag{3.50}$$

Definition 3.3.4 *Consider a Q-noise graphon system with state operator* $\mathbb{A} = \boldsymbol{A} + a\mathbb{I}$*, observation operator* $\boldsymbol{C}$*, Q-noise covariance operator* $\mathbf{Q}$*, and set of initial conditions* $\boldsymbol{X}_0$.

The tuple $(\boldsymbol{C}, \mathbb{A}, \mathbf{Q}, \boldsymbol{X}_0)$ *is Q-observable if:*

1. *The* $\boldsymbol{A}$*-invariant subspace* $\mathcal{S}^{\boldsymbol{A}} \subset L^2[0,1]$ *is equal to the domain of* $\boldsymbol{A}$*, and is spanned by the basis functions* $\{\phi_k\}_{k=1}^M$*, with* M *possibly infinite.*

2. *The noise-controllable, unobservable subspace* $CON_{\mathbf{Q}}UNOB$ *is empty, and the noise-controllable observable subspace is contained in* $\mathcal{S}^{\boldsymbol{A}}$*.*

3. *The set of initial conditions* $\boldsymbol{X}_0$ *is contained in* $\mathcal{S}^{\boldsymbol{A}}$*.*

4. *For* $\boldsymbol{C} = [\langle c_1, \cdot\rangle, ..., \langle c_l, \cdot\rangle]^T$ *defined by Eq. (3.45) and the set* $\{\phi_k\}_{k=1}^M$ *spanning* $\mathcal{S}^{\boldsymbol{A}}$*, for* $1 \leq k \leq M$*,*

$$\text{rank} \begin{bmatrix} \langle c_1, \phi_k \rangle \\ \vdots \\ \langle c_l, \phi_k \rangle \end{bmatrix} \geq 1. \tag{3.51}$$

□

Remark: In standard Kalman filter theory, the system tuple (C, A, B) is typically assumed to be detectable and noise-controllable. Here, as the observable subspace is not necessarily invariant with respect to $\mathbb{A}$, it is necessary to assume that the set of initial conditions $\boldsymbol{X}_0$ and the Q-noise $\boldsymbol{w}_t$ exist are observable and invariant with respect to the graphon $\boldsymbol{A}$.

A trivial example of such a state system is given by

$$d\boldsymbol{x}_t = (\int_0^1 \boldsymbol{x}_t^\alpha d\alpha + \boldsymbol{x}_t)dt + d\boldsymbol{w}_t, \tag{3.52}$$

$$\boldsymbol{x}_0(\alpha) = 1 \ \forall \alpha \in [0,1], \tag{3.53}$$

$$d\boldsymbol{y}_t = \int_0^1 \boldsymbol{x}_t^\alpha d\alpha + d\boldsymbol{v}_t \tag{3.54}$$

with the rank one Q-noise process $\boldsymbol{w}_t(\alpha) = W_t$ for all $\alpha \in [0,1]$. The system is not technically rank one; the state operator $\mathbb{A} = 1 + \mathbb{I}$ includes the identity operator, and any square-

integrable odd function shifted to the right by 0.5 is both unobservable and an eigenfunction of $\mathbb{A}$. However, because the Q-noise, the initial condition, and the observation operator are contained in the subspace of functions which are constant for $\alpha \in [0,1]$, the system trajectory is confined to (and is observable in) that subspace.

With this example in mind, we introduce finite rank decomposition for Kalman filtering, analogous to the decomposition for control in [35] and for deterministic systems in [3].

3.3.2.2 Finite rank decomposition

In general, the Kalman filter requires the solution of an $L^2[0,1]$ operator Riccati differential equation. When the state operators $\mathbb{A}$ and $\mathbf{Q}$ have finite rank, and the tuple $(\boldsymbol{C}, \mathbb{A}, \mathbf{Q}, \boldsymbol{X}_0)$ is Q-observable, then the Kalman filter is equivalent to the solution of a finite-dimensional Riccati equation. Effectively, this is because the limit system exists on a finite-dimensional subspace. For clarity, assume that the system is uncontrolled. The analysis still applies for controlled systems.

Definition 3.3.5 *A Q-observable tuple $(\boldsymbol{C}, \mathbb{A}, \mathbf{Q}, \boldsymbol{X}_0)$ is finite rank if the observable $\boldsymbol{A}$-invariant subspace $\mathcal{S}^{\boldsymbol{A}}$ is spanned by the set of M orthonormal functions denoted $\mathcal{V}^M = span\{\phi_k\}_{k=1}^M$.*

Theorem 3.3.4 *Given a finite rank Q-observable tuple $(\boldsymbol{C}, \mathbb{A}, \mathbf{Q}, \boldsymbol{X}_0)$, assume that the observation operator $\boldsymbol{C}$ is of the form*

$$\boldsymbol{C}\boldsymbol{f} = [\langle c_1, \boldsymbol{f}\rangle \dots \langle c_l, \boldsymbol{f}\rangle], \tag{3.55}$$

and that

$$rank \begin{bmatrix} \langle c_1, \phi_k\rangle \\ \vdots \\ \langle c_l, \phi_k\rangle \end{bmatrix} \geq 1, \quad 1 \leq k \leq M. \tag{3.56}$$

Then, the Riccati equation of the Kalman filter is $M \times M$-dimensional.

Proof: Define the $M \times M$ matrices A and Q as

$$A_{ij} = \langle \phi_i, \boldsymbol{A}\phi_j \rangle \tag{3.57}$$

$$Q_{ij} = \begin{cases} \mu_i, & i = j \\ 0, & i \neq j \end{cases} \tag{3.58}$$

Similarly, define the $l \times M$ observation matrix C by

$$C_{ij} = \begin{bmatrix} \langle c_1, \phi_1 \rangle & \dots & \langle c_1, \phi_M \rangle \\ \vdots & \ddots & \vdots \\ \langle c_l, \phi_1 \rangle & \dots & \langle c_l, \phi_M \rangle \end{bmatrix} \tag{3.59}$$

$$\tag{3.60}$$

This allows the decomposition of the system state $\boldsymbol{x}_t$ into two components: the projection onto the subspace spanned by $\mathcal{V}^M$ (denoted $\mathcal{S}$) and its orthogonal complement (denoted $\mathcal{S}^\perp$),

$$\boldsymbol{x}_t = \boldsymbol{x}_t^{\mathcal{V}} + \boldsymbol{x}_t^{\mathcal{V}\perp}, \tag{3.61}$$

$$\boldsymbol{x}_t^{\mathcal{V}} := \sum_{k=1}^{M} \langle \boldsymbol{x}_t, \phi_k \rangle \phi_k \tag{3.62}$$

$$\boldsymbol{x}_t^{\mathcal{V}\perp} := \boldsymbol{x}_t - \boldsymbol{x}_t^{\mathcal{V}}. \tag{3.63}$$

Note that $\boldsymbol{x}_t^{\mathcal{V}}$ has M dimensions, and $\boldsymbol{x}_0^{\mathcal{V}} \in \boldsymbol{X}_0$. This allows the definition of the M dimen-

sional system x_t^M projecting $\boldsymbol{x}_t$ to $\mathcal{S}$ (as well as the corresponding control u_t^M, if any),

$$x_t^M = \begin{bmatrix} \langle \boldsymbol{x}_t, \phi_1 \rangle \\ \langle \boldsymbol{x}_t, \phi_2 \rangle \\ \vdots \\ \langle \boldsymbol{x}_t, \phi_M \rangle \end{bmatrix}, \quad x_t^M \in \mathcal{R}^M, \tag{3.64}$$

As $\mathbf{Q}$ is assumed to be finite-dimensional, the Q-noise $\boldsymbol{w}_t$ is equivalent to the M dimensional Wiener process

$$w_t^M = \sum_{k=1}^{M} \sqrt{\mu_k} W_t^k, \quad w_t^M \in \mathcal{R}^M. \tag{3.65}$$

Further, this satisfies the M dimensional stochastic differential equation,

$$dx_t^M = [(A + aI)x_t^M]dt + dw_t^M, \tag{3.66}$$

$$x_0^M = \sum_{k=1}^{M} \langle \boldsymbol{x}_0, \phi_k \rangle \phi_k \tag{3.67}$$

By assumption on the span of the observation operator, the observation process only acts on the $\boldsymbol{x}_t^{\mathcal{V}}$ process. The observation noise process $\boldsymbol{v}_t$ (with covariance matrix R) is already l-dimensional, and hence does not need to be redefined. The decomposed system can then be written as the solution to the coupled differential equations,

$$\boldsymbol{x}_t = \boldsymbol{x}_t^{\mathcal{V}} + \boldsymbol{x}_t^{\mathcal{V}^\perp}, \tag{3.68}$$

$$dx_t^M = [(A + aI)x_t^M]dt + dw_t^M, \tag{3.69}$$

$$x_0^M = \begin{bmatrix} \langle \boldsymbol{x}_0, \phi_1 \rangle \\ \vdots \\ \langle \boldsymbol{x}_0, \phi_M \rangle \end{bmatrix}, \qquad x_0^M \in \mathcal{R}^M \tag{3.70}$$

$$d\boldsymbol{x}_t^{\mathcal{V}^\perp} = a\boldsymbol{x}_t^{\mathcal{V}^\perp} dt, \tag{3.71}$$

$$\boldsymbol{x}_0^{\mathcal{V}^\perp} = \boldsymbol{x}_0 - \sum_{k=1}^{M} x_0^M \phi_k, \tag{3.72}$$

$$dy_t = C x_t^M dt + d\boldsymbol{v}_t \tag{3.73}$$

This allows the full decomposition of the Kalman filter process $\hat{\boldsymbol{x}}_t$ on a finite-rank graphon system into the M-dimensional process $\hat{x}_t^M$ and its orthogonal complement, $\hat{\boldsymbol{x}}_t^{\mathcal{V}^\perp}$. These jointly satisfy the following coupled differential equations,

$$\hat{\boldsymbol{x}}_t = \sum_{k=1}^{M} [\hat{x}_t^M]_k \phi_k + \hat{\boldsymbol{x}}_t^{\mathcal{V}^\perp}, \tag{3.74}$$

$$d\hat{\boldsymbol{x}}_t^{\mathcal{V}^\perp} = a\hat{\boldsymbol{x}}_t^{\mathcal{V}^\perp} dt, \qquad \hat{\boldsymbol{x}}_t^{\mathcal{V}^\perp} \in L^2[0,1], \tag{3.75}$$

$$\hat{\boldsymbol{x}}_0^{\mathcal{V}^\perp} = \boldsymbol{x}_0 - \sum_{k=1}^{M} [x_0^M]_k \phi_k, \tag{3.76}$$

$$\begin{aligned} d\hat{x}_t^M =& (A + a\mathbb{I})\hat{x}_t^M dt + P_t^M (C)^{\mathrm{T}} (R)^{\mathrm{T}} (dy_t - C x_t^M dt), \\ & \hat{x}_t^M \in \mathcal{R}^M \hat{x}_0^M \text{ given}, \end{aligned} \tag{3.77}$$

where $P_t^M \geq 0$ is the $M \times M$ dimensional matrix satisfying the Riccati equation,

$$\begin{aligned} \frac{d}{dt} P_t^M =& (A + a\mathbb{I}) P_t^M + P_t^M (A + a_N \mathbb{I})^{\mathrm{T}} \\ & + Q^M - P_t^M (C)^{\mathrm{T}} (R)^{-1} C P_t^M, \end{aligned} \tag{3.78}$$

$$P_0^M = \mathrm{cov}(\hat{x}_0^M - x_0^M, \hat{x}_0^M - x_0^M), \quad P_t \in \mathcal{R}^M \times \mathcal{R}^M. \tag{3.79}$$

□

Note: As the noise-controllable and unobservable subspace is empty, the Q-noise process $\boldsymbol{w}_t$ is wholly contained in the finite-dimensional space spanned by $\mathcal{V}^M$. This allows the calculation of $\hat{\boldsymbol{x}}_t^{\mathcal{V}^\perp}$ as

$$\hat{\boldsymbol{x}}_t^{\mathcal{V}^\perp} = e^{at} \hat{\boldsymbol{x}}_0^{\mathcal{V}^\perp}. \tag{3.80}$$

By the definition of Q-observability, the initial condition is contained in the observable subspace OB. For systems where the initial condition is not known, the filter error is unstable unless the system is stable in any unobserved modes.

The requirement that $\boldsymbol{C}$ only measure the system state contained in the span of $\mathcal{V}^M$ is restrictive. Relaxing this to allow measurement of the orthogonal complement process would not allow the system to be solved with an $M \times M$ Riccati equation, and would instead require an infinite-dimensional Riccati equation.

3.4 Separation Principle

For every graph-averaging system in the sequence x_t^N converging to the graphon limit system $\boldsymbol{x}_t$, the Separation Principle applies. Hence, there is a natural question: under which circumstances does the separation principle apply to the graphon limit system?

For this section, we assume that the limit control operator $\mathbb{B} = \boldsymbol{B} + b\mathbb{I}$ has non-zero local forcing constant b. This ensures that the system is always controllable. First, we restate the linear quadratic regulator problem with fully observed system state:

Definition 3.4.1 (Linear Quadratic Regulator) *Given a linear Q-noise system with state process $\boldsymbol{x}_t$ satisfying*

$$d\boldsymbol{x}_t = (\mathbb{A}\boldsymbol{x}_t + \mathbb{B}\boldsymbol{u}_t)dt + d\boldsymbol{w}_t, \quad \boldsymbol{x}_0 \in L^2[0,1], \tag{3.81}$$

find the control $\boldsymbol{u}_t^o \in L^2[0,1]$ adapted to the filtration consisting of $\{\boldsymbol{x}_s, 0 \leq s \leq t\}$ that infimizes the performance function

$$\begin{aligned} J(\boldsymbol{x}_0, \boldsymbol{u}) =& \mathbb{E}\bigg[\int_0^T \langle \boldsymbol{x}_s, \mathbb{M}\boldsymbol{x}_s\rangle + \langle \boldsymbol{u}_s, \mathbb{R}\boldsymbol{u}_s\rangle\bigg] \\ &+ \mathbb{E}\bigg[\langle \boldsymbol{x}_T, \mathbb{M}_T\boldsymbol{x}_T\rangle\bigg]. \end{aligned} \tag{3.82}$$

where $\mathbb{M} : L^2[0,1] \to L^2[0,1]$, $\mathbb{M} \geq 0$ and $\mathbb{R} : L^2[0,1] \to L^2[0,1]$, $\mathbb{R} > 0$.

This optimal control problem (abbreviated Q-LQG) has the well-known solution given by the following theorem.

Theorem 3.4.1 ([13]) *Suppose that* $\mathbb{M}, \mathbb{R}, \mathbb{M}_T$ *are bounded positive self-adjoint* $L^2[0,1]$ *operators, and that* $\mathbb{R} : L^2[0,1] \to L^2[0,1]$ *is invertible. Then, the performance function (3.82) is minimized by* $\boldsymbol{u}_t = -\mathbb{R}^{-1}\mathbb{B}^* S_t \boldsymbol{x}_t$*, where* $S : [0,1] \times [0,1] \times [0,T] \to \mathcal{R}$ *is an* $L^2[0,1]$ *linear operator for all* t *whose kernel satisfies the following Riccati equation,*

$$\begin{aligned} -\frac{d}{dt}\langle S_t \boldsymbol{v}, \boldsymbol{v}\rangle =& 2\langle \mathbb{A}\boldsymbol{v}, S_t \boldsymbol{v}\rangle - \langle S_t \mathbb{B}\mathbb{R}^{-1}\mathbb{B}^* S_t \boldsymbol{v}, \boldsymbol{v}\rangle + \langle \mathbb{M}\boldsymbol{v}, \boldsymbol{v}\rangle, \qquad \forall \boldsymbol{v} \in L^2[0,1] \\ S_T =& \mathbb{M}_T. \end{aligned} \tag{3.83}$$

Proof: See [13, Sec. 4] with $F = \mathbb{I},\ D = 0,\ C = 0$ (hence $\Gamma(\cdot) = 0$ and $\Delta(S_t) = 0$). □

The convergence of the standard LQG problem on a network sequence to the graphon Q-LQG problem is shown in [35]. The Separation Principle for Q-Wiener Process Linear Quadratic Regulator problems (derived by Curtain and Ichikawa [18]) yields the following optimal control law and linear state estimator for the system adapted to graphon Q-LQG systems:

Theorem 3.4.2 (Separation Principle) *Consider a Q-LQG problem minimizing the performance functional* J *on the time interval* $[0,T]$*,*

$$J(\boldsymbol{x}_0, \boldsymbol{u}) = \mathbb{E}\bigg[\int_0^T \langle \boldsymbol{x}_s, \mathbb{M}\boldsymbol{x}_s\rangle + \langle \boldsymbol{u}_s, \mathbb{R}\boldsymbol{u}_s\rangle\bigg] + \mathbb{E}\bigg[\langle \boldsymbol{x}_T, \mathbb{M}_T \boldsymbol{x}_T\rangle\bigg], \tag{3.84}$$

subject to $\mathbb{M} \geq 0$*,* $\mathbb{R} > 0$*,*

$$d\boldsymbol{x}_t = (\mathbb{A}\boldsymbol{x}_t + \mathbb{B}\boldsymbol{u}_t)dt + d\boldsymbol{w}_t, \quad \boldsymbol{x}_0 \in L^2[0,1], \tag{3.85}$$

with the finite-dimensional observation process

$$d\boldsymbol{y}_t = \boldsymbol{C}\boldsymbol{x}_t dt + d\boldsymbol{v}_t, \quad \boldsymbol{y}_t \in \mathcal{R}^l, \tag{3.86}$$

the optimal linear state estimator $\hat{\boldsymbol{x}}_t$ *satisfies equation (3.21) where* $\boldsymbol{P}_t$ *equation (3.23) and* $\boldsymbol{K}_t = \boldsymbol{P}_t \boldsymbol{C}^T \mathbf{R}^{-1}$*, and the optimal control* $\boldsymbol{u}_t^o = -\mathbb{R}^{-1}\mathbb{B}^* S_t \hat{\boldsymbol{x}}_t$*, where* S_t *is the solution to the infinite-dimensional Riccati equation (3.83), and the optimal control has the value*

$$J(\boldsymbol{x}_0, \boldsymbol{u}^o) = trace(\mathbb{M}_t \boldsymbol{P}_T) + \int_0^T + trace(\mathbb{M}\boldsymbol{P}_s)ds + \int_0^T trace(S_s \boldsymbol{P}_s \boldsymbol{C}^* \mathbf{R}^{-1} \boldsymbol{C} \boldsymbol{P}_s)ds. \tag{3.87}$$

See [14, Section V] for details. □

Finally, for the case of sequences of partially observed Q-LQG problems on graph-averaging systems which converge to graphon Q-LQG problems, we present the following theorem.

Theorem 3.4.3 *Define a graph-averaging Q-LQG problem with partial observations with system parameters* $(\mathbb{A}^{[N]}, \mathbb{B}^{[N]})$*, state noise covariance operator* $\mathbf{Q}^{[N]}$*, cost operators* $(\mathbb{M}^{[N]}, \mathbb{M}_T^{[N]}, \mathbb{R}^{[N]})$*, observation operator* $\boldsymbol{C}^{[N]}$*, and observation noise operator* $\mathbf{R}$ *converging to the respective operators* $(\mathbb{A}, \mathbb{B}, \mathbf{Q}, \mathbb{M}, \mathbb{M}_T, \mathbb{R}, \boldsymbol{C}, \mathbf{R})$ *in operator norm and initial condition* $\boldsymbol{x}_0^{[N]}$ *converging to* $\boldsymbol{x}_0$ *in* $L^2[0,1]$ *norm. Then the optimal linear filter* $\hat{\boldsymbol{x}}_t^{[N]}$ *and the optimal control for the finite graph problem* $\boldsymbol{u}_t^{[N],o}$ *converges to the optimal linear filter* $\hat{\boldsymbol{x}}_t$ *and the optimal control of the graphon problem,* $\boldsymbol{u}_t^o$ *in mean,*

$$\lim_{N\to\infty} \mathbb{E}[||\hat{\boldsymbol{x}}_t^{[N]} - \hat{\boldsymbol{x}}_t||_2] = 0, \quad t \in [0,T], \tag{3.88}$$

$$\lim_{N\to\infty} \mathbb{E}[||\boldsymbol{u}_t^{[N],o} - \boldsymbol{u}_t^o||_2] = 0, \quad t \in [0,T]. \tag{3.89}$$

Proof: The first limit is found by fixing $\hat{\boldsymbol{u}_t^{[N]}}$ as the input for both the finite graph-averaging system and the limit graphon system, and applying Theorem 3.3.2 to find the Kalman filter of the graphon system. The second limit is necessarily true as a consequence of Theorem 2.2.3.

□

Consider a sequence of linear quadratic Gaussian problems on a sequence of increasingly large finite graph systems that converges to the Q-observable finite rank system in the sense that the graphon operators of the LQ Gaussian filtering problems defined on a given sequence of increasingly large finite graph systems converge. Then, the theorem below holds.

Theorem 3.4.4 *Let the piecewise constant tuple* $(\mathbb{A}^{[N]}, \mathbb{B}^{[N]}, \boldsymbol{C}^{[N]}, \mathbf{Q}^{[N]}, \mathbb{M}^{[N]}, \mathbb{M}_T^{[N]}\mathbb{R}^{[N]})$ *converge to the tuple* $(\mathbb{A}, \mathbb{B}, \boldsymbol{C}, \mathbf{Q}, \mathbb{M}, \mathbb{M}_T, \mathbb{R})$ *in* $L^2[0,1]$*-operator norm and the piecewise constant initial condition* $\boldsymbol{x}_0^{[N]}$ *converge to the* $L^2[0,1]$ *initial condition* $\boldsymbol{x}_0$.

Further, assume that the following conditions of the limit system hold:

1. *The tuple* $(\boldsymbol{C}, \mathbb{A}, \mathbf{Q}, \boldsymbol{X}_0)$ *is Q-observable by Definition 3.3.4.*

2. *The tuple* $(\boldsymbol{C}, \mathbb{A}, \mathbf{Q}, \boldsymbol{X}_0)$ *is finite rank by Definition 3.3.5, and satisfies the conditions of Theorem 3.3.4.*

3. *The cost operators satisfy* $\mathbb{M} \geq 0$, $\mathbb{M}_T \geq 0$, *and* $\mathbb{R} > 0$.

Then, the Kalman filter process of the finite graph system $\hat{\boldsymbol{x}}_t^{[N]}$ *converges to the limit graphon Kalman filter* $\hat{\boldsymbol{x}}_t$, *and the optimal control input of the finite graph system* $\boldsymbol{u}_t^{[N]}$ *converges to the optimal control input of the limit graphon system* $\boldsymbol{u}_t$. *Further, the limit graphon Kalman filter* $\hat{\boldsymbol{x}}_t$ *and the limit optimal control input* $\boldsymbol{u}_t$ *are determined by finite-dimensional differential Riccati equations.*

Proof: The result is a direct consequence of a system satisfying Definition 3.3.4, and the assumptions of Theorem 3.3.4, and Theorem 3.4.3.

□

Next, we demonstrate Theorem 3.4.4 by modeling and controlling finite graph systems with many nodes using the finite rank limit.

3.5 Numerical Demonstrations

The strongest motivating case for the convergence results of the graphon Kalman filter is to show that systems on large graphs in a sequence converging to a graphon limit can be analyzed in the limit. In particular, when the limit is low rank, the finite graph system can be approximated with a number of equations lower than the number of nodes of the graph. This would not require the specific structure of the graph to be known. We demonstrate this with two numerical examples. First, it is shown that the Kalman filter on an uncontrolled Erdos-Renyi graph system is well-approximated by the graphon Kalman filter with observation of the average state at each node, though the filter itself is unstable due to the unobserved modes of the random graph system. Then, it is shown that even though the graphon filter is unstable for the finite graph system, the system can be stabilized using the Q-Linear Quadratic Gaussian control applied to the graphon filter.

For each example, a uniform 100-point discretization of the unit interval is used to represent a graph of 100 nodes, and the graph is generated using the W-random graph method [1]. The W-random graph method is as follows:

- Let $\boldsymbol{W} : [0,1] \times [0,1] \to [0,1]$ be a graphon.
- Begin with a set of N vertices in a graph G_N with no edges and a uniform partition $\mathcal{P}$ of the unit interval into $N-1$ segments, each segment denoted $\mathcal{P}_k = [\frac{k-1}{N}, \frac{k}{N})$ $1 \leq k \leq N-2$ and $\mathcal{P}_{N-1} = [\frac{k-1}{N}, \frac{k}{N}]$.
- For $1 \leq k \leq N-1$, assign vertex v_k to the point $\alpha_k = \frac{k-1}{N}$, and assign v_N to the point $\alpha_N = 1$.
- For every pair of vertices $i, j, 1 \leq i, j \leq N$, assign an edge between v_i and v_j with probability $\boldsymbol{W}(\alpha_i, \alpha_j)$ independently.

As N tends to infinity, the adjacency matrix of G_N tends to the graphon $\boldsymbol{W}$ in the cut metric [1]. The following experiments show that, even for relatively small numbers of nodes,

the graphon limit can be used to model stochastic systems on graphs.

3.5.1 Erdos-Renyi system

To demonstrate this on the simplest $L^2[0,1]$ system, set both the graphon $\boldsymbol{A}$ to be the Erdos-Renyi graphon and the Q-noise covariance to be a one-dimensional noise sharing the same eigenspace. Set the graphon limit to be the constant function $\boldsymbol{A}(\alpha,\beta) = 0.2, (\alpha,\beta) \in [0,1]^2$, with the initial state and filter conditions $\boldsymbol{x}_0(\alpha) = 1,\ \alpha \in [0,1]$. The terminal time T is 10.

The adjacency matrix A^N of a finite graph of 100 nodes (generated using the W-random graph method) is shown in Fig. 3.1-A. This is used to create the piecewise constant graphon $\boldsymbol{A}^{[N]}$, as described in Section 2.2.5.

The eigenfunction of the Erdos-Renyi graphon $\boldsymbol{A}$ is the constant function $\phi(\alpha) = 1$. The observation operator $\boldsymbol{C}$ is the average value of the state over the unit interval:

$$\boldsymbol{C}\boldsymbol{x}_t = \int_0^1 \boldsymbol{x}_t(\alpha)d\alpha, \tag{3.90}$$

with the observation error $\boldsymbol{v}_t \sim W(0, 0.1)$, and let $\boldsymbol{w}_t$ be the one-dimensional Q-noise with constant covariance operator $\mathbf{Q}(\alpha,\beta) = 0.05$. Then the system $\boldsymbol{x}_t$ with observation process $\boldsymbol{y}_t$ satisfies

$$d\boldsymbol{x}_t(\alpha) = \left(\int_0^1 \boldsymbol{A}^{[N]}(\alpha,\beta)\boldsymbol{x}_t(\beta)d\beta\right)dt + d\boldsymbol{w}_t, \tag{3.91}$$

$$\boldsymbol{x}_0(\alpha) = 1, \tag{3.92}$$

$$d\boldsymbol{y}_t = \boldsymbol{C}\boldsymbol{x}_t dt + d\boldsymbol{v}_t, \quad \boldsymbol{y}_t \in \mathcal{R}^l, \tag{3.93}$$

and the filter $\hat{\boldsymbol{x}}_t$ satisfies

$$d\hat{\boldsymbol{x}}_t = 0.2\int_0^1 \hat{\boldsymbol{x}}_t(\alpha)d\alpha dt + K_t(d\boldsymbol{y}_t - \boldsymbol{C}\hat{\boldsymbol{x}}_t dt), \tag{3.94}$$

$$\hat{\boldsymbol{x}}_0(\alpha) = 1. \tag{3.95}$$

The finite graph system is not Q-observable, as the random finite graph adjacency matrix (Fig. 3.1-A) is not observable with the observation operator $\boldsymbol{C}$. However, the low rank graphon limit provides a reasonable approximation of the graph system trajectory. Fig. 3.1-B shows the state trajectory of the finite system. The ridges in the node index dimension are caused by the random construction of the adjacency matrix. Fig. 3.1-C shows the Kalman filter of the system calculated using the graphon $\boldsymbol{A}(\alpha, \beta) = 0.2$. The Kalman filter in this instance is one-dimensional, and can be calculated as a single equation.

Fig. 3.1-D shows the root squared distance of the graph system state and the Kalman filter, calculated as

$$rsd(\boldsymbol{x}_t, \boldsymbol{x}_t, t) = \int_0^1 \sqrt{\langle (\boldsymbol{x}_t(\alpha) - \hat{\boldsymbol{x}}_t(\alpha)), (\boldsymbol{x}_t(\alpha) - \hat{\boldsymbol{x}}_t(\alpha)) \rangle} d\alpha,$$

showing that the filter approximates the average state of the system. While the filter accurately tracks the average state value at each time, the filter is unstable due to the random construction of $\boldsymbol{A}^{[N]}$.

Despite the filter of the uncontrolled system being unstable, the graphon limit can be used to stabilize the system. Modifying the system by adding the (local) control $\boldsymbol{u}_t$,

$$\begin{aligned} d\boldsymbol{x}_t(\alpha) =& \left(\int_0^1 \boldsymbol{A}^{[N]}(\alpha, \beta) \boldsymbol{x}_t(\beta) d\beta + \boldsymbol{u}_t(\alpha) \right) dt + d\boldsymbol{w}_t, \\ \boldsymbol{x}_0(\alpha) =& 1, d\boldsymbol{y}_t = \boldsymbol{C}\boldsymbol{x}_t dt + d\boldsymbol{v}_t, \quad \boldsymbol{y}_t \in \mathcal{R}^l, \end{aligned} \tag{3.96}$$

with the filter $\hat{\boldsymbol{x}}_t$ satisfying

$$d\hat{\boldsymbol{x}}_t = \left(0.2 \int_0^1 \hat{\boldsymbol{x}}_t(\alpha) d\alpha + \boldsymbol{u}_t \right) dt + K_t(d\boldsymbol{y}_t - \boldsymbol{C}\hat{\boldsymbol{x}}_t dt), \tag{3.97}$$

$$\hat{\boldsymbol{x}}_0(\alpha) = 1. \tag{3.98}$$

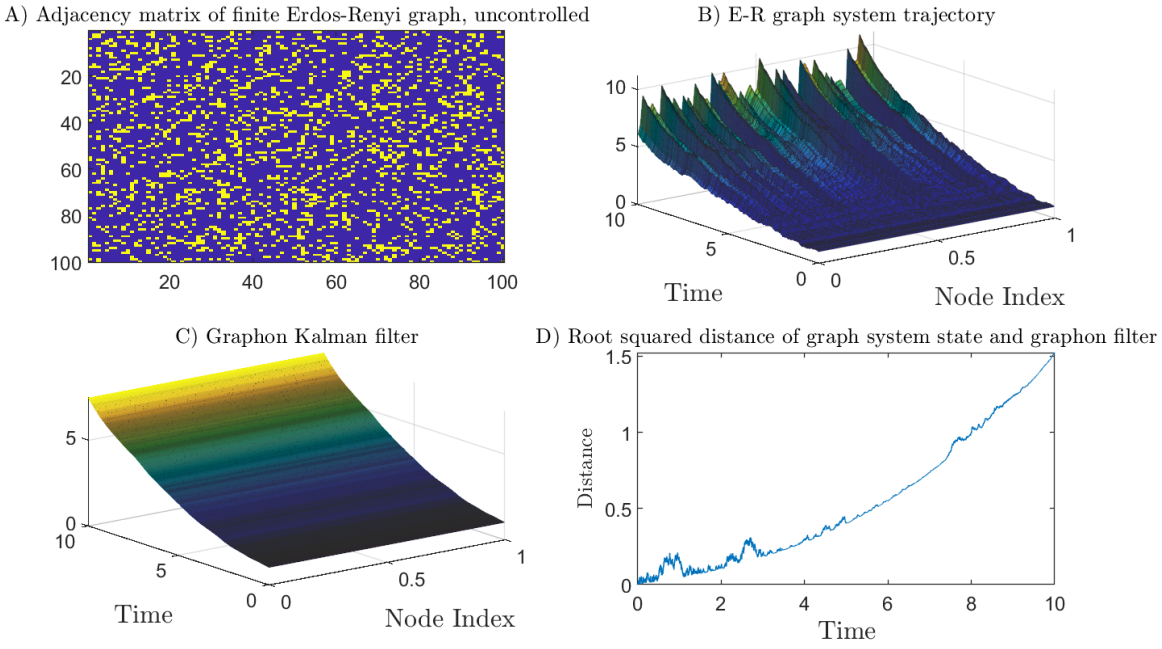

Figure 3.1: A: The finite graph adjacency matrix generated using the W-random graph method. This adjacency matrix is used to define $\boldsymbol{A}^{[N]}$.B: The state trajectory of the finite graph system. There are two sources of randomness: the random generation of the graph and the Q-noise in the system. C: The Kalman filter trajectory of the system. D: The root squared difference of the finite graph system trajectory and the graphon Kalman filter.

We extend the previous system to a Q-Linear Quadratic Gaussian problem by defining the cost operators $\mathbb{M} = \mathbb{I}$, $\mathbb{R} = \mathbb{I}$, and the graphon limit $\boldsymbol{A}$ is used to calculate the LQG solution. The terminal time is extended to $T = 20$ in order to show that the controlled system is stable. Then, the optimal feedback control is the function $\boldsymbol{u}_t = -S_t\hat{\boldsymbol{x}}_t$ satisfying the Separation Principle, Theorem 4.2.

Fig. 3.2-A shows the controlled state trajectory of the graph system, Fig. 3.2-B shows the Kalman filter trajectory, and Fig. 3.2-C shows the root squared distance between the filter and the state trajectory.

Despite the Kalman filter and the LQR control equations using the graphon limit system (the first of which can be calculated with one equation, and the second of which can be calculated with two equations [39]) instead of the full finite graph, the root squared distance between the state and the filter is stable about the origin. This agrees with Theorem 3.4.4. While directly using the full graph A^N to calculate the Kalman filter and LQG solution would yield a more accurate state estimate, this would require the full knowledge of the network and the solution of a 100×100 dimensional Riccati equation.

3.5.2 Uniform Attachment Graphon

For one further uncontrolled system to examine, consider a system where both the graphon $\boldsymbol{A}$ and the covariance operator $\mathbf{Q}$ are given by the Uniform Attachment Graphon (UAG), $\boldsymbol{A}(\alpha, \beta) = 1 - \max(\alpha, \beta)$ ([1]), and $\mathbf{Q} = 0.05\boldsymbol{A}(\alpha, \beta)$. The uniform attachment graphon is infinite rank with strictly positive eigenvalues, and hence the system is unstable.

As shown in [25], the eigenfunctions and eigenvalues of the Uniform Attachment Graphon are

$$(\phi_k(\alpha), \lambda_k) = \left(\sqrt{2}\cos\left(\frac{k\pi\alpha}{2}\right), \frac{4}{k^2\pi^2}\right), \quad k = \{1, 3, 5, ...\}. \tag{3.99}$$

As with the E-R graph, the single observation is the average value of the system at each

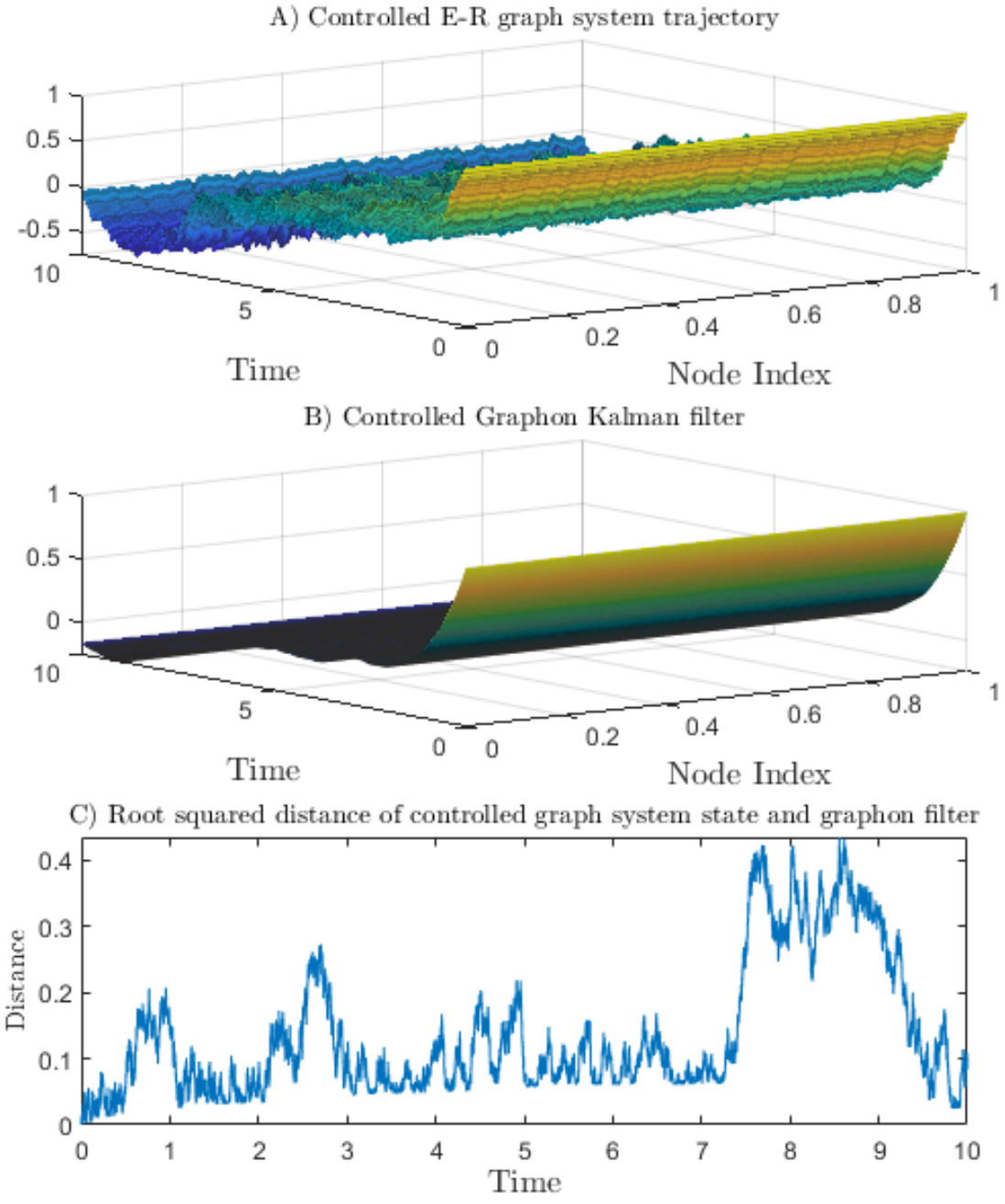

Figure 3.2: A: The state trajectory of the finite graph system controlled using the graphon Kalman filter. B: The graphon Kalman filter of the system. C: The root squared distance of the graph state trajectory and the filter.

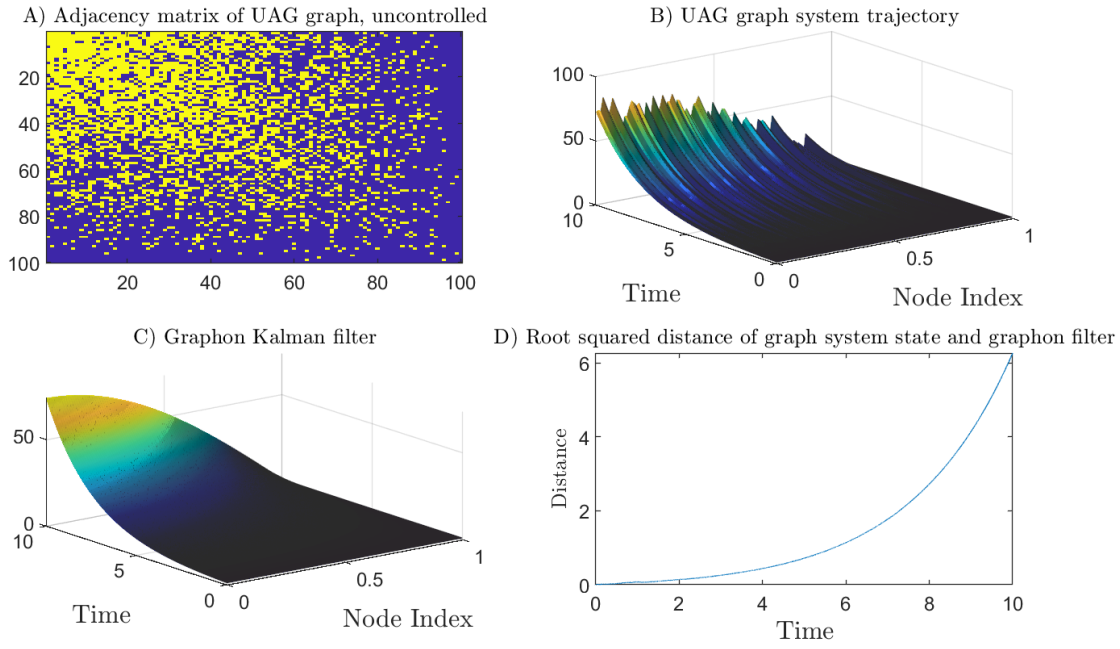

Figure 3.3: A: The finite graph adjacency matrix generated using the W-random graph method with the Uniform Attachment Graphon. This adjacency matrix is used to define $\boldsymbol{A}^{[N]}$. B: The state trajectory of the finite graph system, uncontrolled. There are two sources of randomness: the random generation of the graph and the Q-noise in the system. C: The Kalman filter trajectory of the UAG system. D: The root squared difference of the finite graph system trajectory and the graphon Kalman filter.

time.

Unlike the Erdos-Renyi graph, the adjacency matrix of the UAG shown in Fig. 3.3-A has much more structure based on the node index. As in the Erdos-Renyi case, the state trajectory of the finite graph system (shown in Fig. 3.3-B) is not smooth in the state index as the adjacency matrix is not smooth. The graphon filter (Fig. 3.3-C) effectively tracks the state average, even in the presence of observation and state noise. The root squared distance between the UAG graph system and the graphon limit filter (Fig. 3.3) increases exponentially due to the instability of the uncontrolled system and the difference between the finite graph and the graphon limit in the operator norm.

As with the Erdos-Renyi graph, the unmodelled modes cause the filter to be unstable. As with the Erdos-Renyi graph, the UAG graph system can be stabilized by applying the graphon state estimate in the optimal control feedback, as expected from Theorem 3.4.3.

The controlled UAG system is shown in Fig. 3.4-A, and the graphon Kalman filter is shown in Fig. 3.4-B. The root squared distance (Fig. 3.4-C) shows that the system is stabilized.

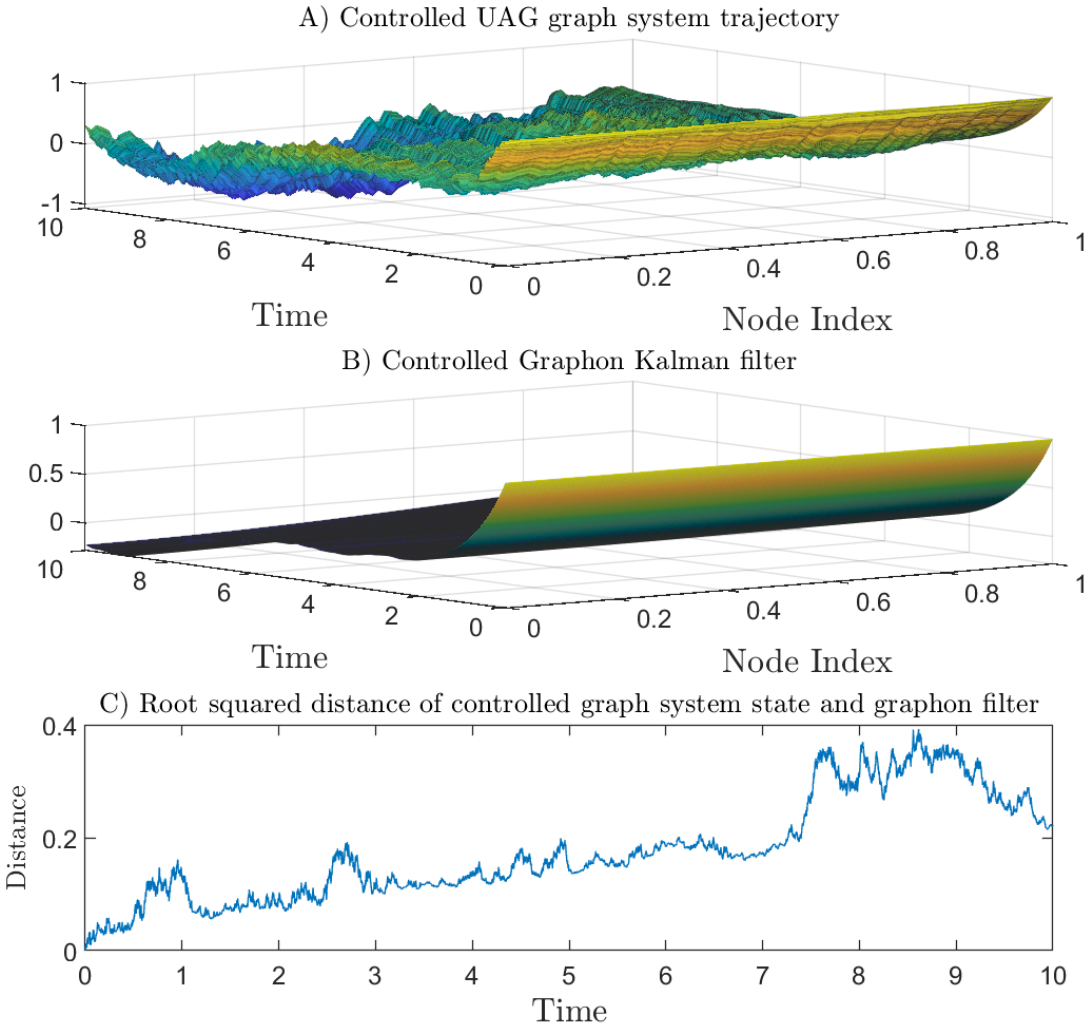

Figure 3.4: A: The state trajectory of the finite UAG system controlled using the graphon Kalman filter. B: The graphon Kalman filter of the system. C: The root squared distance of the graph state trajectory and the filter.

Chapter 4

Field Tracking Games

Chapter 4 extends the work of Gao, Foguen-Tchuendom, and Caines [34] by applying the Q-noise foundations of Dunyak and Caines [9] to discrete-time systems. This model is analogous to the limit behavior of a finite-dimensional graph system with a correlated Gaussian disturbance impacting each node at each time step. It is demonstrated that the discrete-time linear quadratic Q-noise tracking game has an adapted Nash equilibrium solution, and the behavior of the equilibrium solution is demonstrated numerically.

4.1 Introduction

Large systems composed of interacting non-cooperative agents arise in many applications such as cellular networks, financial markets, and electrical grids. The modelling and control of such systems is intractable due to the size and complexity of their respective networks.

In the case of a game with a large number of identical agents, one can use Mean-Field Game theory to find the approximate system behavior by simulating a system with an infinite number of agents and finding the distribution of agents' states under different control methods ([42],[43],[44]). The mean-field game approach simplifies the game, as rather than optimizing with respect to the actions of every individual player, one can optimize with respect to a single representative player.

Standard mean-field games can be extended to games on networks where each node has an infinite population of players by the use of graphons ([23],[45],[22]). Graphon theory [1] allows the adjacency matrix of an infinitely large graph to be represented as a bounded, symmetric operator, providing a limiting object for large, dense graphs. Under the Graphon Mean-Field Games (GMFG) model each node in a network contains a separate, infinite population interacting with the agents local to their node uniformly and the agents in the network through the graphon. As there are an infinite number of agents, the actions of a single agent do not change the mean-field.

Expanding on previous work [46], a linear quadratic game with correlated Gaussian disturbances on an infinitely large dense graph is investigated where each node represents a single agent. A continuous-time, deterministic model with stochastic initial conditions for this type of linear-quadratic game was investigated by Gao, Foguen-Tchuendom, and Caines [34]. To distinguish this from the infinite-agent-per-node GMFG model, this approach was termed the Graphon Field Game model. As in the GMFG model, the actions of any individual agent do not directly affect the field of the system. The Nash equilibria of such a system require the optimality of each agent's chosen actions with respect to the field generated by the ensemble of agents' optimal strategies.

Parise and Ozdaglar [47] present a model for static graphon games. Carmona et al. [48] extend this model to the idiosyncratic noise case using the Fubini extension of standard white noise affecting all agents. Vasal, Mishra, and Vishwanath [49] find a backwards recursive solution to discrete-time graphon games without noise.

This work extends the work of Gao, Foguen-Tchuendom, and Caines [34] by applying the Q-noise foundations of Dunyak and Caines [9] to discrete-time systems. This model is analogous to the limit behavior of a finite-dimensional graph system with a correlated Gaussian disturbance impacting each node at each time step. It is demonstrated that the discrete-time linear quadratic Q-noise tracking game has an adapted Nash equilibrium solution, and the behavior of the equilibrium solution is demonstrated numerically.

Section 4.3 presents the finite network, finite time field-tracking game as motivation for taking the infinite node limit, called the graphon field-tracking game. The general approach used to solve the graphon field tracking game in Section 4.3.2 is:

1. Use the mean-field game principle: a given agent optimizes against an exogenous signal that is indifferent to their own control and state input,

2. Use dynamic programming to find the solution of an arbitrary stochastic tracking problem (Section 4.4.1), and

3. Use the graphon field to recursively generate the tracked signal for each time step (Section 4.4.2).

The second step generates the tracking signal solution in reference to a stochastic adjoint process, which is defined recursively backwards. The third step uses the graphon field to generate the adjoint process for each agent by finding a deterministic backwards operator equation. This is called the Consistency Condition, as it ensures that the graphon field is consistent with each agent's optimizing control input. This behavior is demonstrated numerically in two scenarios: where the maximal eigenvalue of the graphon $\boldsymbol{M}$ is less than one, and where the maximal eigenvalue is equal to one. This causes the state of all players of the game to either stabilize about zero or stabilize about an eigenfunction of the game, respectively.

Section 4.5 extends the analysis to infinite time horizon games with multiplicative discounting. Unlike in the finite time horizon case, the operator equation solutions for the discounted game have multiple solutions. For the case where the graphon $\boldsymbol{M}$ is low rank, a finite number of closed-form solutions are found. It is demonstrated that it is nontrivial to determine which solution is rational for all agents numerically.

For simplicity, the initial formulation is presented where each agent has a scalar state and a scalar control. The extension to games where each agent has multiple states and controls is straightforward, and the notation is presented in Appendix 4.6.1.

4.2 Preliminaries

4.2.1 Notation

- The set of vectors of real numbers of dimension m is denoted $\mathcal{R}^m$.
- Graphons (i.e., bounded symmetric $[0,1]^2$ functions used as the kernels of linear integral operators) are denoted in italicized bold capital letters, and in this chapter are typically written as $\boldsymbol{M}$.
- $L^2[0,1]$ denotes the Hilbert space of real square-integrable functions on the unit interval. In addition, $L^2[0,1]$ is equipped with the standard inner product, denoted $\langle \boldsymbol{u}, \boldsymbol{v} \rangle$. For any function $\boldsymbol{v}$, $\boldsymbol{v}^*$ denotes the adjoint of $\boldsymbol{v}$. As such, $\langle \boldsymbol{u}, \boldsymbol{v} \rangle$ is sometimes written as $\boldsymbol{v}^* \boldsymbol{u}$.
- The identity operator in both $L^2[0,1]$ and finite-dimensional spaces is denoted $\mathbb{I}$.
- A linear integral operator with the kernel $\mathbf{Q} : [0,1]^2 \to \mathcal{R}$ acting on a function $\boldsymbol{f} \in L^2[0,1]$ is defined by

$$(\mathbf{Q}\boldsymbol{f})(x) = \int_0^1 \mathbf{Q}(x,y)\boldsymbol{f}(y)dy, \quad \forall\ x \in [0,1]. \tag{4.1}$$

- The operators $\mathbf{Q}$ are equipped with the standard $L^2[0,1]$ operator norm $||\mathbf{Q}||_{\text{op}}$.
- A symmetric function $\mathbf{Q} : [0,1]^2 \to \mathcal{R}$ is non-negative if the following inequality is satisfied for every function $\boldsymbol{f} \in L^2[0,1]$,

$$\begin{aligned} 0 &\leq \int_0^1 \int_0^1 \mathbf{Q}(x,y)\boldsymbol{f}^*(x)\boldsymbol{f}(y)dxdy \\ &:= \langle \mathbf{Q}\boldsymbol{f}, \boldsymbol{f} \rangle < \infty. \end{aligned} \tag{4.2}$$

  Additionally, denote $\mathcal{Q}$ to be the set of bounded symmetric non-negative functions. All valid Q-noise covariance functions are members of $\mathcal{Q}$.

- Discrete-time Q-noise processes (stochastic processes over the time interval $(0, 1, ..., T)$) will be denoted by the bold font $\boldsymbol{g}_k$. For each $k \in (0, 1, ..., T)$, $\boldsymbol{g}_k$ is an $L^2[0, 1]$ function. The precise definition of a Q-noise process is given in Section 4.2.2.

- The expectation of a random variable at time k with respect to a sigma algebra $\mathcal{F}_k$ is denoted:

$$\mathbb{E}[\cdot|\mathcal{F}_k] := \mathbb{E}_k[\cdot]. \tag{4.3}$$

This chapter focuses on games where each agent possesses a scalar state. The extension to vectors of states is straightforward, and is presented in Section 4.6.1.

4.2.2 Discrete-Time Q-noise Processes

Discrete-time Q-noise processes are $L^2([0, 1])$ valued random processes satisfying the following axioms (modified from [9] for discrete-time processes):

1. Let $\mathbf{Q} \in \mathcal{Q}$, and let $([0, 1] \times \{0, 1, ..., T\} \times \Omega, \mathcal{B}([0, 1] \times \{0, 1, ..., T\} \times \Omega), \mathbb{P})$ be a probability space with the measurable random variable $\boldsymbol{g}_k(\alpha, \omega) : [0, 1] \times \{0, 1, ..., T\} \times \Omega \to \mathbb{R}$ for all $k \in \{0, 1, ..., T\}, \alpha \in [0, 1]$, and $\omega \in \Omega$. For notation, ω is suppressed when the meaning is clear.

2. For all $\alpha \in [0, 1]$, $\boldsymbol{g}_k(\alpha) \sim \mathcal{N}(0, \mathbf{Q}(\alpha, \alpha))$.

3. For all α and β, $\mathbb{E}[\boldsymbol{g}_k(\alpha)\boldsymbol{g}_k(\beta)] = \mathbf{Q}(\alpha, \beta)$.

An orthonormal basis example: Let $\{W_k^1, W_k^2, \cdots\}$ be a sequence of independent standard normal random variables for each $k \in \{0, 1, ..., T\}$. Let $\mathbf{Q} \in \mathcal{Q}$ have a diagonalizing orthonormal basis $\{\phi_r\}_{r=1}^{\infty}$ with eigenvalues $\{\lambda_r\}_{r=1}^{\infty}$. Then

$$\boldsymbol{g}_k(\alpha, \omega) = \sum_{r=1}^{\infty} \sqrt{\lambda_r}\phi_r(\alpha)W_k^r(\omega) \tag{4.4}$$

is a discrete-time Q-noise process. See, for example, [6] and [7] for the construction of general Gaussian measures in Hilbert spaces.

4.3 Problem Statement

4.3.1 Discrete-Time Network System Games

Consider a discrete-time game on a graph $G^N = (V^N, E^N)$ where each node i represents an agent. The state of agent i at time k (denoted x_k^i with control u_k^i) evolves with the following stochastic difference equation:

$$x_{k+1}^i = (ax_k^i + bu_k^i + c\frac{1}{N}\sum_{j=1}^{N} M_{ij}^N x_k^j) + W_k^i \tag{4.5}$$

where $a, b, c \in \mathcal{R}$, M^N is the weighted adjacency matrix of G^N, and $\{W_k^i\}$ is a collection of Gaussian disturbances with covariance matrix Q^N for each k. Subject to the actions of all other agents, each agent i minimizes the expected quadratic cost function with respect to their information set $\mathcal{F}_k^i$, which is the sigma algebra generated by the set $\{x_k^i, z_k^i\}_{i=0}^N$,

$$J^i(u^i, u^{-i}|\{z_k^i\}_{i=1}^N) = \mathbb{E}\left[\sum_{k=0}^{T-1} ||x_k^i - z_k^i||_S^2 + ||u_k^i||_R^2 + ||x_T^i - z_T^i||_S^2 \middle| \mathcal{F}_0^i\right], \tag{4.6}$$

where $z_k^i = \frac{1}{N}\sum_{j=1}^N M_{ij}^N x_k^j$, $||v||_S^2 = Sv^2$ for some $S \in \mathcal{R}$, $R \in \mathcal{R}$, $S \geq 0$ and $R > 0$.

A Nash Equilibrium of the game exists when no agent can benefit by deviating from its current strategy. If the optimal strategy tuple is $\{u^{i*}\}_{i=1}^N$, this implies

$$J^i(u^{i*}, u^{-i*}) \leq J^i(u^i, u^{-i*}) \;\; \forall i \in \{1, ..., N\}. \tag{4.7}$$

As the network size grows, the networked system adjacency matrix M^N approaches its associated *graphon* which is a bounded measurable function mapping $[0,1] \times [0,1] \to [0,1]$, denoted $\boldsymbol{M}$ (see [3], [1]). When the underlying graph is undirected, its graphon is also

symmetric.

4.3.2 Graphon Field Tracking Games

In graphon analysis, as the size of the network tends to infinity, each agent in the system is associated with a point α on the unit interval. Define the discrete-time Q-noise $\boldsymbol{g}_k^\alpha,\ \alpha \in [0,1]$, and the resulting discrete-time system evolves according to

$$\boldsymbol{x}_{k+1}^\alpha = (a\boldsymbol{x}_k^\alpha + b\boldsymbol{u}_k^\alpha + c\boldsymbol{z}_k^\alpha) + \boldsymbol{g}_k^\alpha, \tag{4.8}$$

$$\boldsymbol{z}_k^\alpha = \int_0^1 \boldsymbol{M}(\alpha,\beta)\boldsymbol{x}_k^\beta d\beta \quad \forall\ \alpha \in [0,1]. \tag{4.9}$$

The local field for an agent designated by α refers to the value $\boldsymbol{z}_k^\alpha$ found using the above integral and expectation.

The objective function for the single agent at node α has the limit

$$J^\alpha(\boldsymbol{u}^\alpha, \boldsymbol{x}_0) = \mathbb{E}\left[\sum_{k=0}^{T-1} ||\boldsymbol{x}_k^\alpha - \boldsymbol{z}_k^\alpha||_S^2 + ||\boldsymbol{u}_k^\alpha||_R^2 \middle| \mathcal{F}_0^\alpha\right], \tag{4.10}$$

and its goal is to minimize the objective function for the control strategy $\boldsymbol{u}^\alpha$ adapted to the information pattern $\mathcal{F}_k^\alpha$. For the purposes of this chapter, the full-state information pattern is used, where $\mathcal{F}_k^\alpha = \mathcal{F}_k := \{\boldsymbol{x}_k^\beta,\ \beta \in [0,1]\}$ for each agent α. This is sufficient for each agent to calculate the entire graphon field $\boldsymbol{z}_k$ at time k. This has the value function form:

$$\begin{aligned} V_k^\alpha(\mathcal{F}_k^\alpha) &= \mathbb{E}\big[||\boldsymbol{x}_k^\alpha - \boldsymbol{z}_k^\alpha||_S^2 + ||\boldsymbol{u}_k^\alpha||_R^2 + V_{k+1}(\mathcal{F}_{k+1}^\alpha)|\mathcal{F}_k^\alpha\big], \quad k = (0,1,...,T-1), \\ V_T^\alpha(\mathcal{F}_T^\alpha) &= \mathbb{E}_T[||\boldsymbol{x}_T^\alpha - \boldsymbol{z}_T^\alpha||_S^2] = ||\boldsymbol{x}_T^\alpha - \boldsymbol{d}_T^\alpha||_S^2. \end{aligned} \tag{4.11}$$

The agents are in a Nash equilibrium when the following inequality holds,

$$J^\alpha(\boldsymbol{u}^{\alpha*}, \boldsymbol{u}^{-\alpha*}) \leq J^\alpha(\boldsymbol{u}^\alpha, \boldsymbol{u}^{-\alpha*}),\ \forall\ \alpha \in [0,1]. \tag{4.12}$$

Unlike in the case of finite agent games, taking the limit as the number of agents tends to infinity yields an indifference to the costs of a particular agent α with respect to the strategies of any other specific agent β. Only the strategies of the agents as a mass (taken as a function over the unit interval) affect the cost of a given agent.

As with mean-field games and graphon mean-field games, the graphon field term $\boldsymbol{z}_k^\alpha$ is not dependent on both the state $\boldsymbol{x}_k^\alpha$ and the action $\boldsymbol{u}_k^\alpha$ of any single agent, in the sense that altering $\{\boldsymbol{x}_r^\alpha\}_{0\leq r\leq k}$ or $\{\boldsymbol{u}_r^\alpha\}_{0\leq r\leq k}$ for a particular α does not change $\boldsymbol{z}_k^\alpha$. This is evident from the integral operator definition of $\boldsymbol{z}_k^\alpha$. As with many mean-field game problems, this changes the limit problem from a game to a tracking control problem where each node in the network is penalized for deviating from its associated graphon field.

4.4 Solution to the Q-noise Graphon Field Tracking Game

The game is solved in two steps, first by formulating the response of an individual agent $\alpha \in [0,1]$ as a stochastic tracking problem, then by showing that the individual actions of each agent generate a Nash equilibrium.

4.4.1 Solution to the Stochastic Control Tracking Problem

Assume an agent α is tracking an exogenous square-integrable drift process $\boldsymbol{d}_k(\alpha),\ \alpha \in [0,1]$. Define the state transition equation as

$$\boldsymbol{x}_{k+1}^\alpha = (a\boldsymbol{x}_k^\alpha + b\boldsymbol{u}_k^\alpha + c\boldsymbol{d}_k^\alpha) + \boldsymbol{g}_k^\alpha, \tag{4.13}$$

The value function is found using dynamic programming, and, as above, has the form

$$\begin{aligned} V_k^\alpha(\mathcal{F}_k^\alpha) &= \mathbb{E}\big[||\boldsymbol{x}_k^\alpha - \boldsymbol{d}_k^\alpha||_S^2 + ||\boldsymbol{u}_k^\alpha||_R^2 + V_{k+1}(\mathcal{F}_{k+1}^\alpha)|\mathcal{F}_k^\alpha\big],\quad k = (0,1,...,T-1), \\ V_T^\alpha(\mathcal{F}_T^\alpha) &= \mathbb{E}_T[||\boldsymbol{x}_T^\alpha - \boldsymbol{d}_T^\alpha||_S^2] = ||\boldsymbol{x}_T^\alpha - \boldsymbol{d}_T^\alpha||_S^2. \end{aligned} \tag{4.14}$$

As stated above, this work considers the case where all agents have the full-information set $\mathcal{F}_k$ consisting of $\boldsymbol{x}_k^\eta$ and $\boldsymbol{d}_k^\eta$ for all $\eta \in [0,1]$.

Lemma 4.4.1 *The value function of agent α at time k, V_k^α, is given by*

$$V_k^\alpha(\mathcal{F}_k^\alpha) = \mathbb{E}_k[P_k(\boldsymbol{x}_k^\alpha)^2 + 2\boldsymbol{x}_k^\alpha \boldsymbol{s}_k^\alpha + m_k^\alpha], \tag{4.15}$$
$$k = \{0, ..., T\},$$

where $\mathbb{E}[\cdot|\mathcal{F}_k] := \mathbb{E}_k[\cdot]$. Here, P_k is a positive scalar, and $\boldsymbol{s}_k$ and m_k^α are $L^2([0,1])$ valued functions for all $k = \{0, ..., T\}$ derived from the following backwards recurrence relations:

$$F_k = (R + b^2 P_{k+1})^{-1} abP_{k+1}, \tag{4.16}$$

$$G_k = (R + b^2 P_{k+1})^{-1} bcP_{k+1}, \tag{4.17}$$

$$H_k = (R + b^2 P_{k+1})^{-1} b, \tag{4.18}$$

$$P_k = S + RF_k^2 + P_{k+1}(a - bF_k)^2, \tag{4.19}$$

$$\begin{aligned} \boldsymbol{s}_k^\alpha = &- S\boldsymbol{d}_k^\alpha + F_k R(G_k \boldsymbol{d}_k^\alpha + H_k \mathbb{E}_k[\boldsymbol{s}_{k+1}^\alpha]) \\ &+ (a - bF_k) P_{k+1} \\ &\quad \times \left[(c - bG_k)\boldsymbol{d}_k^\alpha - bH_k \mathbb{E}_k[\boldsymbol{s}_{k+1}^\alpha]\right] \\ &+ (a - bF_k)\mathbb{E}_k[\boldsymbol{s}_{k+1}^\alpha], \end{aligned} \tag{4.20}$$

$$\begin{aligned} m_k^\alpha = &S\boldsymbol{d}_k^\alpha \boldsymbol{d}_k^\alpha + (G_k \boldsymbol{d}_k^\alpha + H_k \mathbb{E}_k[\boldsymbol{s}_{k+1}^\alpha])R \\ &\quad \times (G_k \boldsymbol{d}_k^\alpha + H_k \mathbb{E}_k[\boldsymbol{s}_{k+1}^\alpha]) \\ &+ \left[(c - G_k)\boldsymbol{d}_k^\alpha - bH_k \mathbb{E}_k[\boldsymbol{s}_{k+1}^\alpha]\right] P_{k+1} \\ &\quad \times \left[(c - G_k)\boldsymbol{d}_k^\alpha - bH_k \mathbb{E}_k[\boldsymbol{s}_{k+1}^\alpha]\right] \\ &+ 2\left[(c - G_k)\boldsymbol{d}_k^\alpha - bH_k \mathbb{E}_k[\boldsymbol{s}_{k+1}^\alpha]\right] \mathbb{E}_k[\boldsymbol{s}_{k+1}^\alpha] \\ &+ \mathbf{Q}(\alpha, \alpha) + \mathbb{E}_k[m_{k+1}^\alpha], \end{aligned} \tag{4.21}$$

with the terminal conditions

$$P_T = S, \tag{4.22}$$

$$\boldsymbol{s}_T^\alpha = -S\boldsymbol{d}_T^\alpha, \tag{4.23}$$

$$m_T^\alpha = S||\boldsymbol{d}_T^\alpha||_2^2. \tag{4.24}$$

Further, the optimal control is given by

$$u_k^{o,\alpha} = -(R + b^2 P_{k+1})^{-1} b[P_{k+1}(a\boldsymbol{x}_k^\alpha + c\boldsymbol{d}_k^\alpha) + \mathbb{E}_k[\boldsymbol{s}_{k+1}^\alpha]] \tag{4.25}$$

$$=: -F_k\boldsymbol{x}_k^\alpha - G_k\boldsymbol{d}_k^\alpha - H_k\mathbb{E}_k[\boldsymbol{s}_{k+1}^\alpha]. \tag{4.26}$$

Proof: The proof follows from the ansatz (4.15). See Section 4.6.2. □

The cost m_k^α does not affect the control input $\boldsymbol{u}_k^\alpha$ and does not have a simple closed-form solution, so it is not calculated here. The structure of the tracking control solution (with the feedforward term in the costate $\boldsymbol{s}_{k+1}$) is common in discrete-time tracking problems [50].

The value function above solves the general discrete-time stochastic optimal control problem where an agent α tracks an exogenous signal $\boldsymbol{d}_k^\alpha$. The problem is ill-defined in general since it requires the computation of the expectation of the offset, $\mathbb{E}_k[\boldsymbol{s}_{k+1}^\alpha]$ in terms of the expected terminal value of $\boldsymbol{d}_T^\alpha$, which requires additional assumptions on the process $\boldsymbol{d}_k$.

However, in the graphon field game setting, at each time step k the chosen strategy must generate the local field term $\boldsymbol{z}$, i.e. the optimal input $\{\boldsymbol{u}_k^o,\ k = 0, ..., T-1\}$ must generate a trajectory satisfying $\boldsymbol{z}_k^\alpha = [\boldsymbol{M}\boldsymbol{x}_k](\alpha) = \boldsymbol{d}_k^\alpha$ for all α. This provides additional structure to the tracked stochastic process, and is known as the Consistency Condition for the Nash equilibrium in the limit game [34]. In the full state feedback case, the Consistency Condition allows the expectation of the offset $\boldsymbol{s}_k$ to be explicitly calculated as a linear state process in terms of $\boldsymbol{z}_k$.

4.4.2 Nash Equilibrium Consistency Condition with Full State Information

By the Consistency Condition, for each k, the local field $\boldsymbol{z}_k$ is given by $\boldsymbol{z}_k = \boldsymbol{M}\boldsymbol{x}_k$. As $\boldsymbol{x}_k$ is square-integrable for each k when generated by the optimal strategy $\boldsymbol{u}_k$ and $\boldsymbol{M}$ is an $L^2[0,1]$ to $L^2[0,1]$ operator, the graphon field $\boldsymbol{z}_k$ is square-integrable as well. For the game to yield a Nash equilibrium, it is necessary for all agents to apply their respective control $\boldsymbol{u}_k^\alpha$ and generate the local field process $\boldsymbol{z}_k^\alpha$. To denote the function over the whole index set the superscript α is omitted.

To do this, define two new, time varying operators: $\Gamma_k : L^2[0,1] \to L^2[0,1]$ which calculates the expected graphon field $\boldsymbol{z}_{k+1}$ at the next time-step given the state of all agents at the current time-step, and $\Psi_k : L^2[0,1] \to L^2[0,1]$ which calculates the tracking adjoint process $\boldsymbol{s}_k$ as a linear function of the current graphon field $\boldsymbol{z}_k$.

Lemma 4.4.2 *Let the signal to be tracked be given by $\boldsymbol{z}_k = \boldsymbol{M}\boldsymbol{x}_k$ for time k. Let Γ_k and Ψ_k be $L^2([0,1])$ operators which are defined by the backwards recursion equations*

$$\begin{aligned}\Psi_k =& - S\mathbb{I} + F_k R(G_k\mathbb{I} + H_k\Psi_{k+1}\Gamma_k) \\ &+ (a - bF_k)P_{k+1}\big[(c - bG_k)\mathbb{I} - b\Psi_{k+1}H_k\Gamma_k\big] \\ &+ (a - bF_k)\Psi_{k+1}\Gamma_k, \end{aligned} \tag{4.27}$$

$$\Gamma_k = (\mathbb{I} + bH_k\boldsymbol{M}\Psi_{k+1})^{-1}[(a - bF_k)\mathbb{I} + (c - bG_k)\boldsymbol{M}] \tag{4.28}$$

with the terminal condition

$$\Psi_T = - S\mathbb{I}. \tag{4.29}$$

Assume that for all $k = \{0, ..., T-1\}$, the inverse $(\mathbb{I} + bH_k\boldsymbol{M}\Psi_{k+1})^{-1}$ exists. Then,

$$\mathbb{E}_k[\boldsymbol{z}_{k+1}] = \Gamma_k\boldsymbol{z}_k, \tag{4.30}$$

$$\boldsymbol{s}_k = \Psi_k\boldsymbol{z}_k, \tag{4.31}$$

and the trajectory generated by

$$\boldsymbol{u}_k = -F_k \boldsymbol{x}_k - (G_k \mathbb{I} + H_k \Psi_{k+1} \Gamma_k) \boldsymbol{z}_k \tag{4.32}$$

gives the optimal tracking trajectory for each α*.*

Proof: See Section 4.6.3.

Combining Lemma 4.6.2 and Section 4.6.3 yields the Nash equilibrium of the game.

Theorem 4.4.3 *Given the limit graphon tracking game of the type (4.10) for the family of systems (4.8), where each agent* α *indexed by* $[0,1]$ *has the total information pattern (that is, each agent knows the states of all other agents at the current time step),* $\mathcal{F}_k^\alpha = \{\boldsymbol{x}_k, \boldsymbol{z}_k\}$ *for all* $\alpha \in [0,1]$*, the control strategy given in equations (4.27), (4.28), and (4.32) yields a Nash equilibrium.*

4.4.3 Numerical Simulation

To demonstrate the behavior of the field tracking game, we illustrate some numerical examples. There are two general phenomena depending on the maximal eigenvalue of the graphon $\boldsymbol{M}$. Namely, as the state $\boldsymbol{x}_k^\alpha$ attempts to track the field average $\boldsymbol{z}_k^\alpha$, the optimal trajectory (without noise) would satisfy

$$\boldsymbol{x}_k = \boldsymbol{z}_k := \boldsymbol{M} \boldsymbol{x}_k. \tag{4.33}$$

This is an eigenvalue and eigenfunction relation, satisfied by either the trivial function $\boldsymbol{x}_k^\alpha = 0$ for all agents $\alpha \in [0,1]$, or when $\boldsymbol{x}_k$ is an eigenfunction of the operator $\boldsymbol{M}$ with associated eigenvalue $\lambda = 1$. When $\max(\lambda(\boldsymbol{M})) < 1$, tracking the graphon field contracts the state of all agents to zero. Two contracting examples, with varying graphons and Q-noise disturbances are presented first, and two normalized examples are presented second. In order to create examples where the maximal eigenvalue is one, the graphon $\boldsymbol{M}$ is normalized by its maximal

eigenvalue.

In all examples, the states are scalar, with the system parameters $a = 1$, $b = 1$, and $c = 0.1$. To illustrate that the system effectively tracks the perturbed graphon fields with noise, the disturbance covariance will be scaled to be small relative to the effect of the graphon field.

To verify the definitions of Γ_k and Ψ_k, for all examples we compute $\Delta(\Gamma_k)$, the L^2 norm between the expected value of the graphon field $\boldsymbol{z}_{k+1}$ given $\boldsymbol{z}_k$ and the operator Γ_k acting on the current graphon field $\boldsymbol{z}_k$, i.e.,

$$\Delta(\Gamma) := \max_{0 \leq k \leq T} ||\boldsymbol{M}(a\boldsymbol{x}_k + b\boldsymbol{u}_k + c\boldsymbol{z}_k) - \Gamma_k \boldsymbol{z}_k||_2. \tag{4.34}$$

In all four sample paths below, $\Delta(\Gamma)$ was calculated to be below the order of 10^{-9}, often on the order of 10^{-14}. This confirms numerically that the operator Γ_k is equivalent to the expected value of the graphon field $\boldsymbol{z}_k$ at the next time step.

4.4.4 Contracting graphon, $|\max(\lambda(\boldsymbol{M}))| < 1$

4.4.4.1 Erdos-Renyi: $\boldsymbol{M}(\alpha, \beta) = 0.9$, $\mathbf{Q}(\alpha, \beta) = (1 - \max(\alpha, \beta))/20$

Here, set the initial state for each agent to $\boldsymbol{x}_0^\alpha = 3\sin(\pi\alpha)$. This initial condition is arbitrary, it only needs to be set to be non-constant to demonstrate the graphon field behavior. The state $\boldsymbol{x}_k$ and field $\boldsymbol{z}_k$ are shown in Fig. 4.1, as well as the trajectory of the error between the two, $\boldsymbol{x}_k - \boldsymbol{z}_k$. The error is low, but due to the addition of noise at each time step, it is never zero.

For the contracting Erdos-Renyi graphon, $\Delta(\Gamma)$ is zero on the order of 10^{-14}.

4.4.5 $\boldsymbol{M}(\alpha, \beta) = \sqrt{|x - y|}$, $\mathbf{Q}(\alpha, \beta) = \cos(\alpha - \beta)$

The trajectory of the state in this example is shown in Fig. 4.2. Unlike in the Erdos-Renyi case, the graphon field $\boldsymbol{z}_k$ is non-constant at each k, but the controlled game is still

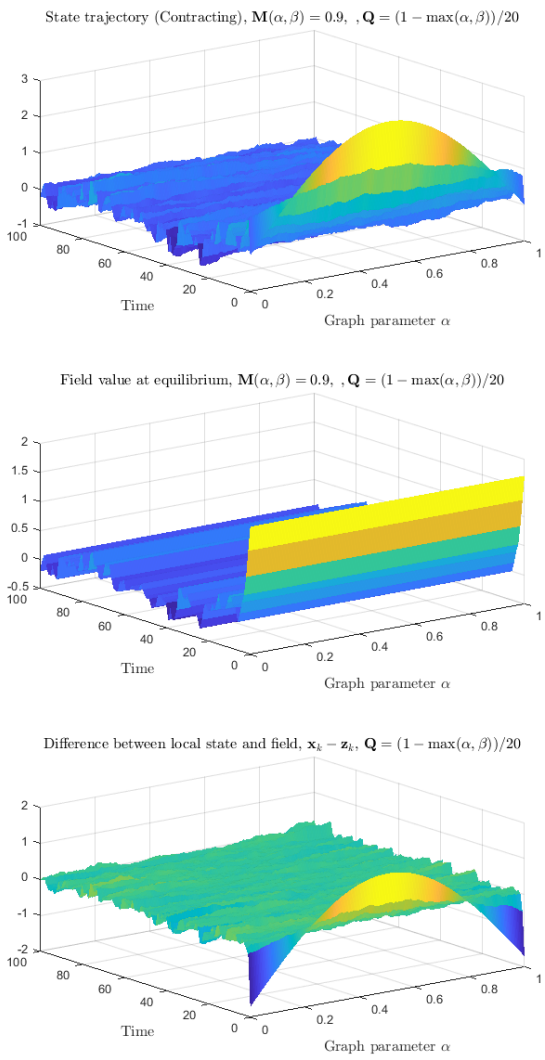

Figure 4.1: Top: The state trajectory of the system $\boldsymbol{x}_k$ when the graphon field is given by the Erdos-Renyi graphon $\boldsymbol{M} = 0.9$. As the graphon is contracting, the controlled state trajectory is near zero for all agents. Middle: The associated graphon field. As this is a rank-one graphon equivalent for all agents, the field is flat at each time step. Bottom: The difference between the graphon field and state, which determines the cost to particular agents.

stable about the origin $x_k^\alpha = 0,\ \alpha \in [0,1]$. For the contracting square root graphon, $\Delta(\Gamma)$ is zero on the order of 10^{-15}.

4.4.6 Normalized graphon, $\max(\lambda(\boldsymbol{M})) = 1$

When the graphon $\boldsymbol{M}$ is normalized by its maximal eigenvalue, instead of sending the state of each agent to zero, the calculated optimal control $\boldsymbol{u}_k$ instead moves the state $\boldsymbol{x}_k$ towards the associated eigenfunction of $\boldsymbol{M}$. As $c = 0.1$ and $a = 1$, the system is unstable, and the system tracks a scaling of an eigenfunction of $\boldsymbol{M}$.

4.4.6.1 Erdos-Renyi: $\boldsymbol{M}(\alpha,\beta) = 1$, $\mathbf{Q}(\alpha,\beta) = (1 - \max(\alpha,\beta))/20$

This trajectory is shown in Fig. 4.3. Unlike the case where $\boldsymbol{M}(\alpha,\beta) = 0.9$, the controlled game is stable near the eigenfunction initial condition. For the normalized Erdos-Renyi graphon, $\Delta(\Gamma)$ is zero on the order of 10^{-9}.

4.4.7 $\boldsymbol{M}(\alpha,\beta) = \sqrt{|x-y|}$ (Normalized), $\mathbf{Q}(\alpha,\beta) = \cos(\alpha - \beta)$

The trajectory shown in Fig. 4.4 shows that the controlled state is attracted to a scaled eigenfunction of the system. For the normalized square root graphon, $\Delta(\Gamma)$ is zero on the order of 10^{-10}.

4.5 Infinite Horizon Discounted Cost

Due to the addition of disturbance of bounded variation, the standard horizon field tracking problem does not have a well-defined value function in the infinite time horizon case. This can be addressed in the standard manner by using a multiplicative, stage-wise discount factor ρ.

Even then, this poses some conceptual questions. The graphon field process to be tracked is non-deterministic and non-constant, and the backwards equation method of deriving the operators Ψ and Γ cannot be used directly. As a starting point, consider the finite time

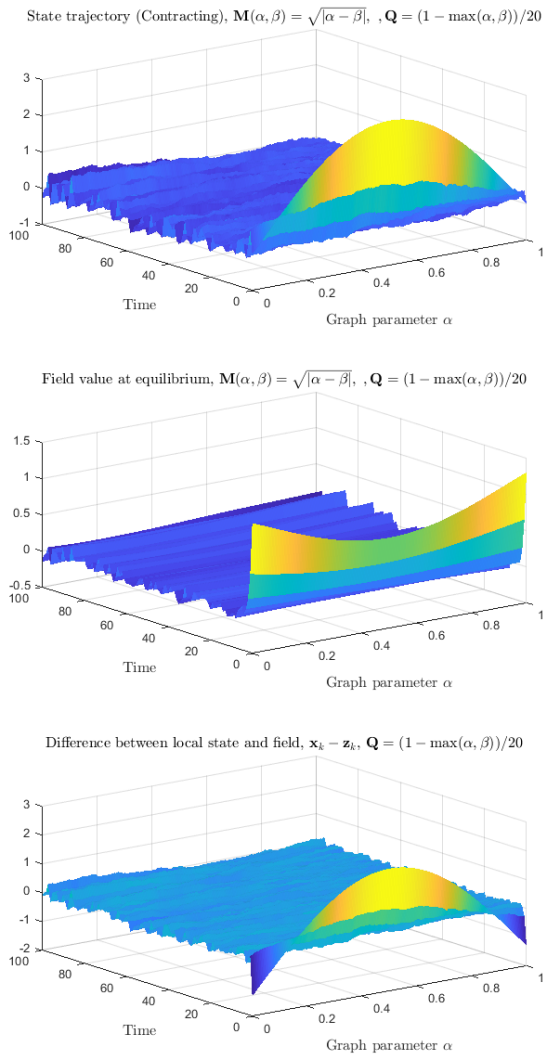

Figure 4.2: Top: The state trajectory of the system $\boldsymbol{x}_k$ when the graphon field is given by the graphon $\boldsymbol{M}(\alpha,\beta) = \sqrt{|\alpha-\beta|}$. This graphon is also contracting, and the controlled state trajectory approaches zero. Middle: The associated graphon field. Bottom: The difference between the agents' states and graphon fields.

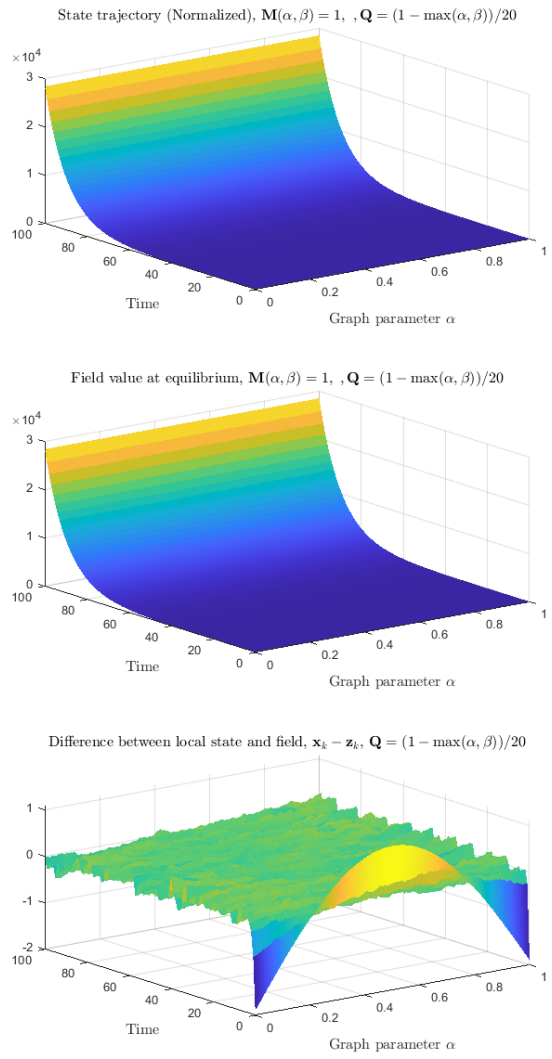

Figure 4.3: Top: The state trajectory of the system $\boldsymbol{x}_k$ when the graphon field is given by the Erdos-Renyi graphon $\boldsymbol{M} = 1$. As the system is unstable ($c = 0.1$), the state of each agent tends to infinity. Middle: The associated graphon field. Bottom: The difference between each agent's state and field. Despite the controlled system being fundamentally unstable, the state of each agent very closely tracks the graphon field.

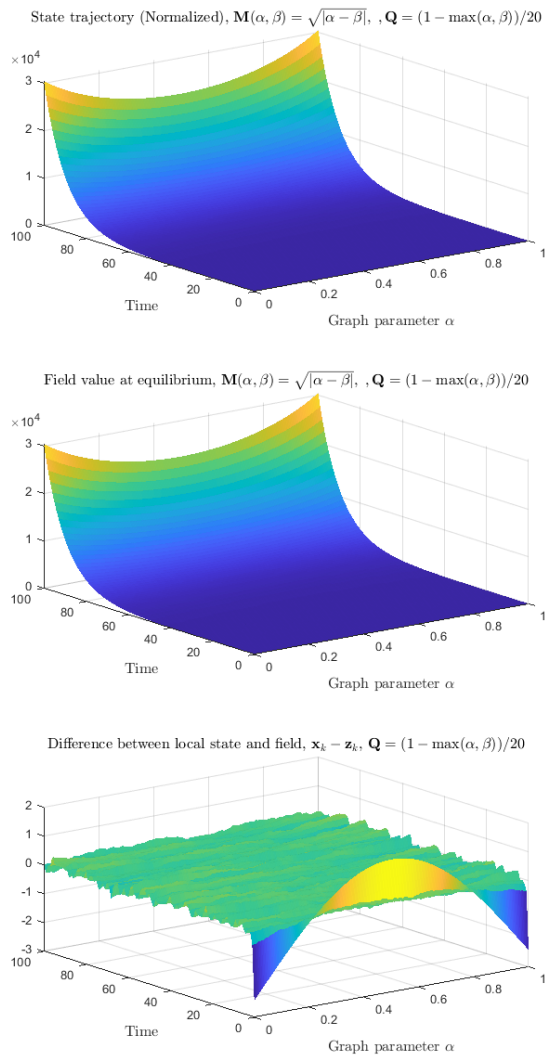

Figure 4.4: Top: The state trajectory of the system $\boldsymbol{x}_k$ when the graphon field is given by the graphon $\boldsymbol{M} = \sqrt{|\alpha - \beta|}$ after normalization by its maximal eigenvalue. As the system is unstable ($c = 0.1$), the state of each agent tends to infinity. Middle: The associated graphon field. Bottom: The difference between each agent's state and field. Despite the controlled system being fundamentally unstable, the state of each agent very closely tracks the graphon field.

horizon discounted case; for $0 < \rho < 1$, define the finite horizon discounted tracking problem for a system of the form (4.13),

$$J_\rho^\alpha(\boldsymbol{u}, \boldsymbol{x}_0) = \sum_{k=0}^{T-1} \rho^k \mathbb{E}[||\boldsymbol{x}_k^\alpha - \boldsymbol{z}_k^\alpha||_S^2 + ||\boldsymbol{u}_k^\alpha||_R^2 \mid \mathcal{F}_0^\alpha] \tag{4.35}$$

$$+ \rho^T \mathbb{E}[||\boldsymbol{x}_T^\alpha - \boldsymbol{z}_T^\alpha||_S^2 | \mathcal{F}_T]. \tag{4.36}$$

By the same proof approach to the finite time non-discounted game, this is associated with the sequence of value functions

$$V_k^\alpha(\mathcal{F}_k^\alpha) = \mathbb{E}_k[P_k(\boldsymbol{x}_k^\alpha)^2 + 2(\boldsymbol{x}_k^\alpha)\boldsymbol{s}_k^\alpha + m_k^\alpha], \tag{4.37}$$

$$k = \{0, ..., T\},$$

where P_k^ρ is an positive scalar, and $\boldsymbol{s}_k$ and m_k^α are $L^2([0,1])$ valued functions for all $k = \{0, ..., T\}$ derived from the following backwards recurrence relations,

$$F_k^\rho = \rho(R + \rho P_{k+1}^\rho b^2)^{-1} P_{k+1}^\rho ab, \tag{4.38}$$

$$G_k^\rho = \rho(R + \rho P_{k+1}^\rho b^2)^{-1} P_{k+1}^\rho bc, \tag{4.39}$$

$$H_k^\rho = \rho(R + \rho P_{k+1}^\rho b^2)^{-1} b, \tag{4.40}$$

$$P_k^\rho = S + R(F_k^\rho)^2 + \rho^2(a - bF_k^\rho)^2 P_{k+1} \tag{4.41}$$

$$\begin{aligned} \boldsymbol{s}_k^\alpha = &- S\boldsymbol{d}_k^\alpha + F_k^\rho R(G_k^\rho \boldsymbol{d}_k^\alpha + H_k^\rho \mathbb{E}_k[\boldsymbol{s}_{k+1}^\alpha]) \\ &+ \rho(a - bF_k^\rho) P_{k+1}^\rho \left[(c - bG_k^\rho)\boldsymbol{d}_k^\alpha - bH_k^\rho \mathbb{E}_k[\boldsymbol{s}_{k+1}^\alpha]\right] \\ &+ \rho(a - bF_k^\rho)\mathbb{E}_k[\boldsymbol{s}_{k+1}^\alpha], \end{aligned} \tag{4.42}$$

$$\begin{aligned} m_k^\alpha = &\boldsymbol{d}_k^{\alpha *} S \boldsymbol{d}_k^\alpha + \rho \Big[(G_k^\rho \boldsymbol{d}_k^\alpha + H_k^\rho \mathbb{E}_k[\boldsymbol{s}_{k+1}^\alpha])^* R (G_k^\rho \boldsymbol{d}_k^\alpha + H_k^\rho \mathbb{E}_k[\boldsymbol{s}_{k+1}^\alpha]) \\ &+ \left[(c - bG_k^\rho)\boldsymbol{d}_k^\alpha - bH_k^\rho \mathbb{E}_k[\boldsymbol{s}_{k+1}^\alpha]\right] P_{k+1}^\rho \left[(c - bG_k^\rho)\boldsymbol{d}_k^\alpha - BH_k^\rho \mathbb{E}_k[\boldsymbol{s}_{k+1}^\alpha]\right] \\ &+ 2\left[(c - bG_k^\rho)\boldsymbol{d}_k^\alpha - BH_k^\rho \mathbb{E}_k[\boldsymbol{s}_{k+1}^\alpha]\right] \mathbb{E}_k[\boldsymbol{s}_{k+1}^\alpha] + \mathbf{Q}(\alpha, \alpha) + \mathbb{E}_k[m_{k+1}^\alpha] \Big], \end{aligned} \tag{4.43}$$

with the terminal conditions

$$P_T^\rho = S, \tag{4.44}$$

$$\boldsymbol{s}_T^\alpha = -S\boldsymbol{d}_T^\alpha, \tag{4.45}$$

$$m_T^\alpha = S||\boldsymbol{d}_T^\alpha||^2. \tag{4.46}$$

Further, the optimal control is given by

$$u_k^{o,\alpha} = -\rho(R+\rho b^2 P_{k+1}^\rho)^{-1}[P_{k+1}^\rho(a\boldsymbol{x}_k^\alpha + c\boldsymbol{d}_k^\alpha) + \mathbb{E}_k[\boldsymbol{s}_{k+1}^\alpha]] \tag{4.47}$$

$$=: -F_k^\rho \boldsymbol{x}_k^\alpha - G_k^\rho \boldsymbol{d}_k^\alpha - H_k^\rho \mathbb{E}_k[\boldsymbol{s}_{k+1}^\alpha]. \tag{4.48}$$

As in the non-discounted case, the process to be tracked is given by $\boldsymbol{z}_k = \boldsymbol{M}\boldsymbol{x}_k$ at time k. Let Γ_k and Ψ_k be $L^2([0,1])$ operators defined by the backwards recursion equations

$$\begin{aligned}\Psi_k^\rho =& -S\mathbb{I} + F_k^\rho R(G_k^\rho \mathbb{I} + H_k^\rho \Psi_{k+1}^\rho \Gamma_k^\rho) \\ &+ \rho(a-bF_k^\rho)^* P_{k+1}^\rho\big[(c-bG_k^\rho)\mathbb{I} - b\Psi_{k+1}H_k\Gamma_k\big] \\ &+ \rho(a-bF_k)^*\Psi_{k+1}\Gamma_k,\end{aligned} \tag{4.49}$$

$$\Gamma_k^\rho = (\mathbb{I}+bH_k^\rho \boldsymbol{M}\Psi_{k+1})^{-1}[(a-bF_k^\rho)\mathbb{I} + (d-bG_k^\rho)\boldsymbol{M}] \tag{4.50}$$

with the terminal conditions

$$\Psi_T^\rho = -S\mathbb{I}. \tag{4.51}$$

Assume that for all $k = \{0,...,T-1\}$, the inverse $(\mathbb{I}+bH_k\boldsymbol{M}\Psi_{k+1})^{-1}$ exists. Then, for the system (4.13) as with the non-discounted game,

$$\mathbb{E}_k[\boldsymbol{z}_{k+1}] = \Gamma_k^\rho \boldsymbol{z}_k, \tag{4.52}$$

$$\boldsymbol{s}_k = \Psi_k^\rho \boldsymbol{z}_k, \tag{4.53}$$

and the trajectory is generated by

$$\boldsymbol{u}_k^\rho = -F_k^\rho \boldsymbol{x}_k - (G_k^\rho \mathbb{I} + H_k^\rho \Psi_{k+1} \Gamma_k^\rho) \boldsymbol{z}_k \tag{4.54}$$

gives the optimal tracking trajectory for each α.

It is assumed that the infinite horizon feedback solution (when it exists) is given by the fixed point to the following algebraic Riccati and operator equations:

$$\begin{aligned}
F_\infty^\rho =& \rho(R + \rho b^2 P_\infty^\rho)^{-1} P_\infty^\rho ab, && (4.55)\\
G_\infty^\rho =& \rho(R + \rho b^2 P_\infty^\rho)^{-1} P_\infty^\rho bc, && (4.56)\\
H_\infty^\rho =& \rho(R + \rho b^2 P_\infty^\rho b)^{-1} b, && (4.57)\\
P_\infty^\rho =& S + F_\infty^{\rho *} R F_\infty^\rho + \rho(a - bF_\infty^\rho)^* P_\infty^\rho (a - bF_\infty^\rho), && (4.58)\\
\Psi_\infty^\rho =& - S\mathbb{I} + F_\infty^\rho R(G_\infty^\rho \mathbb{I} + H_\infty^\rho \Psi_\infty^\rho \Gamma_\infty^\rho) && (4.59)\\
& + \rho(a - bF_\infty^\rho)^* P_\infty^\rho \big[(c - bG_\infty^\rho)\mathbb{I} - bH_\infty \Psi_\infty \Gamma_\infty\big]\\
& + (a - bF_\infty^\rho)^* \Psi_\infty \Gamma_\infty^\rho,\\
\Gamma_\infty^\rho =& (\mathbb{I} + bH_\infty^\rho \boldsymbol{M} \Psi_\infty)^{-1} [(a - bF_\infty^\rho)\mathbb{I} + (c - bG_\infty^\rho)\boldsymbol{M}]. && (4.60)
\end{aligned}$$

Under the condition that $c = 0$ (that is, the states of each agent evolve with strictly local state and controls) and that the graphon $\boldsymbol{M}$ has finite rank K, then the operators can be explicitly solved with $(K \times K) + 1$ equations.

Define the orthogonal subspaces $\mathcal{S}^{\boldsymbol{M}}$ to be the the linear subspace spanned by the basis of the system graphon $\boldsymbol{M}$, and $\breve{\mathcal{S}}$ to be the orthogonal complement of $\mathcal{S}^{\boldsymbol{M}}$ such that

$$L^2[0,1] =: \mathcal{S}^{\boldsymbol{M}} \oplus \breve{\mathcal{S}}. \tag{4.61}$$

Then, define the $K \times K$ matrix M to be

$$M_{i,j} := \langle \boldsymbol{M}\phi_i, \phi_j \rangle, \quad i,j \in (1,...,K) \tag{4.62}$$

and the complement identity operator $\breve{\mathbb{I}} : L^2[0,1] \to \breve{\mathcal{S}}$ to be the projection operator satisfying

$$\breve{\mathbb{I}}\boldsymbol{d} = \boldsymbol{d} - \sum_{k=1}^{K} \langle \boldsymbol{d}, \phi_k \rangle \phi_k, \quad \forall \boldsymbol{d} \in L^2[0,1]. \tag{4.63}$$

Theorem 4.5.1 (Finite Rank Closed-Form Feedback) *If the state of each node is a scalar, $c = 0$, and the system graphon $\boldsymbol{M}$ is of rank $K < \infty$ with associated orthonormal basis $\{\phi_k\}_{k=1}^K$, then Ψ_∞ and Γ_∞ is a solution of the quadratic operator equation*

$$BH_\infty \boldsymbol{M} \Psi_\infty^2 + (C\mathbb{I} + SBH_\infty^\rho \boldsymbol{M})\Psi_\infty^\rho + S\mathbb{I} = 0, \tag{4.64}$$

where

$$C := 1 - (a - bF_\infty^\rho)[F_\infty^\rho R - \rho(a - bF_\infty^\rho)P_\infty^\rho b \tag{4.65}$$

$$- \rho(a - bF_\infty)^2] \tag{4.66}$$

Then, in the low rank case equation (4.64) is solved by the orthogonal operator equations

$$\Psi_\infty := \breve{\Psi}_\infty + \sum_{i=1}^{K}\sum_{j=1}^{K} [\Psi_\infty^{\boldsymbol{M}}]_{ij} \langle \phi_i, \cdot \rangle \tag{4.67}$$

$$c\breve{\Psi}_\infty + S\breve{\mathbb{I}} = 0, \quad \breve{\Psi}_\infty : L^2[0,1] \to \breve{\mathcal{S}} \tag{4.68}$$

$$bH_\infty M(\Psi_\infty^{\boldsymbol{M}})^2 + (C + bSH_\infty)\Psi_\infty^{\boldsymbol{M}} \tag{4.69}$$

$$+ SI_K = 0, \quad \Psi_\infty^{\boldsymbol{M}} \in \mathcal{R}^{K\times K}$$

where I_K is the K-dimensional identity operator.

Proof: Note that if $c = 0$, then $G_\infty = 0$. Equation (4.64) is attained by substituting the definition of Γ_∞ into Eq. (4.59), and multiplying on the right by $\mathbb{I} + bH_\infty \boldsymbol{M} \Psi_\infty$. The equation can then be solved explicitly in two orthogonal subspaces $\mathcal{S}^{\boldsymbol{M}}$ and $\breve{\mathcal{S}}$ using the definitions provided in the lemma. □

Remark: When $\boldsymbol{M}$ is rank one, then equation (4.69) is a simple quadratic equation in one variable. Thus, there are two solutions due to the square root.

In simulations, when the system parameters are changed, the solution of the finite-horizon operator equations (4.49)–(4.51) may converge to either of the solutions of the infinite-horizon quadratic equation. In particular, the operator may converge to the solution with the positive radical when the eigenvalue associated with the eigenfunction of $\boldsymbol{M}$ is less than one, and to the solution with the negative radical when the eigenvalue is equal to one. Further, while the operator found through equations (4.49)–(4.51) is necessarily a Nash equilibrium for the finite-horizon game, this may not be the case for the other solution of the infinite-horizon game.

For $\boldsymbol{M}$ of rank K, a matrix quadratic formula is required, for which there are 2^K solutions. Intuition suggests only one of the solutions will be stable (as in the finite-dimensional analysis of linear quadratic systems), but this has yet to be proven.

As will be explored in the following numerical simulations, there are typically multiple solutions for the operator equations. Given initial conditions aligned with the eigenfunctions of the graphon $\boldsymbol{M}$, some of the generated solutions are clearly worse for all players.

4.5.1 Numerical Simulation

The following numerical solutions demonstrate the existence of multiple solutions of the infinite time horizon discounted problem, and that the finite horizon discounted problem can converge to both of them depending on whether or not the underlying graphon operator is normalized.

For each of the simulations, the discount factor $\rho = 0.95$ is used, with system parameters

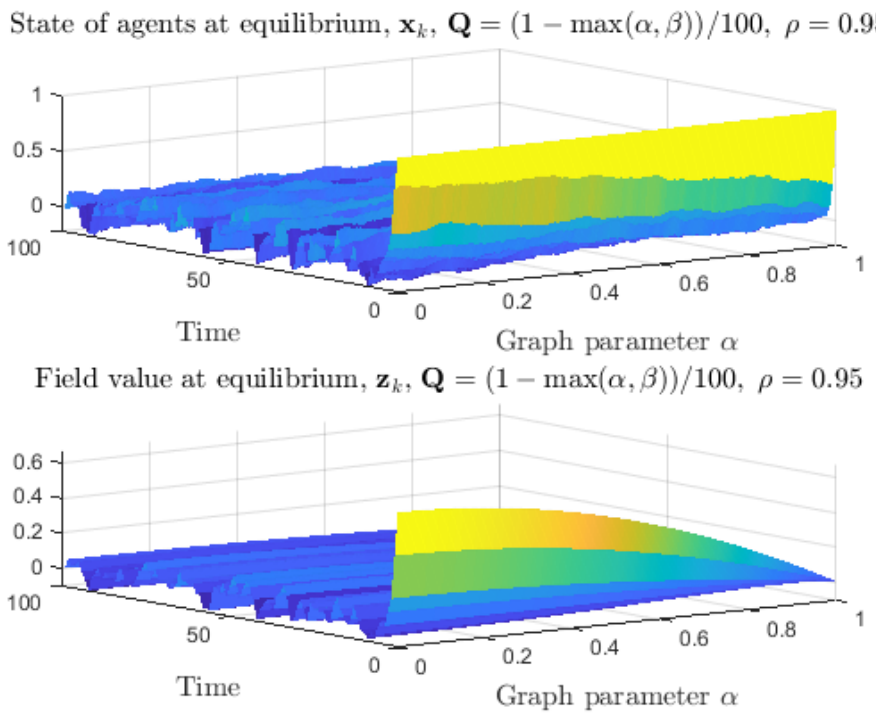

Figure 4.5: Finite time horizon discounted game with a contracting graphon. As expected, the state trajectory of the finite time horizon controlled system approaches zero.

$a = 1$, $b = 1$, $c = 0$ and costs $S = 1$ and $R = 1$ and a 200-node discretization of the unit interval. The rank one graphon $\boldsymbol{M}(\alpha, \beta) = (\alpha^2 - 1)(\beta^2 - 1)$ was used to generate the graphon field. In the first set of three simulations, the graphon is non-normalized (contracting), and for the second set of three simulations, the graphon is normalized. For all agents in all simulations, the initial condition $\boldsymbol{x}_0(\alpha) = 1,\ \alpha \in [0, 1]$ was used.

Figure 4.5 shows the state trajectory of the finite time discounted game when the graphon is non-normalized.

Figure 4.6 demonstrates that when the positive root solution of equation (4.69)is used to calculate Ψ^{ρ}_{∞} and Γ^{ρ}_{∞}, the solution very closely tracks the controlled state trajectory shown in Fig. 4.5. Indeed, the operator norm distance of $\Psi^{\rho}_{2}\Gamma^{\rho}_{1}$ and $\Psi^{\rho}_{\infty}\Gamma^{\rho}_{\infty}$ was on the order of machine precision, indicating that the sequence converged. Meanwhile, Fig. 4.7 shows that when the negative root solution of Eq. (4.69) is used, the controlled state trajectory is exceptionally unstable.

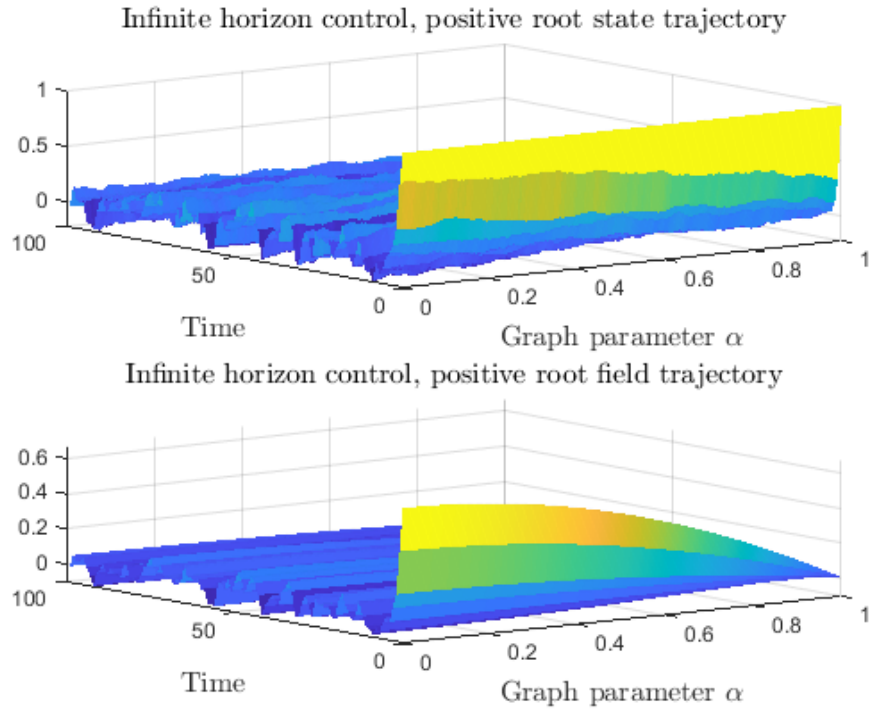

Figure 4.6: The controlled state trajectory of the game when the positive root solution of Eq. (4.69) is used, which closely resembles the finite time horizon discounted game trajectory.

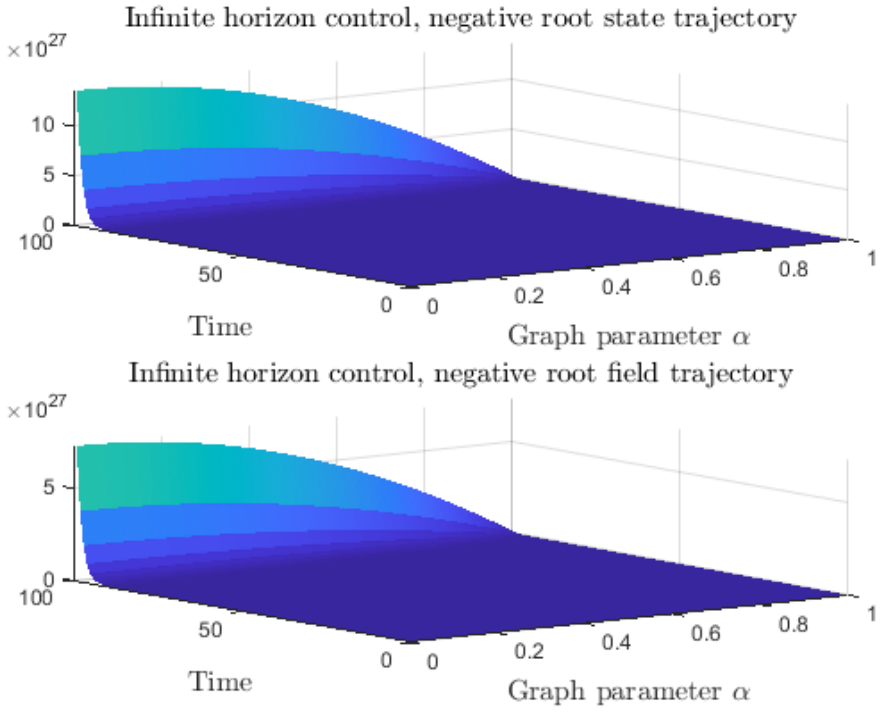

Figure 4.7: The system is unstable using the negative root solution of Eq. (4.69).

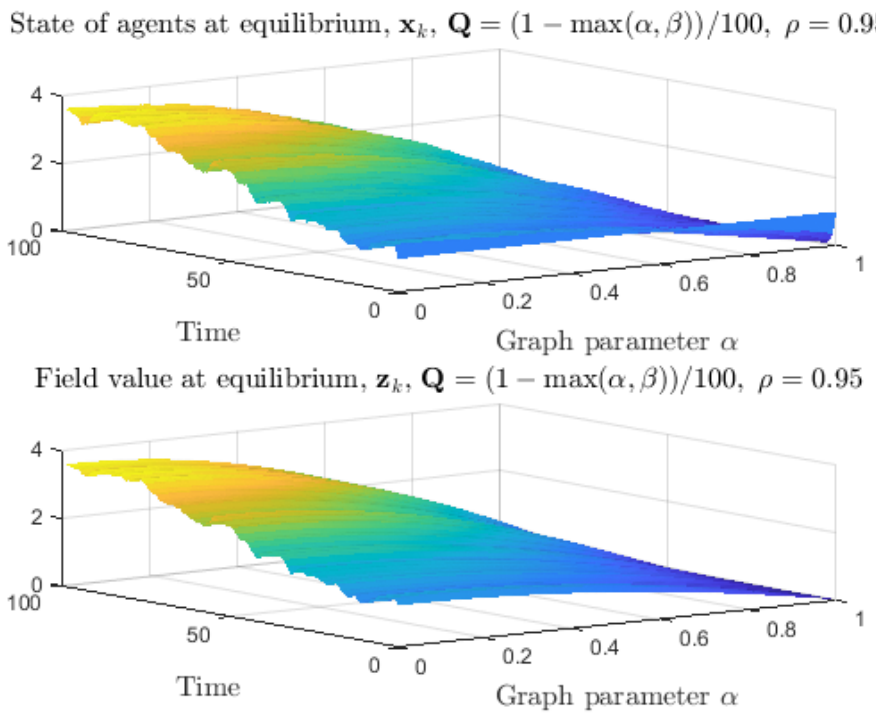

Figure 4.8: The controlled trajectory of the finite horizon discounted game closely tracks the eigenfunction of the system, even under noise, when $\boldsymbol{M}$ is normalized by its largest eigenvalue.

Next, consider the case where the graphon $\boldsymbol{M}$ is normalized by its eigenvalue. As with the nondiscounted game, the solution of the finite time horizon discounted game approaches a scaled eigenfunction of the graphon, in this case, $\phi(\alpha) = \alpha^2 - 1$. Figure 4.8 shows this behavior.

However, unlike the previous case, the positive root solution of equation (4.69) does not create a trajectory that closely matches the finite time horizon game. It instead creates a trajectory that approaches zero for all agents, even though that seems sub-optimal, shown in Fig. 4.9. When the graphon $\boldsymbol{M}$ is normalized, the finite horizon discounted game solution instead converges to the negative root solution. A calculated trajectory of the controlled system using the negative root solution is shown in Fig. 4.10, which approaches an eigenfunction of the graphon $\boldsymbol{M}$ in a similar manner to the finite horizon discounted game trajectory.

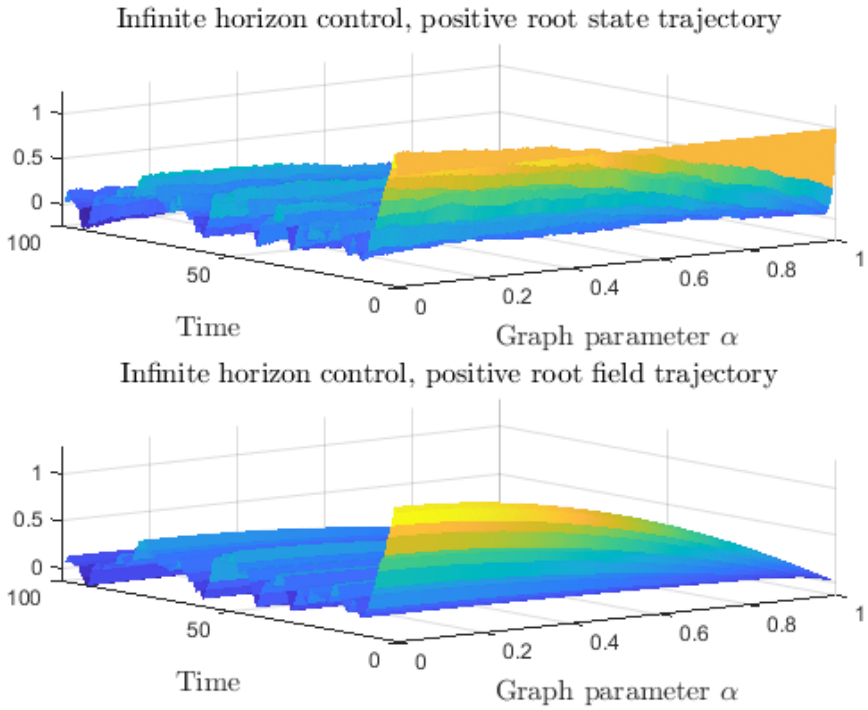

Figure 4.9: The controlled state trajectory of the normalized system using the positive root solution approaches zero for all agents, instead of approaching an eigenfunction.

4.6 Extensions and Proofs

4.6.1 Multivariate State Notation

Let each agent $\alpha \in [0,1]$ have n local states and m local controls, and let $A \in \mathcal{R}^{n\times n}, D \in \mathcal{R}^{n\times n}$, $B \in \mathcal{R}^{n\times m}$. Then, define the state evolution equation as

$$\boldsymbol{x}_{k+1}^{\alpha} = (A\boldsymbol{x}_k^{\alpha} + B\boldsymbol{u}_k^{\alpha} + D\boldsymbol{z}_k^{\alpha}) + \boldsymbol{g}_k^{\alpha}, \tag{4.70}$$

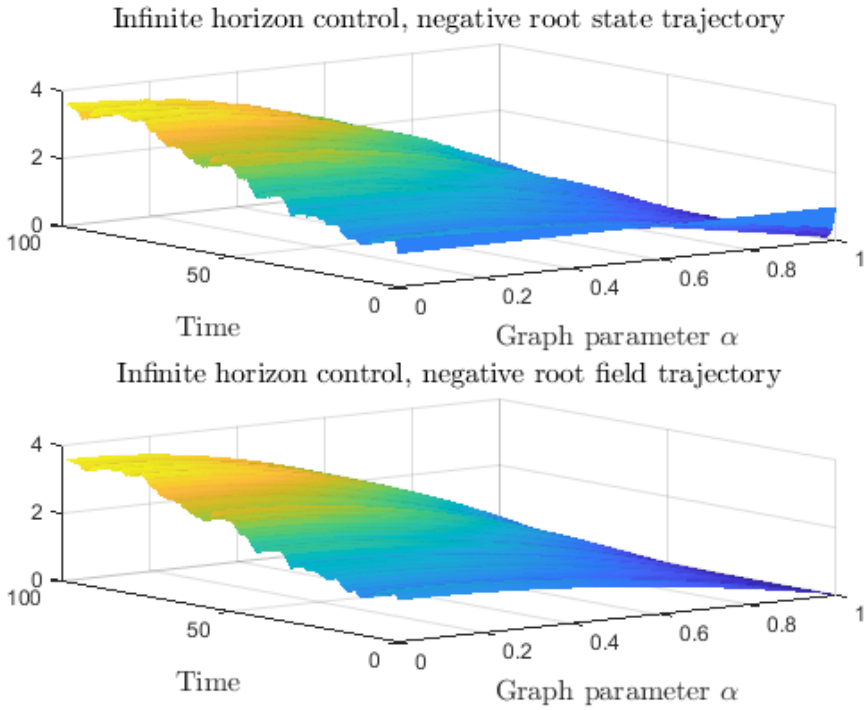

Figure 4.10: When $\boldsymbol{M}$ is normalized, the backwards recursion instead converges to the negative root solution.

where the graphon field $\boldsymbol{z}_k^\alpha$ is an n dimensional real vector for all α defined by the following blockwise form, with graphons $\boldsymbol{M}_{11}, \boldsymbol{M}_{12}, ...\boldsymbol{M}_{nn}$

$$\boldsymbol{z}_k^\alpha := \begin{bmatrix} (\boldsymbol{z}_k^\alpha)_1 \\ (\boldsymbol{z}_k^\alpha)_2 \\ \vdots \\ (\boldsymbol{z}_k^\alpha)_n \end{bmatrix} \tag{4.71}$$

$$= \begin{bmatrix} \int_0^1 \big[\boldsymbol{M}_{11}(\alpha,\beta)(\boldsymbol{x}_k^\beta)_1 + \boldsymbol{M}_{12}(\alpha,\beta)(\boldsymbol{x}_k^\beta)_2 \\ \quad + \cdots + \boldsymbol{M}_{1n}(\alpha,\beta)(\boldsymbol{x}_k^\beta)_n\big] d\beta \\ \int_0^1 \big[\boldsymbol{M}_{21}(\alpha,\beta)(\boldsymbol{x}_k^\beta)_1 + \boldsymbol{M}_{22}(\alpha,\beta)(\boldsymbol{x}_k^\beta)_2 \\ \quad + \cdots + \boldsymbol{M}_{2n}(\alpha,\beta)(\boldsymbol{x}_k^\beta)_n\big] d\beta \\ \vdots \\ \int_0^1 \big[\boldsymbol{M}_{n1}(\alpha,\beta)(\boldsymbol{x}_k^\beta)_1 + \boldsymbol{M}_{n2}(\alpha,\beta)(\boldsymbol{x}_k^\beta)_2 \\ \quad + \cdots + \boldsymbol{M}_{nn}(\alpha,\beta)(\boldsymbol{x}_k^\beta)_n\big] d\beta \end{bmatrix} \tag{4.72}$$

$$= \begin{bmatrix} \boldsymbol{M}_{11} & \boldsymbol{M}_{12} & \cdots & \boldsymbol{M}_{1n} \\ \boldsymbol{M}_{21} & \boldsymbol{M}_{22} & \cdots & \boldsymbol{M}_{2n} \\ \vdots & \vdots & \ddots & \vdots \\ \boldsymbol{M}_{n1} & \boldsymbol{M}_{n2} & \cdots & \boldsymbol{M}_{nn} \end{bmatrix} \begin{bmatrix} (\boldsymbol{z}_k)_1 \\ (\boldsymbol{z}_k)_2 \\ \vdots \\ (\boldsymbol{z}_k)_n \end{bmatrix} \tag{4.73}$$

By abuse of notation, we denote this blockwise form

$$\boldsymbol{z}_k := \boldsymbol{M}\boldsymbol{x}_k \tag{4.74}$$

as in the single-state-per-node case.

Following this, the relevant $\mathcal{R}^m$ dimensional controls for each $\alpha \in [0,1]$ would be defined by

$$F_k = (R + B^* P_{k+1} B)^{-1} B^* P_{k+1} A, \tag{4.75}$$

$$G_k = (R + B^* P_{k+1} B)^{-1} B^* P_{k+1} D, \tag{4.76}$$

$$H_k = (R + B^* P_{k+1} B)^{-1} B^*, \tag{4.77}$$

$$P_k = S + F_k^* R F_k + (A - BF_k)^* P_{k+1} (A - BF_k), \tag{4.78}$$

$$\begin{aligned} \boldsymbol{s}_k^\alpha = &- S\boldsymbol{z}_k^\alpha + F_k^* R(G_k \boldsymbol{z}_k^\alpha + H_k \mathbb{E}_k[\boldsymbol{s}_{k+1}^\alpha]) \\ &+ (A - BF_k)^* P_{k+1}\big[(D - BG_k)\boldsymbol{z}_k^\alpha - BH_k \mathbb{E}_k[\boldsymbol{s}_{k+1}^\alpha]\big] \\ &+ (A - BF_k)^* \mathbb{E}_k[\boldsymbol{s}_{k+1}^\alpha], \end{aligned} \tag{4.79}$$

$$
\begin{aligned}
m_k^\alpha =& \boldsymbol{z}_k^{\alpha *} S \boldsymbol{z}_k^\alpha + (G_k \boldsymbol{z}_k^\alpha + H_k \mathbb{E}_k[\boldsymbol{s}_{k+1}^\alpha])^* R \\
& \quad \times (G_k \boldsymbol{z}_k^\alpha + H_k \mathbb{E}_k[\boldsymbol{s}_{k+1}^\alpha]) \\
& + \left[(D - G_k)\boldsymbol{z}_k^\alpha - B H_k \mathbb{E}_k[\boldsymbol{s}_{k+1}^\alpha]\right]^* P_{k+1} \\
& \quad \times \left[(D - G_k)\boldsymbol{z}_k^\alpha - B H_k \mathbb{E}_k[\boldsymbol{s}_{k+1}^\alpha]\right] \\
& + 2\left[(D - G_k)\boldsymbol{z}_k^\alpha - B H_k \mathbb{E}_k[\boldsymbol{s}_{k+1}^\alpha]\right] \mathbb{E}_k[\boldsymbol{s}_{k+1}^\alpha] \\
& + \mathbf{Q}(\alpha, \alpha) + \mathbb{E}_k[m_{k+1}^\alpha],
\end{aligned} \tag{4.80}
$$

with the terminal conditions

$$
P_T = S, \tag{4.81}
$$

$$
\boldsymbol{s}_T^\alpha = - S \boldsymbol{z}_T^\alpha, \tag{4.82}
$$

$$
m_T^\alpha = S ||\boldsymbol{z}_T^\alpha||_2^2. \tag{4.83}
$$

Further, the optimal control is given by

$$
u_k^{o,\alpha} = - (R + B^* P_{k+1} B)^{-1} B^* [P_{k+1}(A \boldsymbol{x}_k^\alpha + D \boldsymbol{z}_k^\alpha) + \mathbb{E}_k[\boldsymbol{s}_{k+1}^\alpha]] \tag{4.84}
$$

$$
=: - F_k \boldsymbol{x}_k^\alpha - G_k \boldsymbol{z}_k^\alpha - H_k \mathbb{E}_k[\boldsymbol{s}_{k+1}^\alpha]. \tag{4.85}
$$

Similarly, Γ_k and Ψ_k would be defined by

$$
\begin{aligned}
\Psi_k =& - S\mathbb{I} + F_k R(G_k \mathbb{I} + H_k \Psi_{k+1} \Gamma_k) \\
& + (A - B F_k)^* P_{k+1}\left[(D - B G_k)\mathbb{I} - B \Psi_{k+1} H_k \Gamma_k\right] \\
& + (A - B F_k)^* \Psi_{k+1} \Gamma_k,
\end{aligned} \tag{4.86}
$$

$$
\Gamma_k = (\mathbb{I} + B H_k \boldsymbol{M} \Psi_{k+1})^{-1} [(A - B F_k)\mathbb{I} + (D - B G_k)\boldsymbol{M}] \tag{4.87}
$$

with the terminal condition

$$\Psi_T = -S\mathbb{I}. \tag{4.88}$$

The infinite time horizon discounted problem has a similar formulation:

By the same proof approach to the finite time non-discounted game, this is associated with the sequence of value functions

$$\begin{aligned} V_k^\alpha(\mathcal{F}_k^\alpha) =& \mathbb{E}_k[(\boldsymbol{x}_k^\alpha)^* P_k(\boldsymbol{x}_k^\alpha) + 2(\boldsymbol{x}_k^\alpha)^* \boldsymbol{s}_k^\alpha + m_k^\alpha], \\ & k = \{0, ..., T\}, \end{aligned} \tag{4.89}$$

where P_k^ρ is an positive scalar, and $\boldsymbol{s}_k$ and m_k^α are $L^2([0,1])$ valued functions for all $k = \{0, ..., T\}$ derived from the following backwards recurrence relations,

$$F_k^\rho = \rho(R + \rho B^* P_{k+1}^\rho)^{-1} B^* P_{k+1}^\rho A, \tag{4.90}$$

$$G_k^\rho = \rho(R + \rho B^* P_{k+1}^\rho)^{-1} B^* P_{k+1}^\rho D, \tag{4.91}$$

$$H_k^\rho = \rho(R + \rho B^* P_{k+1}^\rho)^{-1} B^*, \tag{4.92}$$

$$P_k^\rho = S + F_k^{\rho *} R F_k^\rho + \rho(A - BF_k^\rho)^* P_{k+1}^\rho (A - BF_k^\rho), \tag{4.93}$$

$$\begin{aligned} \boldsymbol{s}_k^\alpha =& -S\boldsymbol{d}_k^\alpha + F_k^{\rho *} R(G_k^\rho \boldsymbol{d}_k^\alpha + H_k^\rho \mathbb{E}_k[\boldsymbol{s}_{k+1}^\alpha]) \\ & + \rho(A - BF_k^\rho)^* P_{k+1}^\rho \left[(D - BG_k^\rho)\boldsymbol{d}_k^\alpha - BH_k^\rho \mathbb{E}_k[\boldsymbol{s}_{k+1}^\alpha]\right] \\ & + \rho(A - BF_k^\rho)^* \mathbb{E}_k[\boldsymbol{s}_{k+1}^\alpha], \end{aligned} \tag{4.94}$$

$$\begin{aligned} m_k^\alpha =& \boldsymbol{d}_k^{\alpha *} S \boldsymbol{d}_k^\alpha + \rho \Big[(G_k^\rho \boldsymbol{d}_k^\alpha + H_k^\rho \mathbb{E}_k[\boldsymbol{s}_{k+1}^\alpha])^* R \\ & \times (G_k^\rho \boldsymbol{d}_k^\alpha + H_k^\rho \mathbb{E}_k[\boldsymbol{s}_{k+1}^\alpha]) \\ & + \left[(D - BG_k^\rho)\boldsymbol{d}_k^\alpha - BH_k^\rho \mathbb{E}_k[\boldsymbol{s}_{k+1}^\alpha]\right]^* P_{k+1}^\rho \\ & \times \left[(D - G_k^\rho)\boldsymbol{d}_k^\alpha - BH_k^\rho \mathbb{E}_k[\boldsymbol{s}_{k+1}^\alpha]\right] \\ & + 2\left[(D - G_k^\rho)\boldsymbol{d}_k^\alpha - BH_k^\rho \mathbb{E}_k[\boldsymbol{s}_{k+1}^\alpha]\right] \mathbb{E}_k[\boldsymbol{s}_{k+1}^\alpha] \end{aligned} \tag{4.95}$$

$$+ \mathbf{Q}(\alpha,\alpha) + \mathbb{E}_k[m^\alpha_{k+1}]\Big],$$

with the terminal conditions

$$P^\rho_T = S, \tag{4.96}$$

$$\boldsymbol{s}^\alpha_T = -S\boldsymbol{d}^\alpha_T, \tag{4.97}$$

$$m^\alpha_T = S||\boldsymbol{d}^\alpha_T||^2. \tag{4.98}$$

Further, the optimal control is given by

$$u^{o,\alpha}_k = -\rho(R+\rho B^* P^\rho_{k+1})^{-1}B^*[P^\rho_{k+1}(A\boldsymbol{x}^\alpha_k + D\boldsymbol{d}^\alpha_k) + \mathbb{E}_k[\boldsymbol{s}^\alpha_{k+1}]] \tag{4.99}$$

$$=: -F^\rho_k \boldsymbol{x}^\alpha_k - G^\rho_k \boldsymbol{d}^\alpha_k - H^\rho_k \mathbb{E}_k[\boldsymbol{s}^\alpha_{k+1}]. \tag{4.100}$$

Let the process to be tracked be given by $\boldsymbol{z}_k = \boldsymbol{M}\boldsymbol{x}_k$ for time k. Let Γ_k and Ψ_k be $L^2([0,1])$ operators which are defined by the backwards recursion equations

$$\begin{aligned}\Psi^\rho_k =& -S\mathbb{I} + F^\rho_k R(G^\rho_k \mathbb{I} + H^\rho_k \Psi^\rho_{k+1}\Gamma^\rho_k) \\ &+ \rho(A - BF^\rho_k)^* P^\rho_{k+1}\big[(D-BG^\rho_k)\mathbb{I} - B\Psi_{k+1}H_k\Gamma_k\big] \\ &+ \rho(A-BF_k)^*\Psi_{k+1}\Gamma_k, \\ \Gamma^\rho_k =& (\mathbb{I} + BH^\rho_k \boldsymbol{M}\Psi_{k+1})^{-1}[(A-BF^\rho_k)\mathbb{I} + (D-BG^\rho_k)\boldsymbol{M}]\end{aligned} \tag{4.101}$$

with the terminal conditions

$$\Psi^\rho_T = -S\mathbb{I}. \tag{4.102}$$

Assume that for all $k = \{0,...,T-1\}$, the inverse $(\mathbb{I} + BH_k\boldsymbol{M}\Psi_{k+1})^{-1}$ exists. Then, as with

the non-discounted game,

$$\mathbb{E}_k[\boldsymbol{z}_{k+1}] = \Gamma_k^\rho \boldsymbol{z}_k, \tag{4.103}$$

$$\boldsymbol{s}_k = \Psi_k^\rho \boldsymbol{z}_k, \tag{4.104}$$

and the trajectory is generated by

$$\boldsymbol{u}_k^\rho = -F_k^\rho \boldsymbol{x}_k - (G_k^\rho \mathbb{I} + H_k^\rho \Psi_{k+1} \Gamma_k^\rho) \boldsymbol{z}_k \tag{4.105}$$

gives the optimal tracking trajectory for each α.

Assume that the infinite horizon feedback solution (when it exists) is given by the fixed point to the following algebraic Riccati operator equations:

$$F_\infty^\rho = \rho(R + \rho B^* P_\infty^\rho B)^{-1} B^* P_\infty^\rho A, \tag{4.106}$$

$$G_\infty^\rho = \rho(R + \rho B^* P_\infty^\rho B)^{-1} B^* P_\infty^\rho D, \tag{4.107}$$

$$H_\infty^\rho = \rho(R + \rho B^* P_\infty^\rho B)^{-1} B^*, \tag{4.108}$$

$$P_\infty^\rho = S + F_\infty^{\rho *} R F_\infty^\rho + \rho(A - BF_\infty^\rho)^* P_\infty^\rho (A - BF_\infty^\rho), \tag{4.109}$$

$$\begin{aligned} \Psi_\infty^\rho = & -S\mathbb{I} + F_\infty^\rho R(G_\infty^\rho \mathbb{I} + H_\infty^\rho \Psi_\infty^\rho \Gamma_\infty^\rho) \\ & + \rho(A - BF_\infty^\rho)^* P_\infty^\rho \big[(D - BG_\infty^\rho)\mathbb{I} - BH_\infty \Psi_\infty \Gamma_\infty\big] \\ & + (A - BF_\infty^\rho)^* \Psi_\infty \Gamma_\infty^\rho, \end{aligned} \tag{4.110}$$

$$\Gamma_\infty^\rho = (\mathbb{I} + BH_\infty^\rho \boldsymbol{M} \Psi_\infty)^{-1}[(A - BF_\infty^\rho)\mathbb{I} + (D - BG_\infty^\rho)\boldsymbol{M}]. \tag{4.111}$$

4.6.2 Proof of Lemma 4.15

The dynamic programming principle is applied to find the optimal control. From the terminal condition

$$V_T^\alpha(\boldsymbol{x}_k) = ||\boldsymbol{x}_T^\alpha - \boldsymbol{d}_T^\alpha||_S^2. \tag{4.112}$$

Then, $P_T = S,\ \boldsymbol{s}_T^\alpha = -S\boldsymbol{d}_T^\alpha$, and $m_T^\alpha = ||\boldsymbol{d}_T^\alpha||_S^2$.

By the dynamic programming assumption,

$$V_k^\alpha(\boldsymbol{x}_k) = \min_u \mathbb{E}_k\left[||\boldsymbol{x}_k^\alpha - \boldsymbol{d}_k^\alpha||_S^2 + ||u||_R^2 + V_{k+1}^\alpha(\boldsymbol{x}_{k+1})\right] \tag{4.113}$$

$$= \min_u ||\boldsymbol{x}_k^\alpha - \boldsymbol{d}_k^\alpha||_S^2 + ||u||_R^2 + \mathbb{E}_k[V_{k+1}^\alpha(\boldsymbol{x}_{k+1})] \tag{4.114}$$

$$= \min_u ||\boldsymbol{x}_k^\alpha - \boldsymbol{d}_k^\alpha||_S^2 + ||u||_R^2 \tag{4.115}$$
$$+ \mathbb{E}_k[P_{k+1}(\boldsymbol{x}_{k+1}^\alpha)^2 + 2(\boldsymbol{x}_{k+1}^\alpha)\boldsymbol{s}_{k+1}^\alpha + m_{k+1}^\alpha]$$

$$= \min_u ||\boldsymbol{x}_k^\alpha - \boldsymbol{d}_k^\alpha||_S^2 + ||u||_R^2 \tag{4.116}$$
$$+ \mathbb{E}_k[(a\boldsymbol{x}_k^\alpha + b\boldsymbol{u}_k^\alpha + c\boldsymbol{d}_k^\alpha + \boldsymbol{g}_k^\alpha)^2 P_{k+1}]$$
$$+ 2\mathbb{E}_k[a\boldsymbol{x}_k^\alpha + b\boldsymbol{u}_k^\alpha + c\boldsymbol{d}_k^\alpha + \boldsymbol{g}_k^\alpha]\mathbb{E}_k[\boldsymbol{s}_{k+1}^\alpha]$$
$$+ \mathbb{E}_k[m_{k+1}^\alpha]$$

$$= \min_u ||\boldsymbol{x}_k^\alpha - \boldsymbol{d}_k^\alpha||_S^2 + ||u||_R^2 \tag{4.117}$$
$$+ (a\boldsymbol{x}_k^\alpha + b\boldsymbol{u}_k^\alpha + c\boldsymbol{d}_k^\alpha)P_{k+1}(a\boldsymbol{x}_k^\alpha + b\boldsymbol{u}_k^\alpha + c\boldsymbol{d}_k^\alpha) + \mathbf{Q}(\alpha,\alpha)$$
$$+ 2(a\boldsymbol{x}_k^\alpha + b\boldsymbol{u}_k^\alpha + c\boldsymbol{d}_k^\alpha)\mathbb{E}_k[\boldsymbol{s}_{k+1}^\alpha] + \mathbb{E}_k[m_{k+1}^\alpha].$$

Note that the right-hand expression of (4.117) is differentiable and convex in u, and hence the optimal control is

$$u_k^{o,\alpha} = -\left(R + b^2 P_{k+1}\right)^{-1} b[P_{k+1}(a\boldsymbol{x}_k^\alpha + c\boldsymbol{d}_k^\alpha) + \mathbb{E}_k[\boldsymbol{s}_{k+1}^\alpha]] \tag{4.118}$$

$$=: -F_k\boldsymbol{x}_k^\alpha - G_k\boldsymbol{d}_k^\alpha - H_k\mathbb{E}_k[\boldsymbol{s}_{k+1}^\alpha]. \tag{4.119}$$

Applying the optimal control to the value function and rearranging terms gives equations (4.16–4.21) as required. □

4.6.3 Proof of Lemma 4.4.2

First, recall that by definition $\boldsymbol{z}_k = \boldsymbol{M}\boldsymbol{x}_k$, and hence when applying the optimal control at time $k = T-1$,

$$\begin{aligned}
\mathbb{E}_{T-1}[\boldsymbol{z}_T] = \mathbb{E}_{T-1}[\boldsymbol{M}\boldsymbol{x}_T] && (4.120)\\
=\mathbb{E}_{T-1}[\boldsymbol{M}(a\boldsymbol{x}_{T-1} + b\boldsymbol{u}_{T-1} + c\boldsymbol{z}_{T-1} + \boldsymbol{g}_{T-1})]] && (4.121)\\
=\boldsymbol{M}[a\boldsymbol{x}_{T-1} + b(-F_{T-1}\boldsymbol{x}_{T-1} - G_{T-1}\boldsymbol{z}_{T-1} - H_{T-1}\mathbb{E}_{T-1}[\boldsymbol{s}_T]) + c\boldsymbol{z}_{T-1}] && (4.122)\\
=\boldsymbol{M}[(a - bF_{T-1})\boldsymbol{x}_{T-1} + (c - bG_{T-1})\boldsymbol{z}_{T-1} - bG_{T-1}\mathbb{E}_{T-1}[\boldsymbol{s}_T]] && (4.123)\\
=(a - bF_{T-1})\boldsymbol{M}\boldsymbol{x}_{T-1} + (c - bG_{T-1})\boldsymbol{M}\boldsymbol{z}_{T-1} - bH_{T-1}\boldsymbol{M}\mathbb{E}_{T-1}[\boldsymbol{s}_T] && (4.124)\\
=(a - bF_{T-1})\boldsymbol{z}_{T-1} + (c - bG_{T-1})\boldsymbol{M}\boldsymbol{z}_{T-1} - bH_{T-1}\boldsymbol{M}\mathbb{E}_{T-1}[\boldsymbol{s}_T]. && (4.125)
\end{aligned}$$

Then, applying the terminal condition $\boldsymbol{s}_T = -S\boldsymbol{z}_T$,

$$\begin{aligned}
\mathbb{E}_{T-1}[\boldsymbol{z}_T] = (a - bF_{T-1})\boldsymbol{z}_{T-1} + (c - bG_{T-1})\boldsymbol{M}\boldsymbol{z}_{T-1} && (4.126)\\
\quad + bH_{T-1}\boldsymbol{M}\mathbb{E}_{T-1}[S\boldsymbol{z}_T]\\
\mathbb{E}_{T-1}[\boldsymbol{z}_T] - bH_{T-1}\boldsymbol{M}\mathbb{E}_{T-1}[S\boldsymbol{z}_T] = (a - bF_{T-1})\boldsymbol{z}_{T-1} && (4.127)\\
\quad + (c - bG_{T-1})\boldsymbol{M}\boldsymbol{z}_{T-1}.
\end{aligned}$$

Hence,

$$\begin{aligned}
\mathbb{E}_{T-1}[\boldsymbol{z}_T] =&(\mathbb{I} - SBH_{T-1}\boldsymbol{M})^{-1}[(A - BF_{T-1})\mathbb{I} + (c - bG_{T-1})\boldsymbol{M}]\boldsymbol{z}_{T-1} && (4.128)\\
=:& \ \Gamma_{T-1}\boldsymbol{z}_{T-1}. && (4.129)
\end{aligned}$$

Observing this, make the following inductive hypothesis:

$$\begin{aligned}
\mathbb{E}_k[\boldsymbol{z}_{k+1}] =&\Gamma_k\boldsymbol{z}_k, && (4.130)\\
\boldsymbol{s}_k =&\Psi_k\boldsymbol{z}_k, && (4.131)
\end{aligned}$$

where Ψ_k and Γ_k are $L^2([0,1])$ operators for each $k \in \{0, ..., T\}$. Applying the inductive hypotheses to the expectation of $\boldsymbol{z}_{k+1}$,

$$\begin{aligned}
\mathbb{E}_k[\boldsymbol{z}_{k+1}] &= [(a - bF_k)\mathbb{I} + (c - bG_k)\boldsymbol{M}]\boldsymbol{z}_k && (4.132)\\
&\quad - bH_k\boldsymbol{M}\mathbb{E}_k[\boldsymbol{s}_{k+1}] \\
&= [(a - bF_k)\mathbb{I} + (c - bG_k)\boldsymbol{M}]\boldsymbol{z}_k && (4.133)\\
&\quad - bH_k\boldsymbol{M}\mathbb{E}_k[\Psi_{k+1}\boldsymbol{z}_{k+1}] \\
&= (\mathbb{I} + bH_k\boldsymbol{M}\Psi_{k+1})^{-1}[(a - bF_k)\mathbb{I} + (c - bG_k)\boldsymbol{M}]\boldsymbol{z}_k && (4.134)\\
&=: \Gamma_k\boldsymbol{z}_k, && (4.135)
\end{aligned}$$

which shows equation (4.130). Applying the inductive hypotheses to the recursion for $\boldsymbol{s}_k$,

$$\begin{aligned}
\boldsymbol{s}_k &= -S\boldsymbol{z}_k + F_kR(G_k\boldsymbol{z}_k + H_k\mathbb{E}_k[\boldsymbol{s}_{k+1}]) && (4.136)\\
&\quad + (a - bF_k)P_{k+1}\big[(c - bH_k)\boldsymbol{z}_k - bH_k\mathbb{E}_k[\boldsymbol{s}_{k+1}]\big] \\
&\quad + (a - bF_k)^*\mathbb{E}_k[\boldsymbol{s}_{k+1}] \\
&= -S\boldsymbol{z}_k + F_kR(G_k\boldsymbol{z}_k + H_k\mathbb{E}_k[\Psi_{k+1}\boldsymbol{z}_{k+1}]) && (4.137)\\
&\quad + (a - bF_k)P_{k+1}\big[(c - bG_k)\boldsymbol{z}_k - bH_k\mathbb{E}_k[\Psi_{k+1}\boldsymbol{z}_{k+1}]\big] \\
&\quad + (a - bF_k)^*\mathbb{E}_k[\Psi_{k+1}\boldsymbol{z}_{k+1}] \\
&= -S\boldsymbol{z}_k + F_kR(G_k\boldsymbol{z}_k + H_k\Psi_{k+1}\mathbb{E}_k[\boldsymbol{z}_{k+1}]) && (4.138)\\
&\quad + (a - bF_k)^*P_{k+1}\big[(c - bG_k)\boldsymbol{z}_k - b\Psi_{k+1}H_k\mathbb{E}_k[\boldsymbol{z}_{k+1}]\big] \\
&\quad + (a - bF_k)^*\Psi_{k+1}\mathbb{E}_k[\boldsymbol{z}_{k+1}] \\
&= -S\boldsymbol{z}_k + F_kR(G_k\boldsymbol{z}_k + H_k\Psi_{k+1}\Gamma_k\boldsymbol{z}_k) && (4.139)\\
&\quad + (a - bF_k)P_{k+1}\big[(c - bG_k)\boldsymbol{z}_k - b\Psi_{k+1}H_k\Gamma_k\boldsymbol{z}_k\big] \\
&\quad + (a - bF_k)^*\Psi_{k+1}\Gamma_k\boldsymbol{z}_k \\
&=: \Psi_k\boldsymbol{z}_k. && (4.140)
\end{aligned}$$

Then, the optimal control $\boldsymbol{u}_k^o$ is given in

$$\begin{aligned}\boldsymbol{u}_k^o &= -F_k\boldsymbol{x}_k - G_k\boldsymbol{z}_k - H_k\mathbb{E}_k[\boldsymbol{s}_{k+1}] && (4.141)\\ &= -F_k\boldsymbol{x}_k - G_k\boldsymbol{z}_k - H_k\mathbb{E}_k[\Psi_{k+1}\boldsymbol{z}_{k+1}] && (4.142)\\ &= -F_k\boldsymbol{x}_k - (G_k\mathbb{I} + H_k\Psi_{k+1}\Gamma_k)\boldsymbol{z}_k. && (4.143)\end{aligned}$$

□

Chapter 5

Conclusion

Chapter 2 introduced the notions of Q-noise linear systems and defined the Q-noise linear quadratic Gaussian optimal control problem. We then proved the convergence of a system on a finite graph to a system on a limit graphon in mean square. In addition, it was demonstrated that when the limit graphon is low rank, the linear quadratic Gaussian problem could be solved exactly in a finite number of equations.

Chapter 3 accomplished one of the desired research directions of [35] and [39] by demonstrating that partially observed Q-noise linear quadratic systems can be controlled and estimated using the Kalman filter. When the underlying graphon limit is finite rank (and stable in unobserved dimensions), then the state trajectory of the finite graph can be controlled by the finite-dimensional filter approximation.

There are two immediate future directions for this work. First, the extension to graphs embedded in metric spaces using graphexon theory ([31],[51],[52]). This theory generalizes the concept used implicitly in the numerical simulations above, where each node in the graph is located uniformly at a point on the unit interval. Embedded graph limit theory describes graph limits that exist in geometric spaces more general than the unit interval, for instance, those where each node is located in $\mathcal{R}^2$ or $\mathcal{R}^3$. In the dense graph case, this is a straightforward generalization, but may not have a direct solution analog for sparse graphs. So long as the fundamental space the system is embedded in is a Hilbert space, the

Q-noise formalism holds. Further, much of the literature for optimal control and estimation in Hilbert spaces allows for unbounded evolution operators, and it may be possible to extend the convergence analysis of the Q-noise linear quadratic Gaussian problem and graphon Kalman filter to such a system. Second, the systems considered in this work have strictly linear noise. This can be expanded into systems of the form of [53], where the noise intensity depends on the state of the system.

One application that was not explored in Chapter 2 or Chapter 3 is that of "point" control and estimation, a classical method of controlling infinite-dimensional systems [41]. By averaging over a few nodes in the graph system corresponding to a small segment of the unit interval (approximating a point observation without invoking the mathematical and intuitive difficulties associated with unbounded observation operators), the system may still be observable. This would allow the estimation of the graph system from only the observation of a few nodes, and a similar assumption on controllability could allow the system to be stabilizable while only issuing control inputs to a few nodes in the graph. Providing qualitative criteria for the graphon for such a point control and estimation scheme to work would greatly increase the scope of applications for this modelling approach.

One particular area that may be of interest is in the area of epidemic modelling, particularly compartmental SIR models. The system would need to be extended from strictly linear to bilinear systems, as in SIR models; the rate of infection depends upon the proportion of the population that is susceptible as well as infected. A deterministic, uncontrolled graphon SIR model that modelled communities interacting with each other rather than strictly homogeneous models was presented in [54]. By applying filtering methods to this SIR model, one may be able to identify the effects of a public health intervention on the trajectory of an epidemic and compare it to the estimated system trajectory.

The graphon field game model presented in Chapter 4 provided a closed-form control solution for every agent in an infinite-dimensional stochastic system. The proof and optimal control construction for each agent had two major steps. First, the mean-field game

assumption was applied—by taking the limit as the number of agents increases to infinity and fixing the strategies of all other agents, each agent solves an optimal control problem with regard to the graphon field. This problem can be solved using dynamic programming. After this, each agent's response to the graphon field is fixed as a linear function, and it suffices to define a consistent, recursive method of generating the expected graphon field. Because of the linearity of the system, this recursion yields an adapted forwards-backwards stochastic difference equation.

However, there are some ways the work may be extended. First, as with the Q-LQG sections, the graphon field game could be extended to graphexon systems. This would yield a modification of the mean-field games on graphexons presented in [51], in the same way that the graphon field games of Chapter 4 and Gao et al [34] were a modification of the graphon mean-field game model. Unlike the Q-noise linear quadratic Gaussian and filtering problems, there is not as much literature defining the solutions of such systems. They may not have a well-behaved, closed-form solution as there is for the graphon case.

The numerical analysis showed interesting behaviour for the game trajectory depending on whether the graphon was normalized by its maximal eigenvalue. This has interesting parallels with the operator group action convergence proposed by Backhausz and Szegedy [55]. They investigate the different convergence behavior of operators that correspond roughly to sums over rows of the adjacency matrix of a graph scaled by its spectral radius rather than divided by the number of nodes in the graph (which is the standard dense graphon scaling).

The precise criteria for the convergence of the operators Ψ_k^ρ and Γ_k^ρ to Ψ_∞^ρ and Γ_∞^ρ is a topic for open investigation.

Chapter 4 considered Nash equilibria with full state information. This may be expanded to other information sets, such as those where each agent has only local information and, hence, estimation of the status of the overall graphon field may be of value. In particular, applying it to the case where each agent uses Kalman filtering to estimate the overall graphon field would be of interest, as in Chapter 3. Further research in this area would require the

consideration of common noise [44], where, unlike in the full information case, the local state $\boldsymbol{x}_k^\alpha$ would not be conditionally independent of the full state $\{\boldsymbol{x}_k^\beta,\ \beta \in [0,1]\}$.

Bibliography

[1] L. Lovász, *Large Networks and Graph Limits*. 2012.

[2] G. S. Medvedev, "The Nonlinear Heat Equation on W-Random Graphs", en, *Archive for Rational Mechanics and Analysis*, vol. 212, no. 3, pp. 781–803, Jun. 2014.

[3] S. Gao and P. E. Caines, "Graphon Control of Large-Scale Networks of Linear Systems", *IEEE Transactions on Automatic Control*, vol. 65, no. 10, pp. 4090–4105, Oct. 2020, Conference Name: IEEE Transactions on Automatic Control.

[4] S. Gao and P. E. Caines, "Subspace Decomposition for Graphon LQR: Applications to VLSNs of Harmonic Oscillators", en, *IEEE Transactions on Control of Network Systems*, vol. 8, no. 2, pp. 576–586, Jun. 2021.

[5] A. Khintchine and A. Kolmogoroff, "Uber Konvergenz von Reihen, deren Glieder durch den Zufall bestimmt werden", *Math. Sb.*, vol. 32, no. 4, pp. 668–677, 1925.

[6] A. Kukush, *Gaussian Measures in Hilbert Space*, en. Wiley, 2019.

[7] L. Gawarecki and V. Mandrekar, *Stochastic Differential Equations in Infinite Dimensions* (Probability and Its Applications), en. Berlin, Heidelberg: Springer Berlin Heidelberg, 2011.

[8] G. Fabbri, F. Gozzi, and A. Święch, *Stochastic Optimal Control in Infinite Dimension* (Probability Theory and Stochastic Modelling), en. Cham: Springer International Publishing, 2017, vol. 82.

[9] A. Dunyak and P. E. Caines, "Linear Stochastic Graphon Systems with Q-Space Noise", in *2022 IEEE 61st Conference on Decision and Control (CDC)*, ISSN: 2576-2370, Dec. 2022, pp. 3926–3932.

[10] G. S. Medvedev and G. Simpson, "A numerical method for a nonlocal diffusion equation with additive noise", en, *Stochastics and Partial Differential Equations: Analysis and Computations*, vol. 11, no. 4, pp. 1433–1469, Dec. 2023.

[11] S. Gao and P. E. Caines, "Spectral Representations of Graphons in Very Large Network Systems Control", in *2019 IEEE 58th Conference on Decision and Control (CDC)*, ISSN: 2576-2370, Dec. 2019, pp. 5068–5075.

[12] S.-J. Liu, P. E. Caines, and S. Gao, *Optimal Control of Large-Scale Networks of Stochastic Linear Systems*, 2019.

[13] A. Ichikawa, "Dynamic Programming Approach to Stochastic Evolution Equations", *SIAM Journal on Control and Optimization*, vol. 17, no. 1, pp. 152–174, Jan. 1979, Publisher: Society for Industrial and Applied Mathematics.

[14] R. F. Curtain, "Estimation and Stochastic Control for Linear Infinite-Dimensional Systems", in *Probabilistic Analysis and Related Topics*, A. T. Bharucha-reid, Ed., Academic Press, Jan. 1978, pp. 45–86.

[15] R. S. Bucy 1935- and P. D. Joseph 1936-, *Filtering for stochastic processes with applications to guidance* (Interscience tracts in pure and applied mathematics; no. 23), English. New York: Interscience Publishers, 1968, Section: xviii, 195 pages 24 cm.

[16] P. L. Falb, "Infinite-dimensional filtering: The Kalman\3-Bucy filter in Hilbert space", en, *Information and Control*, vol. 11, no. 1-2, pp. 102–137, Jul. 1967.

[17] R. F. Curtain, "Infinite-Dimensional Filtering", *SIAM Journal on Control*, vol. 13, no. 1, pp. 89–104, Jan. 1975, Publisher: Society for Industrial and Applied Mathematics.

[18] R. F. Curtain and A. Ichikawa, "The Separation Principle for Stochastic Evolution Equations", *SIAM Journal on Control and Optimization*, vol. 15, no. 3, pp. 367–383, May 1977, Publisher: Society for Industrial and Applied Mathematics.

[19] L. Shi, "Kalman Filtering Over Graphs: Theory and Applications", *IEEE Transactions on Automatic Control*, vol. 54, no. 9, pp. 2230–2234, Sep. 2009, Conference Name: IEEE Transactions on Automatic Control.

[20] R. Olfati-Saber, "Distributed Kalman filtering for sensor networks", in *2007 46th IEEE Conference on Decision and Control*, ISSN: 0191-2216, Dec. 2007, pp. 5492–5498.

[21] U. A. Khan and J. M. F. Moura, "Distributed Kalman Filters in Sensor Networks: Bipartite Fusion Graphs", in *2007 IEEE/SP 14th Workshop on Statistical Signal Processing*, ISSN: 2373-0803, Aug. 2007, pp. 700–704.

[22] P. E. Caines and M. Huang, "Graphon Mean Field Games and Their Equations", *SIAM Journal on Control and Optimization*, vol. 59, no. 6, pp. 4373–4399, Jan. 2021, Publisher: Society for Industrial and Applied Mathematics.

[23] P. E. Caines and M. Huang, "Graphon Mean Field Games and the GMFG Equations", in *2018 IEEE Conference on Decision and Control (CDC)*, ISSN: 2576-2370, Dec. 2018, pp. 4129–4134.

[24] R. F. Tchuendom, P. E. Caines, and M. Huang, "On the Master Equation for Linear Quadratic Graphon Mean Field Games", in *2020 59th IEEE Conference on Decision and Control (CDC)*, ISSN: 2576-2370, Dec. 2020, pp. 1026–1031.

[25] S. Gao, P. E. Caines, and M. Huang, "LQG Graphon Mean Field Games: Graphon Invariant Subspaces", in *2021 60th IEEE Conference on Decision and Control (CDC)*, ISSN: 2576-2370, Dec. 2021, pp. 5253–5260.

[26] D. Lacker and A. Soret, "A Label-State Formulation of Stochastic Graphon Games and Approximate Equilibria on Large Networks", *Mathematics of Operations Research*, vol. 48, no. 4, pp. 1987–2018, Nov. 2023, Publisher: INFORMS.

[27] I. Karatzas and S. E. Shreve, *Brownian Motion and Stochastic Calculus* (Graduate Texts in Mathematics), en. New York, NY: Springer, 1998, vol. 113.

[28] H. Liu and D. Firoozi, "Hilbert Space-Valued LQ Mean Field Games: An Infinite-Dimensional Analysis", en, *SIAM Journal on Control and Optimization (to appear)*, 2025.

[29] D. Lacker and A. Soret, "A Case Study on Stochastic Games on Large Graphs in Mean Field and Sparse Regimes", *Mathematics of Operations Research*, vol. 47, no. 2, pp. 1530–1565, May 2022, Publisher: INFORMS.

[30] K. Cui and H. Koeppl, *Learning Graphon Mean Field Games and Approximate Nash Equilibria*, en, arXiv:2112.01280 [cs, math], Feb. 2022.

[31] P. E. Caines, "Embedded Vertexon-Graphons and Embedded GMFG Systems", in *IEEE Conference on Decision and Control*, Dec. 2022.

[32] A. Aurell, R. Carmona, and M. Laurière, "Stochastic Graphon Games: II. The Linear-Quadratic Case", en, *Applied Mathematics & Optimization*, vol. 85, no. 3, p. 39, May 2022.

[33] A. Aurell, R. Carmona, G. Dayanıklı, and M. Laurière, "Finite State Graphon Games with Applications to Epidemics", en, *Dynamic Games and Applications*, vol. 12, no. 1, pp. 49–81, Mar. 2022.

[34] S. Gao, R. F. Tchuendom, and P. E. Caines, "Linear quadratic graphon field games", en, *Communications in Information and Systems*, vol. 21, no. 3, pp. 341–369, Jun. 2021, Publisher: International Press of Boston.

[35] A. Dunyak and P. E. Caines, *Quadratic Optimal Control of Graphon Q-noise Linear Systems*, en, arXiv:2407.00212 [math], Jun. 2024.

[36] I. Gohberg and S. Goldberg, *Basic Operator Theory*, en. Boston, MA: Birkhäuser Boston, 1981.

[37] M. O. Jackson, "Social and Economic Networks", in *Social and Economic Networks*, Princeton University Press, Nov. 2010.

[38] D. J. Watts, *Small Worlds: The Dynamics of Networks between Order and Randomness*, en. Princeton University Press, Jun. 2018.

[39] A. Dunyak and P. E. Caines, "Linear Stochastic Processes on Networks and Low Rank Graph Limits", en, in *Complex Networks & Their Applications XII*, H. Cherifi, L. M. Rocha, C. Cherifi, and M. Donduran, Eds., Cham: Springer Nature Switzerland, 2024, pp. 395–407.

[40] A. Dunyak and P. E. Caines, "Stochastic Control on Large Networks: A Q-noise Formulation", Toronto, Canada, Jul. 2024.

[41] R. Curtain and H. Zwart, *Introduction to Infinite-Dimensional Systems Theory: A State-Space Approach* (Texts in Applied Mathematics), en. New York, NY: Springer, 2020, vol. 71.

[42] M. Huang, P. E. Caines, and R. P. Malhame, "The NCE (Mean Field) Principle With Locality Dependent Cost Interactions", *IEEE Transactions on Automatic Control*, vol. 55, no. 12, pp. 2799–2805, Dec. 2010, Conference Name: IEEE Transactions on Automatic Control.

[43] A. Bensoussan, J. Frehse, and P. Yam, *Mean Field Games and Mean Field Type Control Theory* (SpringerBriefs in Mathematics). New York, NY: Springer, 2013.

[44] R. Carmona and F. Delarue, *Probabilistic Theory of Mean Field Games with Applications II*, en. 2018.

[45] P. E. Caines and M. Huang, "Graphon Mean Field Games and the GMFG Equations: Epsilon-Nash Equilibria", in *2019 IEEE 58th Conference on Decision and Control (CDC)*, ISSN: 2576-2370, Dec. 2019, pp. 286–292.

[46] A. Dunyak and P. E. Caines, "Graphon Field Tracking Games with Discrete Time Q-noise", en, in *2023 62nd IEEE Conference on Decision and Control (CDC)*, Singapore, Singapore: IEEE, Dec. 2023, pp. 8194–8199.

[47] F. Parise and A. Ozdaglar, "Graphon Games: A Statistical Framework for Network Games and Interventions", en, *Econometrica*, vol. 91, no. 1, pp. 191–225, 2023, _eprint: https://onlinelibrary.wiley.com/doi/pdf/10.3982/ECTA17564.

[48] R. Carmona, D. B. Cooney, C. V. Graves, and M. Laurière, "Stochastic Graphon Games: I. The Static Case", en, *Mathematics of Operations Research*, vol. 47, no. 1, pp. 750–778, Feb. 2022.

[49] D. Vasal, R. Mishra, and S. Vishwanath, "Sequential Decomposition of Graphon Mean Field Games", in *2021 American Control Conference (ACC)*, ISSN: 2378-5861, May 2021, pp. 730–736.

[50] F. L. Lewis, D. Vrabie, and V. Syrmos, "The Tracking Problem and Other LQR Extensions", en, in *Optimal Control*, Section: 4 _eprint: https://onlinelibrary.wiley.com/doi/pdf/10.1002/97 John Wiley & Sons, Ltd, 2012, pp. 177–212.

[51] P. E. Caines and M. Huang, "Mean Field Games on Dense and Sparse Networks: The Graphexon MFG Equations", in *2024 American Control Conference (ACC)*, ISSN: 2378-5861, Jul. 2024, pp. 4230–4235.

[52] P. E. Caines and M. Huang, "Sparse Network Mean Field Games: Ring Structures and Related Topologies", in *Proceedings of the 63rd IEEE Conference on Decision and Control*, Milan, Italy: IEEE, 2024.

[53] Q. Lü and X. Zhang, *Mathematical Control Theory for Stochastic Partial Differential Equations* (Probability Theory and Stochastic Modelling), en. Cham: Springer International Publishing, 2021, vol. 101.

[54] A. Dunyak and P. E. Caines, "Large Scale Systems and SIR Models: A Featured Graphon Approach", in *2021 60th IEEE Conference on Decision and Control (CDC)*, ISSN: 2576-2370, Dec. 2021, pp. 6928–6933.

[55] Á. Backhausz and B. Szegedy, "Action convergence of operators and graphs", en, *Canadian Journal of Mathematics*, vol. 74, no. 1, pp. 72–121, Feb. 2022.